On the Design and Operation of Heat Pump Systems for Zero Carbon Districts

Bahador Samadzadegan

A Thesis in

The Department of

Building, Civil and Environmental Engineering

Presented in Partial Fulfillment of the Requirements

for the Degree of

Master of Applied Science (Building Engineering)

at Concordia University

Montréal, Québec, Canada

April 2021

CONCORDIA UNIVERSITY
School of Graduate Studies

This is to certify that the thesis prepared

By: **Bahador Samadzadegan**

Entitled: **On the Design and Operation of Heat Pump Systems for Zero Carbon Districts**

and submitted in partial fulfillment of the requirements for the degree of

Master of Applied Science (Building engineering)

complies with the regulations of this University and meets the accepted standards with respect to originality and quality.

Signed by the Final Examining Committee:

Dr. R. Zmeureanu.. Chair

Dr. H. Ge.. BCEE Examiner

Dr. R. Zmeureanu..BCEE Examiner

Dr. A. K. Athienitis..BCEE Examiner

Dr. U. Eicker..Supervisor

Approved by

Dr. M. Nokken

Graduate Program Director

Dr. M. Debbabi, Dean

Gina Cody School of Engineering and Computer Science

April 28, 2021

Abstract

On the Design and Operation of Heat Pump Systems for Zero Carbon Districts

Bahador Samadzadegan

Global warming and climate change are no longer just a topic for expert panel discussions since we started to observe real-life impacts of such phenomenon for more than a decade. Reducing and gradual elimination of greenhouse gas (GHG) emissions is the best and only solution. Buildings, districts, and cities are responsible for a significant portion of GHG emissions, and concepts such as sustainability, energy efficiency, and renewable energies support the transition towards zero-carbon districts. Efficient, reliable, and accessible tools are crucial to plan, design and analyze such districts and cities.

The prepared manuscript-based thesis focuses on introducing an automated framework for designing and sizing energy systems in a zero-carbon district context. The framework has been developed using the simulation environment INSEL 8.2 combined with Python coding and contains a variety of complex components, including but not limited to heat pumps (HP), photovoltaic panels (PV), inverter, maximum power point tracker, domestic hot water tank, energy metering, and simplified battery and thermal storage systems. The integrated framework covers demand profiles, energy system sizing, components' interaction, and performance analysis.

An urban energy system model (UESM) has been developed and used for different scenarios and use cases such as sensitivity analysis, optimization using genetic algorithm (GA), economic analysis, and the comparison of different energy systems configurations (Central vs. Decentral scenario). Simulation with an hourly resolution, while considering various detailed models, is the most critical capability of this framework compared to available UESMs. Moreover, all tools developed are open-source with a high level of flexibility, which can be the foundation for other researchers by adding and modifying different domains' components.

Acknowledgments

I would like to thank my supervisor Prof. Dr. U. Eicker, who has guided and supported me through my journey from the day we met to the last day of my graduation. She is a world-class scientist and a role model with an incredible personality and a heart of gold. She touched my life in many ways and will always have a place in my memories.

Also, I would like to thank my best friend and wife, Mohadese, who has always been there for me without a doubt. I saw her patience and sacrifices to push me toward my goals. Besides, I would like to express my appreciation to my parents, who were available whenever I needed a hand and devoted their lives to support me.

Moreover, I want to express my gratitude to all my friends and colleagues at CERC for their unwavering support.

Finally, I would like to mention Jürgen Schumacher, creator and the spiritual father of INSEL, and I hope this work helps to keep his memories alive.

Contribution of Authors

Chapter 2:

Soroush Samareh Abolhassani (Ph.D. candidate) and Sanam Dabirian (Ph.D. candidate) have contributed to the urban building energy model (UBEM) and, along with Azin Sanei (Master's student), has provided data for the Lachine-Est case study, including building geometries and heating and cooling demand profiles. Both Ph.D. candidates helped with writing the manuscript. Saeed Ranjbar (Ph.D. candidate) helped with organizing and writing the manuscript. Hadise Rasoulian (Master's student) helped with data gathering.

This chapter is accepted in "Frontiers in Sustainable Cities-Urban Energy End-Use" journal entitled "Novel energy system design workflow for zero-carbon energy district development"

Chapter 3:

Soroush Samareh Abolhassani (Ph.D. candidate) has contributed to the UBEM and, along with Azin Sanei (Master's student), has provided data for the Lachine-Est case study, including building geometries and heating and cooling demand profiles. Abolfazl Rezaei (Ph.D. candidate) has contributed to the district heating and cooling network design and calculations. Saeed Ranjbar (Ph.D. candidate) and Hadise Rasoulian (Master's student) have contributed to economic analysis and data gathering.

This chapter is published in "Energies" journal special issue "Municipal Energy System Planning: New Approaches, Applications, and Future Research Needs" entitled "A New Modeling Approach for Low-Carbon District Energy System Planning"

Dr. U. Eicker has supervised both papers' preparation.

The thesis author's contribution was essential to both publications. Except "demand calculation" which is the input of the proposed workflow of the thesis, and "economic assessment" and "hydraulic network modeling" which are small section of the process, the rest is the outcome of the thesis author, including but not limited to developing framework, modeling and simulation using INSEL, coding and integrating the model to Python and analysing the results.

All authors reviewed the final manuscript and approved the contents.

Table of Contents

List of Figures

List of Tables

List of Abbreviations

Air Source Heat Pump (ASHP)	Heat Pumps (HP)
Water Source Heat Pump (WSHP)	Coefficient of Performance (COP)
Ground Source Heat Pump (GSHP)	Photovoltaic (PV)
Urban Energy Systems Modeling (UESM)	2°C Scenario (2DS)
Urban Building Energy Modeling (UBEM)	Greenhouse Gas (GHG)
Domestic Hot Water (DHW)	Department of Energy (DOE)
Building Characteristics Dictionary (BCD)	Renewable Energy Sources (RES)
CityGML (City Geographic Markup Language)	net present value (NPV)
Seasonal Coefficient of Performance (SCOP)	Levelized Cost of Energy (LCOE)
Maximum Power Point Tracker (MPPT)	Genetic Algorithm (GA)
INSEL (Integrated Simulation Environment Language)	District Heating Network (DHN)
Energy system analysis (ESA)	District Heating (DH)
Energy system model (ESM)	Net present value (NPV)
Heating, ventilation, and air conditioning (HVAC)	

Nomenclature

A	Incident matrix	$\dot{m}$	Mass flow rate (kg/s)
c_p	Specific heat capacity ($J/kg\ °C$)	P	Pressure (Pa)
D	Diameter of the pipe (m)	Q_C	HP heat output (kWh) in cooling cycle
E_C	Electricity consumption (kWh) in cooling cycle	Q_H	HP heat output (kWh) in heating cycle
E_H	Electricity consumption (kWh) on heating cycle	r	Interest rate
E_t	Energy generation	S	Surface area of the pipe (m^2)
f	Friction factor	T	Temperature ($°C$)
F_t	Fuel expenditures	U	Global heat transfer coefficient ($W/m^2\ °C$)
I_t	Investment expenditures	v	Design velocity (m/s)
L	Length of the pipe (m)	ρ	Density (kg/m^3)
M_t	Operations and maintenance costs	β	Total loss coefficient

Chapter 1: Introduction

1-1- Background

Global awareness about climate change and global warming has pushed policymakers to move their respective countries and organizations toward controlling greenhouse gas (GHG) emissions, lowering fossil fuel consumption, and making the most of renewable energy sources (RES). 2 °C scenario (2DS) is the most well-known and commonly used international policy goal that is part of the Paris Agreement to reach net-zero CO2 emissions by 2060. Such achievement requires extensive use of renewable energy for power generation with an estimated portion of 74% ("Energy Technology Perspectives 2017 Catalysing Energy Technology Transformations INTERNATIONAL ENERGY AGENCY" 2017).

Numerous terms and concepts have been proposed and used by researchers and regulating bodies to define a better structure for all the building sector stakeholders, such as Net-zero energy building, Net-zero energy district, Zero-emission building, etc., which are summarized in (Lindholm, Rehman, and Reda 2021). All these terms have the common intention to prevent further global warming impacts. Electrification providing decarbonized power generation is considered the primary substitute for fossil fuels. This trend will make electricity the most significant final energy carrier, ahead of oil, and increases electricity share in final energy demand by 8% to the final value of 26% by 2060 ("Energy Technology Perspectives 2017 Catalysing Energy Technology Transformations INTERNATIONAL ENERGY AGENCY" 2017). Urban districts account for half of the global population with more than two-thirds of total GHG emissions, and the rates are expected to grow even more by 2050 (Intergovernmental Panel on Climate Change 2014).

Heating and cooling demands in buildings have the largest share of final energy consumption (almost 40%), with 65% reliance on non-renewable sources worldwide. Likewise, 13% and 20% of total energy are being used only in residential buildings in Canada and Quebec, respectively (Government of Canada 2020). Implementing new technologies and growing renewable resources' share can reduce fossil fuel consumption by 50% in 2060 ("Energy Technology Perspectives 2017

Catalysing Energy Technology Transformations INTERNATIONAL ENERGY AGENCY" 2017). It takes ambitious goals and intentions from all countries, especially developed countries. For instance, currently, Denmark provides one-third of heating for buildings with renewable energy sources and is planning to become fossil fuel independent by 2050 (Kontu 2014). Alternatively, the USA has established regulation that requires converting half and all commercial buildings to zero energy buildings by 2040 and 2050 (Crawley, Pless, and Torcellini 2009). Similarly, the EU planned to lower the GHG emission rates to 80% lower than the level of the 1990s (Commission et al. 2018).

During the past two decades transitioning from local energy systems to long-term, large-scale energy systems have become an integrated part of strategic energy planning, especially among 40 megacities worldwide, also known as C40 (C40 2019). All these regulations, codes, and guidelines eventually require a planning framework for estimating and simulating projects' possible outcomes regardless of size and scale.

1-2- Urban Energy Systems Modeling (UESM)

UESMs are tools that are becoming essential in strategic energy planning carried out by cities that are determined to mitigate climate change and are moving sustainability up in their priority list. These tools provide users with quantitative frameworks contributing to the energy sector's decision-making process and strategic development (Yazdanie and Orehounig 2021). During the 1970s oil crisis, using the first generation of UESMs to solve linear programming problems started to become a trend (Pfenninger, Hawkes, and Keirstead 2014). Until the 1990s, UESMs became an integral part of decision-makers' toolbox as their value became more evident by broadening their applications and improving their time resolutions (Keirstead, Jennings, and Sivakumar 2012).

Over time, emerging new technologies and concepts such as sustainability and resiliency, the complexity of energy systems, variable energy systems formations, escalating uncertainties due to various systems interaction, to name a few reasons, have made crucial changes to the energy sector and taken expectancy of UESMs to another level.

1-2-1-UESM Challenges and Gaps

UESMs are getting more noticed in recent years by becoming more reliable and equipped with various features. Many review studies have been carried out to point out the pros and cons of each tool or method. Two of the most cited studies investigating UESM tools and their capabilities for integrating renewable energies into energy systems are (Connolly et al. 2010), which explored 37 models and (Sinha and Chandel 2014) followed by recent work of (Ringkjøb, Haugan, and Solbrekke 2018) which gives a comprehensive and detailed review of 75 tools and methods. Other studies which should not go unnoticed are including but not limited to International Energy Agency's report looking into different models and scenarios (Mai et al. 2013), a review study on implementing energy models in the UK by (Hall and Buckley 2016), and, providing an extensive overview of more than thirty review studies in (Yazdanie and Orehounig 2021).

Among all observations and investigations, there are common conclusions among all reviews regarding the shortcoming of UESMs. Although each model and method has different assumptions, methodology, and temporal scale, the temporal scale importance is usually underestimated. Above all, due to the intermittent nature of renewable energies (e.g., solar and wind energy), a lower temporal resolution will result in over or underestimating power generation, cost, or system size (Collins et al. 2017). For instance, in (Welsch et al. 2014), the comparison between two temporal scales (monthly vs. hourly resolution) in the same use case showed a 21.4% divergence in the results by overestimating the RES power generation capacity. On the other hand, a study carried out in (Pfenninger 2017) suggests that higher temporal resolution is not the solution to all energy system modeling problems, and due to difference in data availability and concerning the nature of the energy system that is being modeled, the adjustable time resolution is much more preferred.

Similarly, transparency and openness of models are among the top points that stand out when looking for improvement and contributing to future UESMs. That being said, models are highly responsive to slight changes in their assumptions, which will drastically affect the results. Since most of the cases are commercial products, understanding the calculation, assumption, and default values of many tools is impossible, let alone changing them. With reference to (Ringkjøb, Haugan, and Solbrekke 2018), UESMs could become more reliable resources for bridging between science

and policy by extending productivity and relevance to social debates. This issue refers to explaining assumptions, ruling equations, and the interaction between components being accessible through proper documenting, providing source code, and result verification if applicable.

As mentioned in (Yazdanie & Orehounig, 2021), reproducibility comes with transparency and opens the opportunity for other researchers to reproduce the model for either conducting research or to verify and calibrate the models. In contrast, lack of transparency lowers the feedback receiving chance from stakeholders and communities by limiting proper understanding of the model and results. Consequently, helpful insights that can contribute to the model itself will be a lost ring in a UESM's improvement chain. Furthermore, transparency of an energy model directly impacts communities' acceptance and eventually being implemented (Zoellner, Schweizer-Ries, and Wemheuer 2008).

Last but not least, despite the known fact that combining energy system modeling with urban planning and modeling strategies can contribute to improving results and all involving models (Cajot et al. 2017), insufficient efforts are focused on introducing an integrated workflow among different disciplines (Keirstead, Jennings, and Sivakumar 2012). A flexible framework with the capability to integrate multiple sectors covering topics such as urban building energy modeling, energy system modeling, transportation sector, and waste management seems to be the next generation of models. Developing such a framework requires immense expertise, efforts, and motivation to gather all modeling and planning aspects.

1-3- Heat Pumps in Urban Energy Systems

Heat pumps are energy systems that transfer heat from an external source to the medium desired by consuming electricity. HPs can extract heat from a heat source and turn it into useful heat used for space heating, domestic hot water (DHW) generation, process heat, or other required applications. Unlike most energy systems, since the process is merely transferring heat rather than energy conversion, heat pumps (HP) have relatively high efficiencies. HPs are regarded as the topmost efficient and environmentally friendly energy systems that will have a crucial role in mitigating climate change, owing to their high efficiency and capability to integrate into

intermittent RES (Yunna and Ruhang 2013). By referring to the literature, it can be concluded that HPs are a critical part of global warming remediation (Bloess, Schill, and Zerrahn 2018).

HP is not a new technology and is being used for many decades. However, recently they have significantly gained traction and become more prevalent in policymakers and strategic planners' eyes. Currently, HPs have a low penetration level in heating in buildings, as low as 5%, but the share will grow dramatically (Abergel 2020). A literature review on HPs done in (Gaur, Fitiwi, and Curtis 2021) shows that the focus on HPs has increased exponentially due to the intention to find solutions for lowering GHG emissions while electrifying heating and cooling systems is a hot topic and also relevant to HPs.

Providing a fully reversible working cycle, HPs can fully or partially meet the heating and cooling demands, and DHW, which seems like a complete solution considering the shown fact about HPs contributing to decarbonizing, saving primary energy, and booming system's efficiency (Yunna and Ruhang 2013). Many studies are showing the impact of HPs in reducing emissions and energy consumption. For instance, a California-based case study reports 50% emission reduction by integrating HP into energy systems (Brockway and Delforge 2018), or the Danish energy system, including HPs, cost 16% less of the scenario without them by 2035 (Renaldi, Kiprakis, and Friedrich 2017). In another study, HPs could provide space heating with 30% less primary energy consumption and emissions than gas boilers, thanks to their high coefficient of performance (COP) (Jarre, Noussan, and Simonetti 2018).

1-3-1-HP Classifications

HPs can be categorized in different ways, such as their heat source type, application, or technological feature like compressor type. One of the broadly used classifications is based on the medium from which HPs extract the required heat. In this categorization, two main branches are air source HPs (ASHP) and water source HP (WSHP), followed by less common types such as HPs working with process heat (industrial HPs). Among the WSHPs, ground source HP (GSHP) is the most commonly used type (Figure 1-1). ASHPs extract heat from surrounding air and, by consuming electricity and based on the reversed refrigeration cycle, boost its energy and transfer high-grade energy into the heat transfer fluid as the final energy carrier going to the indoor space. Similarly, WSHPs have different subcategories of whether they use a lake, river, or an aquifer to

extract heat or use boreholes and geothermal energy. Other than GSHPs, WSHPs are of limited application as a large volume of water bodies are required to support required HP operation and provide sufficient resistance against heat source temperature fluctuations due to heat extraction or injection.

The HP system's heat transfer fluid could be water (or a mixture) or air, resulting in four types of air to water, air to air, water to water, and water to air. GSHPs rely on a much more stable heat source giving the proper system sizing, as the high heat capacity of water prevents drastic changes in the source temperature. On the other hand, ASHPs are utterly dependent on the outdoor air temperature, which can vary significantly unless an auxiliary preheating system is considered, i.e., preheated air using solar walls. With that in mind, GSHPs have relatively more stable COPs compare to ASHPs, especially in colder climates in which temperature can be as harsh as -30 °C.

Several studies have shown the effectiveness of HPs in reducing primary energy consumption and emission while increasing the system's efficiency. To mention some, a study on retrofitting Canadian houses with ASHPs shows a reduction in energy consumption by 36% (Asaee, Ugursal, and Beausoleil-Morrison 2017). Alternatively, using ASHP for the floor heating system can provide satisfactory thermal comfort with lower operating costs compared to the radiator heating system (Hu et al. 2019). Likewise, for GSHPs, multiple studies have pointed out the benefits of using such energy systems. Besides, different studies focused on the advantage of stable COP level of GSHPs due to almost constant heat source temperatures for an entire year, even in cold regions like Canada and Scandinavian climates (Bach et al. 2016; Safa, Fung, and Kumar 2015)
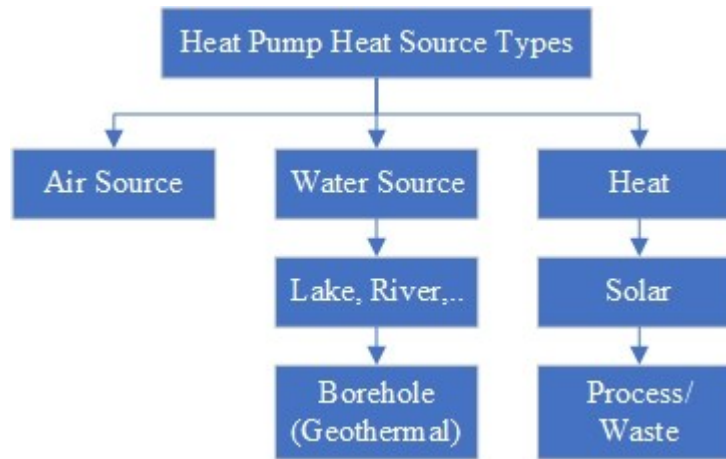
Figure 1-1. Heat pump classification based on heat source types (Gaur, Fitiwi, and Curtis 2021).

1-3-2- HP Modeling Challenges

Both ASHP and GSHP are efficient energy systems, but with respect to heat source temperature changes in both cases, GSHPs tend to be more efficient in the case of COP. Although ASHPs' COP fluctuates more extensively, this equipment has become much more resilient to harsh weather thanks to technological improvements and can have high seasonal COPs. A high level of sensitivity in COP has pushed energy system modelers to find creative solutions other than previously used constant COP value.

Moreover, using a mathematical approach to solve governing thermodynamic equations to simulate the HP working cycle will make the modeling vastly complex and requires extensive calculations. Furthermore, the detailed design of HPs due to system complexity takes lots of effort and can not be overgeneralized to different brands and models. Thus, a simplified but still viable modeling approach should capture all COP fluctuations in high temporal resolution while minimizing detailed modeling up to a sufficient level.

1-4- Objectives and Outline

Mitigating climate change needs to move toward decarbonizing existing infrastructures and systems while planning to build sustainable, green buildings with a minimized carbon footprint. To have a reliable estimation of the current situation and propose future strategies, some tools and frameworks are needed, which are also known as UESM. Although numerous UESMs are

developed, the extensive literature review showed multiple gaps between tools in hand and favorable ones, discussed in previous sections. Primary issues are:

- Lack of adjustable temporal resolution with regards to the problem and available data.
- Lack of openness and transparency in models.
- Focusing on one topic instead of giving a holistic overview by considering interactions between sections (e.g., demand and energy system sizing)
- Due to the lack of a holistic view, implementing demand-side management strategies is not possible.
- Preparing a flexible foundation for users to adjust, change and add desired sections in the model and framework

After considering the need for a reliable UESM framework, the next step is to focus on the energy system's essential components. As mentioned in previous sections, HPs are the focal point of transitioning to zero-carbon energy systems. They provide useful energy and thermal comfort at a relatively lower price with higher efficiency, as well as supporting the integration into RES. Since the electricity is the single required fuel/ input of HP systems, the carbon footprint cannot be reduced unless decarbonized (low carbon) power generation is coupled with HPs. That being said, local solar power generation using photovoltaic panels (PV) is considered to meet the system's electricity demand.

All in all, in this manuscript-based thesis, an automated framework for selecting and sizing ASHP and GSHP is presented. With the inverter, local PV, the maximum power point tracker integrated into the HP system to support renewable power generation and meet the HP electrical demand. DHW tank, auxiliary electrical heater, and two simplified thermal storage and battery models are added to propose a holistic energy system for cooling, heating, and hot water demands while practicing demand-side management strategies and increasing system flexibility. Figure 1-2 shows the schematic overview of the proposed energy system. The model has been tested in multiple use cases, and the results are summarized in the following chapters.

Chapter 2 introduces an integrated urban building energy modeling (UBEM) workflow to calculate existing or designed buildings' cooling and heating demand, coupled with an automated UESM to compare ASHP and GSHP in a decentralized scenario. A detailed explanation regarding

automated PV system sizing and HP modeling is presented in the methodology section. In the results section, the possibility of designing a positive energy district with the support of a local PV generation system as the only renewable energy source is investigated

Chapter 3: The proposed model is used in a case study to compare centralized (district heating and cooling network) and decentralized (individual heat pump systems for each building) scenarios regarding energy and economic analysis.

Chapter 4: Other system capabilities are presented through different case studies, such as optimization features, domestic hot water generation using HP, automated HP sizing, load shifting, and storage system impacts on system efficiency.

Chapter 5: Conclusion and discussion.
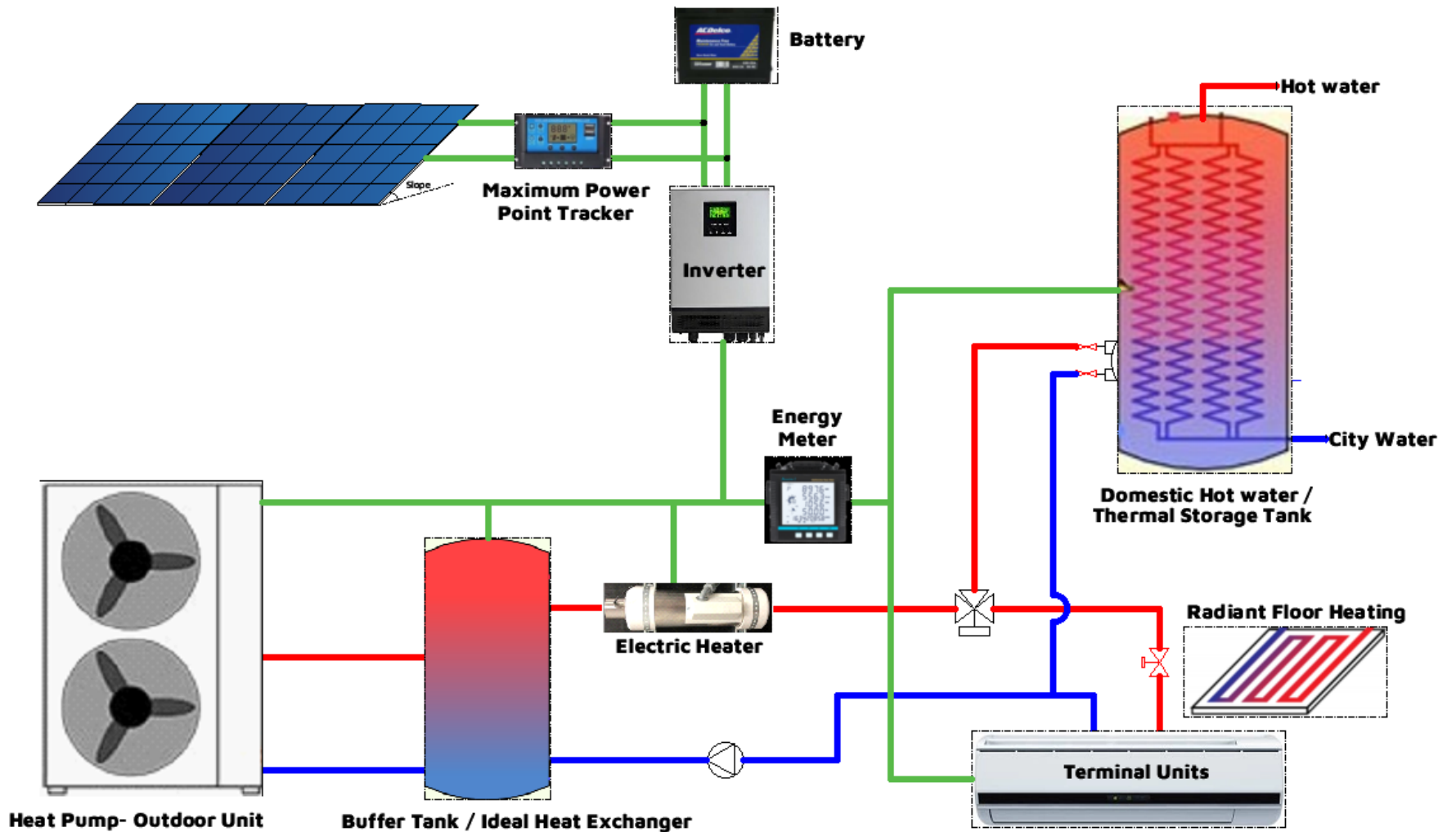
Figure 1-2 Schematic overview of the proposed energy system.

Chapter 2: Novel Energy System Design Workflow for Zero-Carbon Energy District Development[1]

Authors' Contribution

This chapter is published in Frontiers journal and it generally explores implementing the novel framework introduced in this thesis into action. Although the demand-side of the framework is made available by the contribution of co-authors, the general concept, idea, methodology, simulation and results are based on the outcome of the presented thesis. The demand profiles for heating and cooling are the input of the INSEL model and the energy system modeling workflow, simulates the energy system's behaviour regarding the context and the case study. The thesis author is the first name author of this publication.

2-1- Introduction

Many cities worldwide have a climate strategy to become carbon neutral by 2050 (Dominković et al. 2016). Currently, 54% of the world's population lives in urban areas, and this figure will rise to 66 % by 2050 (Pless and Polly 2018). Buildings' energy consumption account for about 30% of the world's energy consumption, and 60% of this is due to heating and cooling demand (Lizana et al. 2017). Based on Natural Resources Canada's data, the residential sector accounts for 13% of the end-use consumption in Canada, while this share is 20% in Quebec (Government of Canada 2020). The successful implementation of net-zero energy buildings has led to applying this concept to a group of buildings and, finally, developing zero-carbon or even positive energy districts. These zero-carbon or positive energy districts have several advantages, including economies of scale, an opportunity to use waste heat from one building in another, and sharing energy resources (Pless and Polly 2018).

In the sustainable development of cities toward carbon neutrality, municipalities' role, efficient energy system design, and buildings' energy consumption should be considered (Wiseman 2018). Municipalities' plans and goals define the scope of changes and enhancements in different sectors. To evaluate different scenarios for municipalities or private developers'

---

[1] This chapter is Published in "Frontiers in Sustainable Cities-Urban Energy End-Use" journal entitled "Novel energy system design workflow for zero-carbon energy district development"

decision-making, dynamic energy demand simulation is beneficial to optimally size the urban renewable energy system to achieve a zero-carbon district. Urban Building Energy Modeling (UBEM) is a physics-based approach to analyze and predict a group of buildings' energy consumption considering the indoor and outdoor conditions (Hong et al. 2018). UBEM is a novel tool to support and improve sustainable development and energy efficiency measures in districts or cities which considers the thermal load diversity of a group of buildings to design on-site renewable energy systems, estimate CO_2 emission, and predict building energy use (Johari et al. 2020).

An appropriate energy system should be designed and sized to supply those demands after calculating a building or a building cluster's energy demand. Utilizing renewable energy systems is a solution to decarbonize buildings' consumption and reduce the urban ecological footprint. There are several tools under development to ease the process of modeling multiple buildings. City Energy Analyst is a modeling framework to integrate the spatiotemporal analysis of building energy performance, local energy potential assessment, and energy system optimization and analysis in neighborhoods and city districts for urban planning and policymaking (Fonseca et al. 2016). TEASER is a design-driven reduced-order UBEM platform for energy performance analysis on network efficiency and management on different spatial scales (Remmen et al. 2018). Besides, TEASER is integrated with the urban energy systems design to optimize energy systems and networks for both building and urban scales (Ferrando and Causone 2020).

A reliable and accurate energy system modeling framework can help compare different technical and environmental indicators of the proposed energy system alternatives. Due to the uncertainties, modeling renewable urban energy systems, whether in a standalone configuration or hybrid mode, is a more complex procedure than conventional energy systems. According to Yazdanie et al. (Yazdanie and Orehounig 2021), many studies in urban energy system modeling (UESM) suffer from the lack of detailed input data. Therefore, there is a need for a comprehensive and detailed UBEM to provide load input data for UESM. Many detailed UBEM software such as UMI and City Energy Analyst are developed and available, but they do not contain comprehensive UESM, nor are they explicitly designed for such purpose (Reinhart and Cerezo Davila 2016)(Fonseca et al. 2016).

Numerous studies are focusing on integrating different energy sources, including renewable energies, into energy system design. To name a few, Petkov and Gabrielli (2020) developed a framework to design, select, and size a low carbon Multi-Energy System. Their objective was to minimize the annual costs and emissions. They showed that emissions could decrease by 90% if a renewable energy system with short-term storage is used. The same objective functions were used by Sohrabi Tabar et al. (2021) to use waste heat recovery, power to gas, and carbon capture technologies in an energy system framework. In simulation models, the aim is to predict the energy system's performance, such as TRNSYS (Li et al. 2015)(Soutullo et al. 2016). Yuan et al. used TRNSYS to design and assess a distributed energy system serving a university campus (Yuan et al. 2020). The proposed system consisted of an internal combustion engine, absorption chiller, thermal energy storage unit, heat pump (HP), and boiler. They realized that integrating thermal storage and distributed energy system leads to higher primary energy efficiency.

Furthermore, Hsieh et al. used quasi-steady state simulation models to study short-term and long-term TES integration with solar collectors in different scales from single buildings to neighborhoods (Hsieh et al. 2017). They reported that using decentral short-term and long-term storage for each building has the best performance, with 48% of the energy being covered by solar energy. Dominkovic et al. (2016)investigated a methodology in the transition to carbon-free and 100% renewable energy in South-Eastern Europe. Their results show that a single renewable energy source typically has no more than 30% share in an energy system. Usually, a variety of technologies is needed to supply the demand. Pilpola et al. developed a techno-economic model at the national and city-level scale to investigate the possibility of using different renewable energy systems to achieve low and zero-carbon goals in Finland and specifically the town of Helsinki (Pilpola et al. 2019). After coupling multiple technologies, each scenario's cost efficiency is discussed and considered as a variable to compare the proposed scenario's overall efficiency.

Also, there are studies trying to point out the required framework and features of a suitable workflow. Eicker et al. discussed the required concepts of an urban energy modeling platform to model the energy demand and intricate urban renewable energy systems design (Eicker et al. 2020). The platform will include models of buildings, transportation, energy and distribution systems, food and water infrastructure to compare different energy system operation scenarios. In another study, Weiler et al. proposed an automated method to calculate central energy generation

and supply scenarios using the simulated heating demand based on a CityGML-based model (Weiler et al. 2019). Although several UBEM models have been proposed, they are mostly still in prototype status, and a reliable urban energy simulation model is still a challenge.

For the current study, the role of energy system design and UBEM in the transition to energy-efficient districts are studied. This paper aims to investigate the challenges of a developed integrated UBEM and energy system design workflow. A novel automated framework combining a Python-based UBEM model with a renewable energy system model is developed to calculate and predict new or existing districts' energy demand and then design a renewable energy system. In this work, photovoltaic panels (PV) have been coupled with ground source and air source HPs for covering the heating and cooling demands for a district.

This work uses a detailed UBEM workflow based on 3D urban geometry with different energy-related data from various sources with different formats to calculate the heating and cooling demand. The developed UBEM is highly flexible in providing relevant input data for energy system sizing in any spatiotemporal scale from a thermal zone to a district and hourly to annual results. This allows combining the building demand modeling with international database sources on construction or occupancy, which is often a limitation in urban modeling tools. Furthermore, designing energy systems with considering component-level details has added a higher value to the proposed UESM's flexibility as well as accuracy. Introducing a sufficiently detailed and comprehensive model as a substitute to the high-level energy system design in an urban context increased modeling resolution by capturing the impact of components' performance on other components and the system's efficiency. In addition to the detailed design of a PV system, HPs have been modeled with varying coefficients of performance (COP) to cover the gaps in many previous studies (Lund et al. 2016) (Rinne and Syri 2013), that have considered a fixed monthly or annual value COPs.

2-2- Methodology

The following sections describe the integrated workflow of the UBEM and UESM. Figure 2-1 illustrates an overview of the methodology used in this paper.

2-2-1-UBEM

The importance of a correct pre-design process for a successful design at the building or city scale is undeniable. Overviewing the site's limitations and the client requests cannot be executed without a feasibility study. The feasibility study shows what is possible for the project based on the site, existing conditions, zoning, building codes, local regulations, and other legal restrictions (Green 2018). The site and climate analysis are also part of the pre-design process. These analyses focus on potentials and conditions around the site (Spreiregen and Beatriz 2007). The site analysis aims to provide external information about the site, limitations, and assets and connect them to the design's internal needs (Halil et al. 2016). Looking at the neighborhood context, vegetation, climate, historical factors, and many others is part of this process. Spatial design or building massing helps to make a better connection between the site and future buildings. Early-stage building shadow studies, wind flow or radiation analysis, and any other analysis related to urban comfort and façade control, can be executed in this stage. Then the process continues reaching the building design. In this stage, the building's location, orientation, and massing form are defined, so the project reaches to more detailed design like adding façade detail, form detail, or shading properties.

A novel, highly flexible, and dynamic Python-based UBEM workflow is developed in the current study. The proposed model can cover all aspects of the building energy modeling in detail and dynamically change all input parameters based on building use-type. Due to the massive amount of input parameters in UBEM models, high computational cost, and considerable uncertainty involved in simulation, it remains a challenge to have a practical and accurate UBEM model. The energy system sizing is highly dependent on building energy demand results and energy demand changes based on building use-type. Thus, all input parameters of the developed UBEM model change based on building use-type to increase the model's accuracy by using more relevant input parameters for each building use-type.

Simulating the urban building energy system requires coupling with an accurate UBEM (Hong et al. 2018). The urban energy system sizing, especially PV system sizing, is highly dependent on the building's roof shape and area (Mohajeri et al. 2018). Most previous studies simplified the building geometry for energy demand calculation which can cause high uncertainty in their

building energy demand and energy system sizing calculation (Strzalka et al. 2011). The roof shape and area from the architectural design step are used for energy system sizing in the current study. It is necessary to use the same roof shape in urban building energy demand and energy system sizing calculation to have a compatible and accurate model. In the developed UBEM, buildings and mostly the roofs are modeled in detail and close to reality. The main advantage and contribution of the proposed UBEM model is its compatibility with the energy system sizing. Many downsides of energy system sizing in the previous studies are studied and rectified through the proposed UBEM model.

CityGML (City Geographic Markup Language) (Gröger et al. 2012) was used as an open data model similar to an XML format suitable for storing the geospatial information of the 3D buildings. The CityGML files are parsed, and building coordinates and attributes are extracted using a Python code, and the building objects are stored in a Python dictionary hierarchically based in the order of a) Building ID b) Building use-type c) Building coordinates (x,y,z)
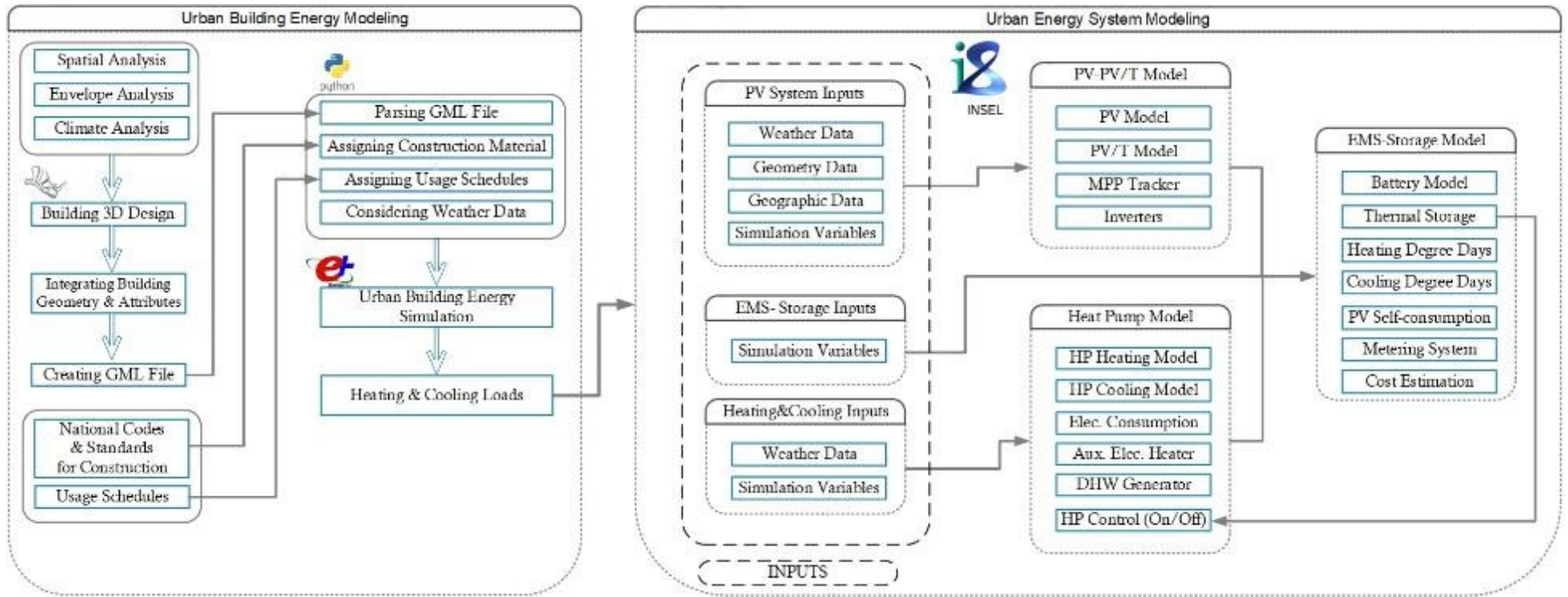
Figure 2-1 Methodology overview.

Using hierarchical building characteristics in the Python dictionary makes it possible to add all the other building information based on the surface type and building use-type. In the next step, the high performance building materials and constructions (standard 189.1-2009) are extracted based on the building use-type from the National Renewable Energy Laboratory (NREL) (NREL 2018) (Building Component Library 2021) and stored in a JSON format called JCM. The JCM file is parsed and embedded in a Python dictionary called building construction archetypes (BCA). Each polygon in the building coordinate's part is categorized into the wall surface, roof surface, and ground surface and are stored as a subcategory of building 3D coordinates (Figure 2-2). The construction and material archetypes are assigned to each surface based on its type (roof, ground, or wall) and related building use-type. Consequently, each surface can be added to the building energy simulation software with its construction and material features automatically using Python code.
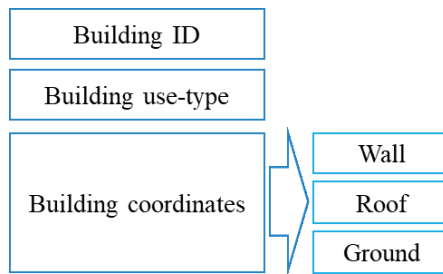
Figure 2-2 The building characteristics dictionary.

EnergyPlus is used as the building energy simulation program to simulate the energy demand considering the effect of the built environment, the interaction between buildings, and internal gains (Chowdhury et al. 2016) (Rao et al. 2018). By iterating through the building characteristics dictionary (BCD), the first item (building IDs) is used for defining building zones. In the next step, the building surface information should be added to EnergyPlus. Hence, the surface coordinates are the successive objects that should be added to EnergyPlus. The coordinates of each building surface are mapped, and the coordinates' connection leads to the creation of the 3D model of buildings and, subsequently, the 3D urban building model in EnergyPlus. Next, the construction and material are assigned to each surface. As each surface is connected to a building use-type in the BCD, a Python code is written to search for each surface based on the building use-type related to the surface type in BCD. The information is extracted from the JCM based on surface building-

related use-type and surface type obtained from the BCD search in the last step. Finally, each surface construction archetype obtained from the NREL JSON search is assigned to each surface and are added to EnergyPlus.

The urban buildings' geometry enriched with materials and construction features is only part of the urban building energy analysis and energy system sizing. To improve the accuracy of the urban building energy demand calculation, building usage schedules need to be considered as follows:

1) Occupancy schedule

2) Lighting schedule

3) Electrical equipment schedule

4) Ventilation schedule

These schedules significantly affect energy demand and, consequently, on energy system sizing (Happle et al. 2018); however, most of the time, a fixed schedule for different building use-types is used, which increases the uncertainty of the urban energy demand calculation. Hence, it is necessary to define the schedules based on the building use-type. Usage schedules (e.g., occupancy parameters, lighting, electrical equipment, and ventilation) have been created by the Department of Energy (DOE). They are available for sixteen different building use-types on the DOE website (US DOE 2013). All schedules are extracted from the EnergyPlus IDF files provided on the DOE website for four different building use-types, including large office, secondary school, small office, and midrise apartment.

In this work, a district case study in Montreal, Canada, has been chosen. These Lachine district case study's building use-types are civic center, school, commercial, residential, and office, which are not the same as the DOE building use-types. Therefore, the chosen building use-types for extracting the DOE website schedules are based on their similarities to the real building use-types in the Lachine district. After extracting the schedules, each schedule of occupancy, lighting, electrical equipment, and ventilation is automatically assigned to each building in the district based on the building use-types. All schedules are fed into EnergyPlus along with the 3D urban model and construction archetypes to calculate the heating and cooling demand in the last step. All the

other settings of EnergyPlus for the UBEM model are shown in Table 2-1. Occupancy, electrical equipment, lighting, and ventilation are set through comparison with other studies (Signelković et al. 2016) (Kim et al. 2013) (Sarfraz et al. 2018) . The simulated heating and cooling demand are input to the UESM model.

Table 2-1 EnergyPlus setting parameters for UBEM.

Parameters	Settings	
Window to wall ratio	0.35	
Constant heating set point	22 ℃	
Constant cooling set point	25 ℃	
HVAC Templates	Ideal loads air system	
Solar distribution	Full interior and exterior	
Shading calculation	**Calculation method**	**Average over days in frequency**
	Calculation frequency	Every 20 days
	Maximum figures in shadow overlap calculations	15000
	Polygon clipping algorithm	SutherlandHodgman
	Sky diffuse modeling algorithm	Simple sky diffuse modeling
	External shading calculation method	Internal calculation
Surface convection algorithm: inside	TARP	
Surface convection algorithm: outside	DOE-2	
Heat balance algorithm	Conduction transfer function	
Sizing period: design day	Winter design day Summer design day	
Solar model indicator	ASHRAE clear sky	
Occupancy	**Number of the people calculation method**	**People/Area**
	People per zone floor area	0.05 people/m2
Lighting	**Design level calculation method**	**Watts/Area**
	Watts per zone floor area	10 W/m2
Equipment	**Design level calculation method**	**Watts/Area**
	Watts per zone floor area	6.5 W/m2
Infiltration	**Design flow rate calculation method**	**Residential: Flow/ExteriorArea and Commercial: Flow/ExteriorWall Area**
	Flow per exterior surface area	Residential: 0.0002 m3/s-m2 Commercial: 0.0005 m3/s-m2
HVAC	**Outdoor air method**	**Flow/Area**
	Outdoor airflow rate per zone floor area	0.00043 m3/s-m2

2-3- UESM

Designing energy systems is of great importance for achieving higher efficiency for a single building, let alone a district or an urban area. Accurate demand forecasting and calculation should be accompanied by an appropriately sized, designed, and installed energy system to have a complete cycle of a sustainable and energy-efficient project. The proposed energy system analysis includes renewable energy sources to reduce carbon and greenhouse gas (GHG) emissions, embodied carbon, and fossil fuel usages. The positive energy concept goes further in utilizing more renewable resources than is consumed while minimizing demand and energy losses and maximizing energy efficiency.

UESM is a block-based simulation model using INSEL 8.2. (Integrated Simulation Environment Language), which comprises many models programmed as independent modular such as meteorological models, PV systems, heat pumps (HP), battery and thermal storage, controllers, auxiliary electrical heaters, and more. In this study, the general workflow of UESM will be discussed as well as PV, HP, metering, and auxiliary electrical heater sections. Eventually, the results of a case study will be provided and discussed.

2-3-1- UESM Platform and Workflow

INSEL is a graphical programming language using blocks with a focus on renewable energy systems. Its usage domain includes but is not limited to building modeling and meteorology. The graphical environment made it easy for users with limited coding experience to implement their ideas using pre-existing blocks to create system models or even prepare their own user blocks. User-defined blocks can be written in different languages, including Fortran and C, and in the next software versions Python, which adds flexibility to the INSEL block concept (Eicker et al. 2020)(Weiler et al. 2019). Moreover, INSEL comes with a comprehensive library for a few energy system components such as PV panels and inverters, which saves the time required for gathering data from manufacturers.

The UESM workflow starts with acquiring hourly demand (heating, cooling, hot water, and plug load) from the UBEM section as input and calculating solar energy parameters, PV panels potential, HP performance, HP energy output, and energy metering. The high-level connection

between different sections is illustrated in Figure 2-3. Internal connections and links between models and blocks are not shown for the clearance of the general concept.
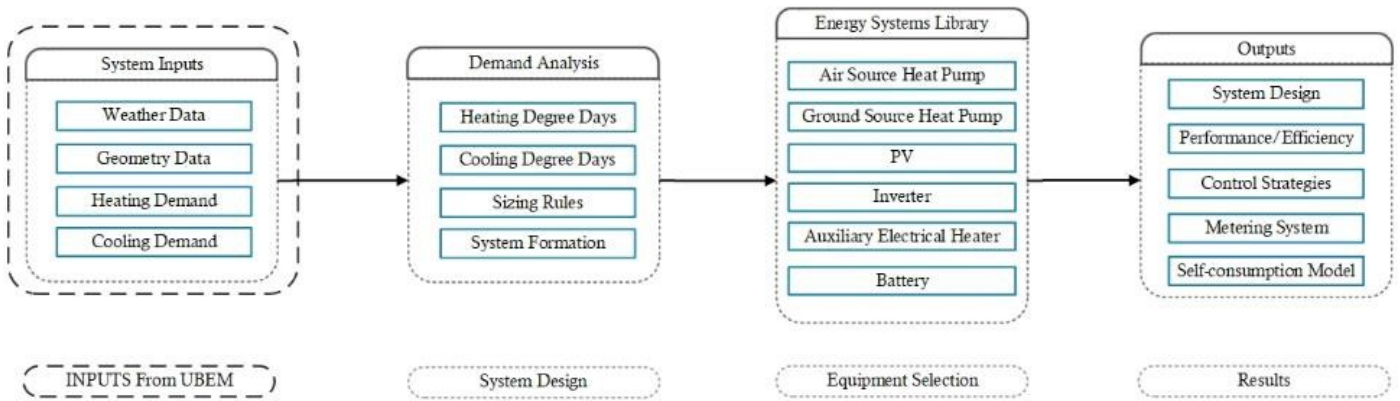
Figure 2-3 Modified UESM flow diagram showing categories of inputs, demand analysis, energy systems, and outputs.

2-3-2-PV Systems

By taking the roof surface area information from UBEM, the PV system model can automatically select the PV placement (by width or length) to maximize the PV generation based on the panel dimensions available in the INSEL PV library. To do so, a rectangular surface (a portion of the roof available for PV panels, which we assumed as 65 % of the total area) with a given length and width is considered. PV panels will be placed by both the short and long sides, and the formation with the highest number of PV panels will be selected. The gap between PV rows is determined with the highest strictness to minimize PVs' shadowing effect (Figure 2-4).
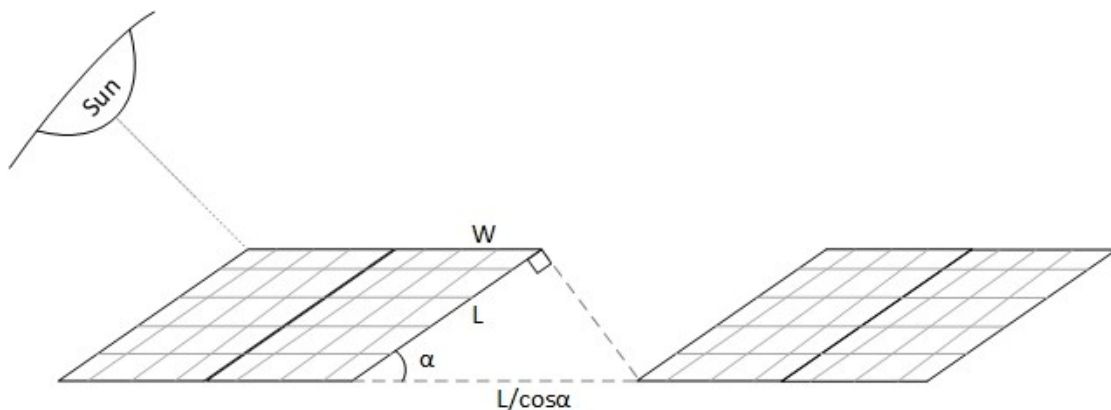
Figure 2-4 Illustrating the gap between PV rows for minimizing shadows on panels.

The PV block simulates the selected PV panel's hourly current-voltage curve using a module-specific parameter set from the INSEL library, with meteorological data inputs, including temperature, global radiation, wind speed, and the user inputs like tilt angle and azimuth for each project. It is worth mentioning that a maximum power point tracker block is integrated into the system to get maximum power at each time step. A selected inverter (appropriately sized for the project) converts the PV-generated DC power to AC and provides the PV system output to the energy metering section of UESM. The characteristics of the used PV panel and PV system design parameters are shown in Table 2-2. The remaining parameters will be determined in each time step and will be fed to the PV block.

Table 2-2 Selected PV panel and PV system design parameters for the Montreal case study

Tilt angle (Degrees)	31
Azimuth Angle	180
Ground reflectance	0.2
Latitude	45.5
Longitude	73.62
Nominal Power (W)	300
MPP Voltage (V)	53.76
MPP Current (A)	5.54
Efficiency (%)	17.24
Width (mm)	1072
Height (mm)	1623

2-3-3- HP System

Electrification of heating systems using HPs and electric boilers has been suggested in recent years to reduce GHG emissions of the heating sector (Thomaßen et al. 2021). Integrating HPs with PV or PV/T panels could enhance renewable energy utilization in urban areas. Aguilar et al. conducted a techno-economic assessment of a PV-HP system supplying an office building's heat demand in Spain (Aguilar et al. 2019). This system reduced the primary non-renewable energy consumption and CO_2 emissions by 74%.

HPs are included in many projects aiming for energy efficiency and decarbonizing due to their high COP, the capability of integrating into heat recovery systems (process heat or waste heat), their flexibility in using different energy sources, including renewables, and the availability in varying capacities and features. The COP is a unitless HP performance indicator. The COP is highly dependent on different parameters. It cannot be referred to as the best and only equipment selection criteria. The COP is determined by dividing useful energy generated (transferred) by the HP's electricity consumption and varies mainly due to source and sink temperatures, resulting in different values in different working conditions.

Researchers have made numerous attempts to determine a correlation between each project's unique properties (heat sink and source temperatures, demand values) and HP's performance to reach an acceptable range of matching results between simulation and real-world experimental data (Jesper et al. 2021)(Heat Pump & Thermal Storage Technology Center of Japan 2010)(Arpagaus et al. 2018). The availability of various technologies and different technical specifications and details for HPs does not allow for a single parameter set to model all HPs.

In the current study, a previously implemented procedure (Weiler et al. 2019) has been used as an accurate HP system model in different conditions. This model uses HP manufacturers' published performance data and interpolation to specify a correlation between COP, HP's heat output, and electricity consumption in different conditions, including additional heat source and heat sink temperatures and heat demand levels. It is worth mentioning that the third parameter can be derived easily in the presence of the two parameters mentioned above. Moreover, instead of COP, which is only accurate in a single condition, seasonal COP (SCOP) has been used, which can be calculated as follows where Q and E are HP heat output (kWh) and electricity consumption (kWh) and E, and H subscripts relate to the heating and cooling cycles.

$$SCOP_H = \frac{\sum_{i=1} Q_H}{\sum_{i=1} E_H} \tag{2-1}$$

$$SCOP_C = \frac{\sum_{i=1} Q_C}{\sum_{i=1} E_C} \tag{2-2}$$

Low-temperature heating is crucial for lowering energy loss and improving systems energy and exergy efficiencies. Heating supply temperatures as low as 30 °C and 35 °C are shown to be

feasible for surface heating and fan coil systems (Hesaraki et al. 2015). Furthermore, many studies have shown that a supply temperature of 40 °C is sufficient for meeting the domestic hot water demand. At the same time, the risk of Legionella can be eliminated via supplementary heating or point of use heating (Henrik Lund et al. 2014)(Lee 2018). By reviewing literature regarding the low-temperature heating concept, supply temperatures of 40 °C and 11-12 °C are selected for heating and cooling, respectively(Huang et al. 2019) (Nordman et al. 2009).

In each time step, the HP model will take heating and cooling demand (kW) from the input file provided by UBEM. With respect to the outdoor temperature, the model interpolates values for HP's electricity consumption, its COP, and the HP output energy. Then the model divides demand by HP output and rounds the quotient up to the closest integer to obtain the number HPs required to meet the demand in each time step. The HP system's electricity consumption will be scaled up accordingly. Besides, electricity balance, PV self-consumption, energy exported and imported from the grid, and SCOPs are calculated in each iteration. The highest value will be reported as the number of HPs required in heating and cooling cycles.

2-4- Case Study

As the second-largest municipality in Canada, Montreal has provided an action plan that includes goals, challenges, and requirements needed to become more sustainable. In the pathway toward sustainability and carbon mitigation goals, the city has three main sustainable development challenges, which are (Montr 2020):

- Reduction of GHG emissions by 80% (3,003-kilo tonnes of CO2 equivalents) by the year 2050 compared to the year 1990 baseline.
- Enhancing access to services and facilities among different city neighborhoods and the ethical distribution of resources for every dwelling.
- To become an exemplary model for other cities by integrating sustainability plans into all aspects of the city.

The developed workflow was applied to a district development called Dominion Bridge in Montreal's Lachine East borough. Lachine-East is a former industrial hub bordered by the Lachine Canal on its southern part, 6th Avenue to the west, Victoria Street to the north, and the east's

Canadian Pacific Railway line. This project's area is 63.8 hectares and includes two heritage buildings that are going to be preserved.

Location is one of the main factors in this project, considered in all design stages. The urban plan should respect the site's identity as the former Dominion Bridge steel bridge company represents Canadian industry's golden age. On the other hand, since an urban farm will be located on the south of the site, the entire building roof area can be considered for PV panels installation, as the green spaces requirements of the municipally are already met. The 3D building geometry of the case study is generated in the Rhinoceros3D software with a total floor area of 277,000 sqm. The model consists of six building blocks with different heights and floor areas. Table 2-3 indicates the buildings' geometrical characteristics.

Table 2-3 Case study buildings' geometrical characteristics.

Building ID	Floor Area (sqm)	No. of Floors	Total floor area	Total surface area
Building A	13637	9	122737	25673
Building B	5174	6	31044	7434
Building C	5469	9	49224	12033
Building D	7882	6	47292	7266
Building E	5890	2	11782	2702
Building F	1690	9	15210	5166

The buildings are mixed-use with residential, commercial, civic center, and school use-types. In this massing model, 90 % of the total area is considered for residential buildings and 10% for the rest of the buildings. The offices and retails are considered on the buildings' ground floor to make this design respond to eco-district policies. The area of the office and retails are around 9500 sqm.

New zoning is proposed for the Lachine-Est area in which buildings with distinct shapes, sizes, and orientations and, therefore, different demand profiles are designed. Moreover, two options are considered for the energy systems: air source heat pump (ASHP) and ground source heat pump (GSHP). As a renewable source, an identical PV system, including a maximum power point tracker and inverter, will provide electricity in both cases. For each building, two energy systems will be selected separately regarding its demand profile to understand better and compare GSHP and ASHP performances.

26

Figure 2-5 a) Master plan of the Lachine East project. b) 3D model of the case study

The construction and architectural features and other thermal properties are assigned based on the building use-type. The definition of the building use-types in this model is not precisely the same as DOE building use-types. Therefore, the closest similarities between the DOE building use-types and real building use-types in the Lachine district are shown in Table 2-4:

Table 2-4 Matching building use-types in DOE with the case study buildings' use-types.

Lachine building use type	DOE building use-types
Civic center	Large office
School	Secondary School
Commercial	Large Office
Residential	Midrise Apartment
Office	Small Office

Regarding modeling borehole temperatures to compare GSHP and ASHP, the correlation between borehole temperature and outdoor air temperature is assumed to be based on the values in Table 2-5.

Table 2-5 Borehole and outdoor air temperature correlation.

Borehole Temp °C	-5	-4.2	-3.9	-3	-2	-1.1	1.7	4.4	7.2	10
Outdoor Air Temp °C	-30	-25	-15	-10	-5	0	5	10	20	30

2-5- Results and Discussion

The developed UBEM model was used to simulate the energy consumption of the Lachine East project based on the assumptions listed in Table 2-1. The monthly heating and cooling demand were estimated at the building and district levels. The specific energy demand is shown in
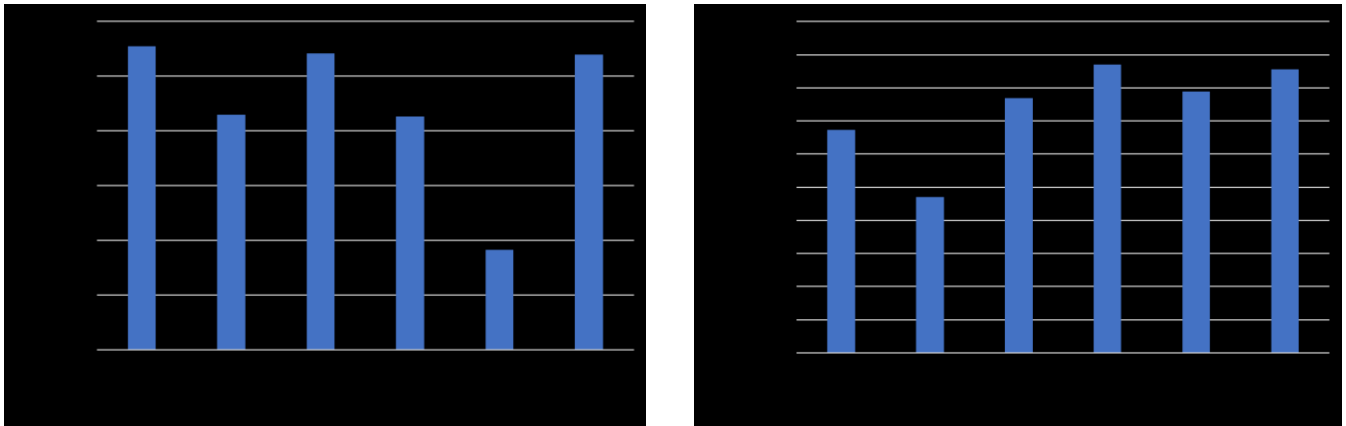
Figure 2-6 a) Specific cooling demand (kWh/sqm/year). b) Specific heating demand (kWh/sqm/year).

Figure 2-6. According to Figure 6a, the different cooling and heating demand for each building is influenced by the surface area to volume ratio of buildings, which changes solar gain and ventilation. The solar gain through the glazing and wall surface and ventilation have a different effect on building energy demand. Increasing the solar gain increases the cooling demand while increasing the ventilation can prevent heat trapped in the buildings and consequently decrease the cooling demand. Figure 2-6a shows that building A has the highest specific cooling demand. Figure 2-6b indicates that the building D and F have the highest specific heating demand, respectively.

Figure 2-7 shows the simulated monthly cooling and heating demand of the buildings. The figure reveals that the cooling load peak is mainly in July, while the heating load peak is between December and January. Building C and D's heating load, and building B, E, and F follow a similar trend, with a slight difference. Building A shows the highest monthly cooling and heating load in a whole year.

The annual district heating and cooling demands are 20 and 7 GWh, respectively. The district's predicted heating and cooling loads are used to calculate the energy system performance using UESM.

UESM results for both energy system scenarios are summarized in Table 2-6. As mentioned before, energy systems are selected to be compatible with low-temperature heating systems with high efficiency. In each scenario, two types of HPs (ASHP and GSHP) were considered to provide heating and cooling demands. HP sizes were selected regarding two criteria, seasonal COPs and demand, and to have a reasonable comparison between two HP types, a 70-ton (245 kW) HP model
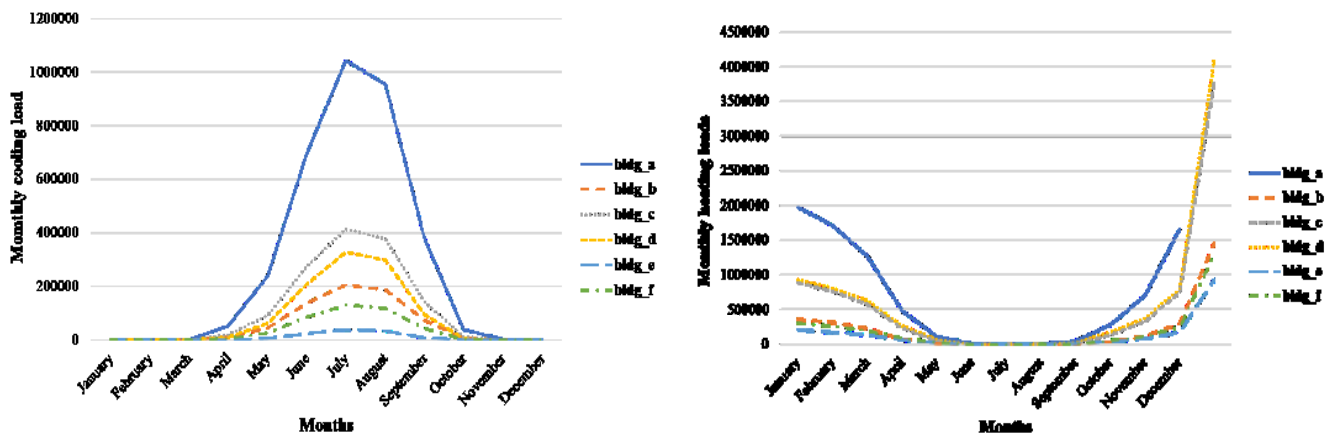
Figure 2-7 a) Monthly cooling loads (kWh). b) Monthly heating loads (kWh).

is selected for each HP type. HPs are modeled using thorough performance documentation provided by manufacturers (Maritime Geothermal 2018)(Trane 2015). Performance data of the chosen ASHP and GSHPs are shown in Table 2-7 and Table 2-8. This data is used to simulate the HP performance in each time step and condition precisely.

Table 2-6 UESM results. Air source and ground source HPs, energy metering, and PV system output for each building.

6 Large scale buildings	Building A		Building B		Building C		Building D		Building E		Building F	
HP Type	GS	AS	GS	AS	GS	AS	GS	AS	GS	AS	GS	AS
Heating SCOP	3.28	3.12	3.28	3.13	3.32	3.21	3.30	3.15	3.40	3.39	3.43	3.44
Cooling SCOP	5.63	5.05	5.66	5.04	5.64	5.05	5.63	5.05	5.59	5.05	5.68	5.05
Elec. Demand (kWh/yr)	3,452	3,783	780	899	1,711	1,903	1,686	1,867	542	637	803	931
PV Generation (MWh/yr)	1,836		673		724		899		752		205	
PV Self-Consumption ratio	0.50	0.53	0.38	0.42	0.60	0.63	0.48	0.51	0.26	0.30	0.83	0.88
Number of Panels	4,347		1,593		1,716		2,130		1,782		486	
Number of HPs (Heating)	30	25	6	5	14	11	14	12	3	3	5	4
Number of HPs (Cooling)	20	16	5	4	9	7	8	6	2	2	3	3
Cooling Temp (C)	12	11	12	11	12	11	12	11	12	11	12	11
Heating Temp (C)	40	40	40	40	40	40	40	40	40	40	40	40
PV Gen./ Elec. Demand	0.53	0.49	0.86	0.75	0.42	0.38	0.53	0.48	1.39	1.18	0.26	0.22

In the present study, due to the sizeable conditioned floor area of the buildings and limited space for PV panels as the only local renewable power generation system, not reaching energy positivity is a foreseeable outcome. The UESM result backed the claim above that low roof area to total floor area ratio plays a vital role in getting closer to energy-positive districts. Figure 2-8shows that except for Building E, which has the smallest total floor area among all buildings, the AC electricity generated by PV is insufficient for covering HP's electricity demand. The higher the floor number in a building, the smaller the relative contribution of roof PV generation to the buildings' energy consumption.
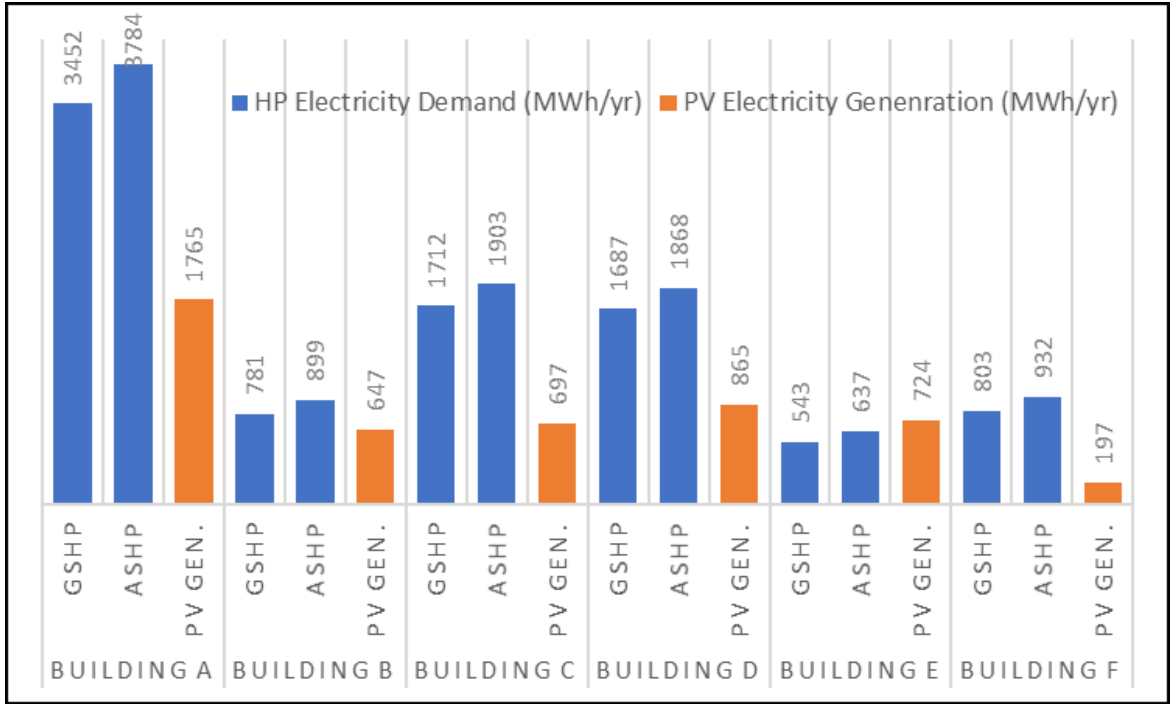
Figure 2-8 HP total electricity demand vs. AC electricity generated by on-site PV system.

For the HP system, in most time steps the number of operating HPs, consequently, the HPs heat generated is greater than the demand values, as it was designed for maximum load conditions. Thus, the system is not optimized regarding cost or energy efficiency on the system level, as the paper's focus is on introducing an automatized simulation workflow merely.

Table 2-7 W900 GSHP heating performance (Maritime Geothermal 2018).

Supply Temp (°C)	Source Temp (Borehole) (°C)	Electrical Consumption (kW)	COP
40	-3.9	56.63	3.04
40	-1.1	57.28	3.36
40	1.7	57.98	3.66
40	4.4	58.64	3.95
40	7.2	59.14	4.22
40	10	59.47	4.51
40	12.8	60.18	4.74
40	15.6	59.95	5.03

Table 2-8 CMAA 070 ASHP heating performance (Trane 2015).

Supply Temp (°C)	Source Temp (Outdoor Air) (°C)	Electrical Consumption (kW)	COP
40	-30	100.2	2.00
40	-25	97.4	2.05
40	-5	70.2	3.01
40	0	70.1	3.43
40	7	69.9	4.09
40	10	69.8	4.42
40	15	69.8	5.01
40	25	69	4.64

Although the result of case studies are not necessarily comparable or interchangeably usable for result validation, the study by (Xu et al. 2020), due to the similarity of context, is interesting. They studied a 108-ton air source HP system in China's severe cold region (similar weather to Montreal) with a supply temperature of 36 °C. They calculated HP's COP and electricity demand to be 3.2 and 10.65 kWh/m2yr, respectively, compared to 3.24 and 22.12 kWh/m2yr in this study. It should be noted that the difference in HP annual electricity demand is entirely compatible with the difference in the heating energy demand of both studies (34.10 and 72 kWh/m2).

Energy-related parameters should be investigated carefully to identify any possible barriers to achieving higher energy efficiency. Parameters such as heating and cooling SCOPs, HPs electricity demand, electricity to/ from grid, and PV self-consumption ratios are considered key performance indicators to UESM. Moreover, in some cases, there might be a restriction that can affect the whole design concept. For instance, having an upper limit for electricity exporting to the grid can be interpreted as a definite need for adding battery storage.

There are some pros and cons associated with each choice in a more focused comparison between two types of HPs. Since the GSHPs heat is mostly provided by boreholes, wells, lakes, or underground water, a GSHP typically has higher source temperature levels than ASHPs. The latter depend on outdoor air temperature, which can be as harsh as -30 °C under Canadian conditions. As a result, ASHP needs a significantly higher compression ratio to transfer heat from the outdoor air to the condenser, especially in cold climates such as the case study location, leading to higher electricity consumption and lower COP than GSHPs. The technology improvements and

innovations should not be taken for granted as a few years ago, ASHPs could only work down to -8 °C, and using ASHPs in cold climates was not a standard option.

ASHPs are generally more sophisticated equipment, with more power and costlier. On the other hand, there are costs associated with GSHPs such as drilling, piping, heat exchanger, or pumps, which might change the balance of cost between two systems. The number of ASHPs and GSHPs required in different buildings shows that the lower number of equipment can be counted toward ASHP systems' advantage.

2-6- Challenges

Developing an integrated UBEM and UESM is a challenge due to the difference in their spatial and temporal input, output, and calculation process resolution. The developed UBEM model was designed to be highly flexible in terms of its temporal and spatial input and output resolution. This flexibility gives the capability to the UBEM to provide suitable input in any temporal and spatial resolution for UESM. As the proposed UESM requires hourly heating and cooling demand for each thermal zone and the whole district, the UBEM can correctly provide these inputs. The resolution of the UBEM heating and cooling demand results can spatially alter the fine-grained resolution, such as in thermal zones scale, to the low resolution of an entire building or a whole district. The temporal resolution can change between yearly to sub-hourly resolution. Although the proposed UBEM uses archetypes for some input parameters, analyzing the heating and cooling demand of UBEM was correlated to the real geometry, building total floor area, and building use-type of the district Lachine. On the other hand, using highly accurate and the same building geometry resolution for renewable potential calculations, the combined UBEM and UESM can calculate the heating and cooling demand and size of different energy systems in any spatial and temporal resolution.

In the current case study, compact, rectangular-shaped buildings with high thermal insulation levels are an excellent start, but not enough toward having a positive energy district. Even though there are always site limits that constrain architects and urban planners' abilities, changing some buildings' orientation so that the longer side faces south could have a significant impact on decreasing the heating demands. Also, in projects with large areas, it can be good practice for implementing innovative ideas like dedicating areas to small urban farms on the site, which

reduces food-related transportation energy demands. The residue could be used as an input for biofuel production.

From the energy efficiency point of view and considering the proposed geometry's size and scale, reaching the zero-energy goal with local photovoltaics sounds unattainable, let alone positive energy. Using 65% of the roof area for PV installation and using HPs with high-efficiency ratings are the only measures put into the design process. Although this paper's focus differs from optimization or defining a more detailed energy system design process, a number of improvements out of many are discussed. For instance, adding thermal storage could be beneficial for the system due to the excessive heat generated in each time step (referring to HP section), which lowers the number of HPs required for meeting demands in subsequent hours and, consequently, the HPs electricity demand. Moreover, properly sized battery storage improves the PV self-consumption ratios. It helps the system to meet the upper limit for electricity export to the grid, if there are any. A cost-benefit analysis of the system would be essential for the system, knowing the high cost of batteries and thermal storage systems.

Regarding the energy systems design, using lower heating temperature for heating (40 °C) instead of conventional values of up to 60 °C or higher is a smart choice that not only can meet the expectations but also increases both energy and exergy efficiencies and lowers heat losses. Adding heat-recovery equipment in the ventilation process could be a significant improvement for lowering heating and cooling demands and associated electricity consumption. The other point that could not go unnoticed is the HP system sizing that needs improvement. Other than sizing based on the maximum demand, a lower percentile like 98% could be a smarter choice. It means that the system is currently sized for 100% of a year's hours and results in the system oversizing for 8585 hours of a year. By designing for lower percentiles, which can be done in either the demand calculation step (UBEM) or limiting the number of HPs (UESM), considerable savings can be achieved.

2-7- Conclusion

Decarbonization of the urban area acquires the maximum renewable energy and considers the energy demand reduction measures. This work described a novel workflow integrating an urban building energy simulation module accompanied by an urban energy system simulation model.

Combining the UBEM and UESM models allows this opportunity to dynamically predict the district energy demand, calculate the renewable energy systems capacity, and sizing energy systems. To have a compatible UBEM and UESM, the UBEM is designed to be highly flexible capable of calculating the heating and cooling demand in any spatial and temporal resolution. The developed model was tested on a case study, a future district in Montreal, Canada. The heating and cooling demand were simulated at the building and district levels and used as input to the UESM model to size the energy systems. It was shown that reaching the zero-carbon goals requires applying stricter constraints on design parameters. Moreover, owners, planners, and designers ought to illustrate realistic goals for each project. For instance, in the Lachine-East case study, considering the buildings' size and scale made reaching carbon neutrality on a local scale almost impossible given the available renewable resources. Nevertheless, implementing some green and sustainable design strategies could mitigate climate impact and GHG emissions. It is of great importance to distinguish between the PV self-consumption ratio and the net value of HPs' electricity demand covered by local PV production. Table 2-6 and Figure 2-8 show that in small buildings like Building E, local PV produces 75 to 100% of the HP electricity demand, while this value for larger buildings like Building C can be as low as 38%. The proposed integrated workflow promotes advantages including, but not limited to, accurate demand calculations in complex geometries from building scale to urban areas, autonomous PV system sizing and PV potential calculation, HPs system sizing, and energy metering. However, adding a feedback loop in the sense that makes the workflow dynamically update and optimize the demand calculation parameters will bring a much more efficient and sustainable tool to the table.

Chapter 3: A New Modeling Approach for Low-Carbon District Energy System Planning[2]

Authors' Contribution

This chapter is published in Energies journal and it is shaped around the energy system sizing capability of the proposed framework in this thesis. As in previous chapter, heating and cooling demands are available through the contribution of co-authors. Heat pump system is modeled for both ground source and air source systems and based on the demand profiles, the proposed workflow, calculates seasonal coefficient of performance and generates demand and supply curves. Also, Automated PV potential calculation gives the renewable electricity penetration of the system. Like the previous chapter, the idea, concept, methodology and resutls shown in this chapters are extracted from the proposed framework. The thesis author is the second name author of this publication.

3-1- Introduction

With the dramatic increase in the world's population during the last two centuries, the energy demand has also increased. The U.S. energy information administration reported that the contribution of heating and cooling of buildings to the total energy consumption is 40%, which mostly depends on fossil fuels ("Energy Technology Perspectives 2017 Catalysing Energy Technology Transformations INTERNATIONAL ENERGY AGENCY" 2017). Utilizing renewable energy resources leads to the decrement in the consumption of fossil fuels and, thus, the related emissions. Facing climate change, the general attitude toward energy consumption is to lower it and also to reduce the emission of greenhouse gases. For example, the European Council decided to reduce the EU's energy consumption by 32.5% in 2030 compared to 1990 levels by increasing the energy efficiency (European Commission 2020). Integrating renewable energy resources with different energy systems is one of the leading solutions for changing energy production systems (H. Lund et al. 2010; P. A. Østergaard and Lund 2011).

---

[2] This chapter is published in "Energies" journal special issue "Municipal Energy System Planning: New Approaches, Applications, and Future Research Needs" entitled "A New Modeling Approach for Low-Carbon District Energy System Planning"

Ground-source heat pumps (GSHP) use the renewable energy stored in the ground to provide heating, cooling, and domestic hot water in a clean and energy-efficient way for various buildings. Since the ground environment provides a higher temperature for heating and a lower temperature for cooling, GSHP systems' efficiency is higher than the conventional heating and cooling systems. The electricity demand for driving the GSHP could be supplied by renewable sources (Mustafa Omer 2008; Sarbu and Sebarchievici 2014).

GSHP systems can provide heating and cooling for a single building or can be used in a district heating system to respond to a set of buildings' energy demand. District heating systems supply the energy demand of either a single building, for instance, a mall or an industrial building, or a district in a city. These systems are in service in several cities, including New York, Moscow, Vienna, etc. Four generations have already been introduced: (1) first-generation systems (1880-1930) use steam boilers with coal as the fuel and steam as heat carrier, (2) second-generation systems (1930-1980) use pressurized hot water with temperatures more than 100 °C as heat carrier, (3) third generation systems (1980-2020) use large-scale combined heat and power (CHP) systems and also pressurized hot water, with a temperature lower than 100 °C, and (4) fourth-generation systems (2020-2050) use low-temperature water as a thermal carrier and renewable energy sources (Lake, Rezaie, and Beyerlein 2017; Henrik Lund et al. 2014).

A district energy system comprises supply units, distribution networks and sub-networks, and demand or users. A distribution network is required for delivering cooling, heating, and hot water demand through a pipeline network to a district (Vesaoja et al. 2014; Brange, Englund, and Lauenburg 2016; Di Pietra, Zanghirella, and Puglisi 2015). Having a network with long distances ultimately leads to heat losses and pressure drops affecting the overall performance of the heating system (Çomakli, Yüksel, and Çomakli 2004).

Heat losses through the distribution network play a significant role in designing an optimal district heating system. Thus, researchers have focused on the optimal simulation of distribution networks. Larsen et al. (Larsen et al. 2002) presented a simple model for district heating networks simulation by reducing the physical complexity of such systems. They used a network which was equivalent to the original one but with fewer branches. In other words, they removed some of the internal nodes. Furthermore, a paper focusing on the dynamic characteristic of district heating networks was published presenting a model for calculating the lag time and the attenuation degree

of a system. Hassine and Eicker (Ben Hassine and Eicker 2013) proposed a cooling and heating network model, employing a graph-theoretical method and the Newton algorithm for solving the equations. Flow and pressure equations were solved statically in their work, while the temperature field has been calculated dynamically.

In addition to the losses within the distribution network, predicting consumers' energy consumption (energy demand of end-users) plays a remarkable role in designing efficient energy systems. Therefore, researchers have widely focused on this issue by considering various influential parameters. The end-user's demands are chiefly related to three factors: (1) physical and environmental features of buildings, (2) the behavior of the occupants, and (3) uncertainty factors (Talebi et al. 2016). Dotzauer (Dotzauer 2002) developed a simple model for predicting heat demand in a district energy system, based on the outdoor air temperature and the behavior pattern of consumers. In 2015, Monsalvete et al. (Monsalvete, Robinson, and Eicker 2015) presented a modular dynamic model for predicting the energy demands of cities. Moreover, recently, a method for predicting the end-user's consumption pattern was proposed (Calikus et al. 2019). Their methodology is based on the distinction of the users' profiles by finding deviating profiles from the typical ones using clustering. Another method on the basis of the available mass flow and temperature data from the smart meters was also presented (Guelpa, Marincioni, and Verda 2019). In addition to its high accuracy and low computational cost, the method is suitable for districts with a large number of buildings. That being said, providing an automated solution for energy demand calculation and energy system design, is of great importance.

Following many cities' sustainability goals, the share of using renewable energy, especially in district heating, is growing (R. Lund et al. 2017). Besides environmental aspects, the economic feasibility of energy systems is a crucial factor (Hennessy et al. 2018). Tanguay (Tanguay 2016) analyzed the economic performance of residential GSHP in North America's market. The study includes comparing equipment and energy costs in four provinces: Quebec, Manitoba, British Colombia, and Ontario. Results show that the average cost of GSHP for residential buildings in Quebec is 164 $ per square meter of surface area. Aditya et al. (Aditya et al. 2020) conducted a cost comparison of using GSHP compared to other technologies. An essential parameter in this study is the climate. Montreal, London, Singapore, and seven Austrian cities were chosen as case studies to show the effect of climate. A two-bedroom residential building was chosen as a case

study and modeled in different cities. Results show that due to high heating demand in Montreal, and its low electricity costs, the city ranks as the cheapest city for GSHP installation among other nine case studies (Aditya et al. 2020). Furthermore, a comparison between Levelized Cost of Energy (LCOE) and Energy System Analysis (ESA) method was made for decentralized heating and district heating systems (Hansen 2019). Both methods show similar ranking results for district heating networks, whereas results of decentralized heating systems vary.

Centralized district heating and distributed renewable energy systems are widely studied during the past years. Dolla Rosa et al. (Dalla Rosa and Christensen 2011) studied the effect of human behavior on load patterns in a low-temperature district heating. They also carried out a socio-economic comparison between district heating and distributed GSHP for a low heat density area. They showed that the low-energy district heating's levelized cost of energy is competitive with the GSHP-based scenario for low heat density areas. Moreover, according to this study, the optimal design of the network is of utmost importance since an optimal design decreases the average pipe size required, reducing the costs. Rämä and Mohammadi (Dalla Rosa and Christensen 2011) studied centralized and distributed solar collectors in an existing district heating system. The showed that both scenarios are feasible; however, integrating renewable energy with a district heating system has higher economic feasibility than the distributed one. Although many works have been done in the field of renewable District heating and cooling network in urban areas, there is still a gap in integrating building energy modeling with energy system sizing and energy distribution network design. In this paper, a novel methodology integrating these 3 modules and automatizing the whole process have been presented. The current study is based on the Dominion Bridge area in Lachine-Est in Montreal, Canada. Figure 3-1 shows the location of the case study and the newly proposed designs. Developers intend to design an eco-quartier with an energy-efficient and cost-effective energy system.

Two scenarios have been considered for the energy system of the mentioned area. Both scenarios share the same sets of buildings with the same characteristics, schedule, usage, and material. In the first scenario, a decentral energy system comprised of GSHP provides heating and cooling demands for each building, while in the second scenario, a district heating and cooling system has been designed. Automatic urban building energy modeling (AUBEM) was used to calculate the energy demand of buildings. Then, a model was prepared in the INSEL simulation

environment and implemented to design the energy systems for both scenarios. This model provides heat pump capacity and the number of required HPs, the number of PV panels, and AC electricity generation potential using PV. After designing the piping system and calculation of the heat losses for the centralized scenario, an economic assessment was carried out to choose the most cost-effective energy system scenario for the studied area.

Figure 3-1 The case study area: (a) and (b) The location of the Lachine-Est quartier in the former Dominion Bridge Area; (c) bird view of buildings distribution in the newly proposed design.

3-2- Methodology

3-2-1- Automatic urban building energy modeling (AUBEM)

One way to store the detailed geometrical information of buildings to be readable by computer programming is to structure the data into the City Geography Markup Language (CtiyGML) format (Gröger et al. 2008). CityGML is a text-based format similar to the XML format, which uses the hierarchal structure to store objects and attributes related to buildings. Since CityGML is readable using Python programming language, a CityGML file of the new design is used in the present study. In the current study, the term automatic UBEM refers to our software workflow that carries out the whole process of 3D building modeling for the energy demand analysis and the entire process of energy system modeling in an automatic manner. A Python code was written to perform the following tasks:

- Extracting the building coordinates and building characteristics (building use-type, year of construction, etc.) from CityGML format.

- Merging the building surface coordinates with their related characteristics in the same list and organize the data to be suitable for energy simulation soft-ware.

- Assigning the building materials and constructions to each surface based on building use-types and surface types, whether they are walls, roof surfaces, or ground surfaces.

- Reading and organizing the occupancy, electrical equipment, lighting, and ventilation schedule and assigning them to each building based on building usage.

- Feeding the data into EnergyPlus (U.S. Department of Energy 2020) for energy demand calculation.

Figure 3-2 shows the AUBEM system workflow. The CityGML is parsed through Python to extract each building's ID and their related information and organizing them with regards to a hierarchical structure to be callable in the next steps. The hierarchical structure starts with building IDs as a root, followed by the building use type and then their surface information as a subcategory. This hierarchical structure paves the way for accessing detailed building geometry and attributes information in the next steps for each building.

41
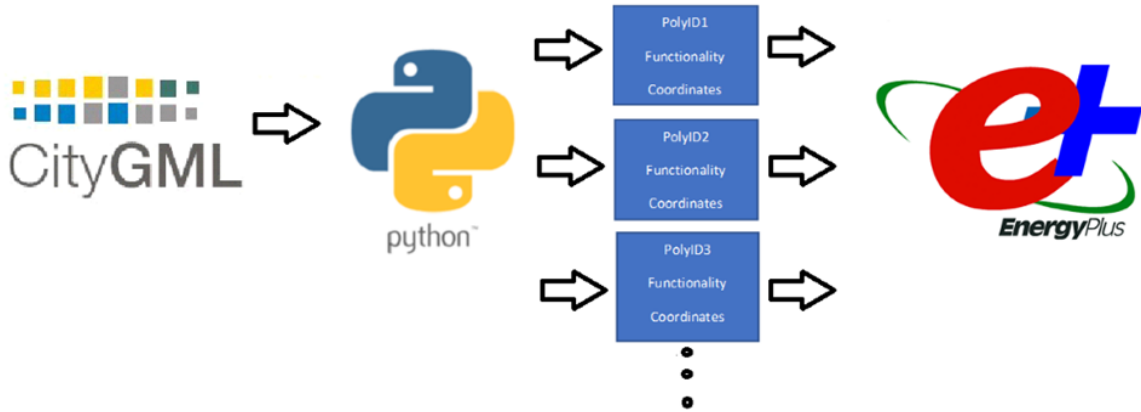
Figure 3-2 Automatic Urban Building Energy Modeling System.

EnergyPlus is a physics-based model that captures the full dynamic of the building performance to provide a detailed analysis of buildings (U.S. Department of Energy 2020). Due to the enough flexibility and accuracy of EnergyPlus, it is used for building energy demand calculations.

EnergyPlus first defines the building zones and then creates 3D building models. Building IDs are used for naming the zones. It is necessary to assign each building's sur-face to its related building zones. Therefore, each surface has its zone name which is de-fined based on the building ID and should be defined automatically before adding the surface coordinates into EnergyPlus.

The building materials and constructions are extracted from the National Renewable Energy Laboratory (NREL) website (NREL 2018) and stored in a JSON format. The JSON format is parsed, and the building constructions and materials are categorized based on the building use-type, and stored in a Python dictionary, and named as NREL building construction archetypes. The building construction archetypes are assigned to each building's surface based on the building use-type. Building use-types are extracted from CityGML. On the other hand, the occupancy, electrical equipment, lighting, and ventilation sched-ules are extracted from the Department of Energy (DOE) building archetypes website (DOE 2020) for a large office, secondary school, small office, and midrise apartment buildings. Since DOE has limited building archetypes, we had to consider the most similar building archetype for each building use-type in the Lachine district. The large office archetype is considered for the Civic Center building type, the secondary school for school,

the large office for a commercial, the midrise apartment for a residential, and the small office for office.

The extracted archetypes are stored in a text file and are read through Python to be as-signed to each building. In the last step, each surface with all their related information along with the building occupancy, electrical equipment, lighting, and ventilation sched-ules are fed to the EnergyPlus to calculate the heating and cooling demands. EnergyPlus positions the surfaces in their specific location and connects them to form a 3D building urban model. Other parameters used in the EnergyPlus model are summarized in Table 3-1. Moreover, the building surfaces are categorized into three groups of walls, roof surfaces, and ground surfaces, and their related archetypes are assigned to each group accordingly. The other required parameters for having an accurate building energy demand calculation such as occupancy, electrical equipment, lighting, and ventilation schedules are changing dynamically based on building use-types, and all are assigned to each building automatically. Occupancy, electrical equipment, lighting, and infiltration values are collected from (Kim et al. 2013)(Wilkins, C.; Hosni 2011)(Signelković et al. 2016)

Table 3-1 EnergyPlus setting parameters for Urban Building Energy Modeling.

Parameters	Settings	
Window to wall ratio	0.35	
Constant heating set point	22 ℃	
Constant cooling set point	25 ℃	
HVAC Templates	Ideal loads air system	
Solar distribution	Full interior and exterior	
	Calculation method	**Average over days in frequency**
	Calculation frequency	Every 20 days
Shading calculation	Maximum figures in shadow overlap calculations	15000
	Polygon clipping algorithm	SutherlandHodgman
	Sky diffuse modeling algorithm	Simple sky diffuse modeling
	External shading calculation method	Internal calculation
Surface convection algorithm: inside	TARP	
Surface convection algorithm: outside	DOE-2	
Heat balance algorithm	Conduction transfer function	
Sizing period: design day	Winter design day Summer design day	
Solar model indicator	ASHRAE clear sky	

Occupancy	**Number of the people calculation method**	**People/Area**
	People per zone floor area	0.05 people/m2
Lighting	**Design level calculation method**	**Watts/Area**
	Watts per zone floor area	10W/m2
Equipment	**Design level calculation method**	**Watts/Area**
	Watts per zone floor area	5 W/m2
Infiltration	**Design flow rate calculation method**	**Residential: Flow/ExteriorArea and Commercial: Flow/ExteriorWall Area**
	Flow per exterior surface area	Residential: 0.0002 m3/s-m2 Commercial: 0.0005 m3/s-m2
HVAC	**Outdoor air method**	**Flow/Area**
	Outdoor airflow rate per zone floor area	0.00043 m3/s-m2

3-3- Energy System Model

A model for designing an energy system is prepared using INSEL 8.2. INSEL (Integrated Simulation Environment Language) is a simulation environment using a flexible graphical programming language comprised of ready to use blocks. Moreover, new extensions or completely user-defined blocks can also be added and used. INSEL's main functionalities are meteorology, building modeling, and renewable energy systems modeling (Weiler, Stave, and Eicker 2019; Eicker, Weiler, et al. 2020). The proposed energy system model gets hourly energy demand for both cooling and heating, the geometry of building (Roof dimension exclusively) and temperature as input and provides heat pump capacity and the number of required HPs to best fit the demand curve, the number of PV panels and AC electricity generation potential using PV.

The complete energy system model (ESM) includes different parts and features. However, in this study, only the heat pump section and the PV system will be discussed briefly. The ESM workflow starts with obtaining and analyzing heating and cooling de-mand and ends with various results, including energy consumption, system's coefficient of performance (COP), PV self-consumption, equipment selection, and the rest. The summary of related parts to the scope of this paper is shown in Figure 3-3.
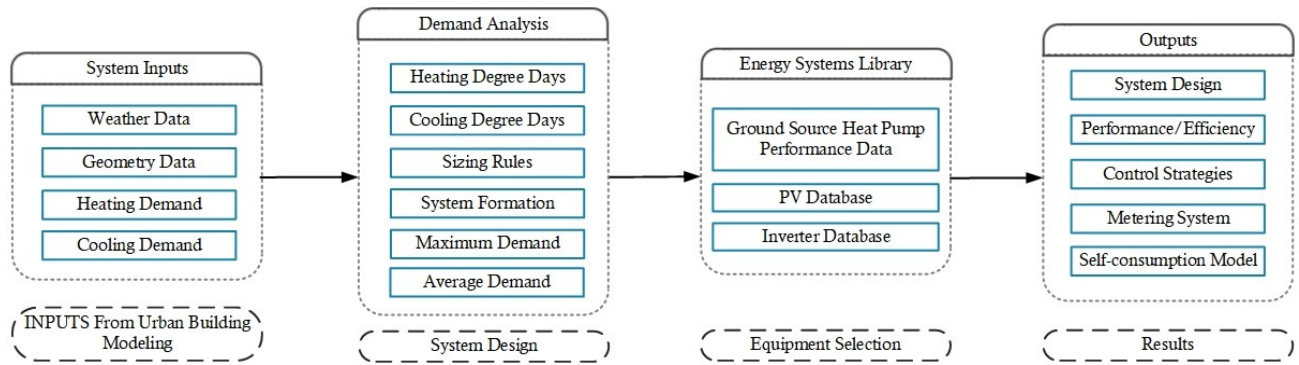
Figure 3-3 Energy System Model Workflow.

3-3-1-Heat Pump Model

The most common HP performance indicator is COP, a unitless parameter that can be interpreted as the thermal energy transferred by the HP to the HP electricity consumption. Since a heat pump COP is highly dependent on heat source and heat sink temperatures COP fluctuations during different conditions should be taken into consideration. In the case of GSHP, the heat transfer fluid temperature leaving boreholes and going to the building is used as a heat source input to the HP.

Based on HP manufacturers' performance data, a correlation between HP energy generation, electricity consumption, sink, and source temperature can be found. Usually, reversible HPs' COP is higher than 1.0 due to the fact that they transfer heat from a heat source to a heat sink. That being said, by referring to the Carnot theorem (theoretical highest efficiency of an HP), it can be seen that by lowering the supply temperature or increasing the boreholes return temperature, higher COPs can be achieved. In our case study, 40 °C and 12 °C are used in calculations for heating and cooling supply temperatures, respectively, which are consistent with the low-temperature heating/cooling concept.

In addition to improving COP, lower heating supply temperature will lower heat losses in piping and storage and enables the heating system to achieve higher exergies. These values have been studied and investigated for low temperature and ultra-low temperature district heating (DH) systems (Henrik Lund et al. 2014; D. S. Østergaard and Svendsen 2016; Yang and Svendsen 2018; Brand and Svendsen 2013). Although 40 °C is sufficient for providing domestic hot water (directly or with supplementary heating) (Lee 2018), the focus of the study is merely on heating and cooling demand and the electricity consumption of HPs covering demand.

45

Previously, Weiler et al. (Weiler, Stave, and Eicker 2019) proposed a model for an Air Source Heat Pump (ASHP), which uses a polynomial fit to the manufacturer's data. In this study, the same approach is used and further developed for GSHP. In this method, two out of three HP parameters, including COP, electricity consumption, and heat output, are defined as a function of supply temperature and heat source temperature (boreholes to HP), based on HP performance data manufacturers provide. Table 3-2 is extracted from Maritime Geothermal Ltd. W series GSHP catalogue (Maritime Geothermal 2018), which shows the W900 70-ton HP's electrical consumption and COP for constant supply temperature (heating) but various source temperatures. As a result, HP output heat can be determined, which will then be used to calculate the number of HPs required to cover the demand in each time step (1 hour).

Table 3-2 Maritime Geothermal Ltd. W900 model GSHP performance data (Maritime Geothermal 2018).

Supply Temp (°C)	Source Temp (Borehole) (°C)	Electrical Consumption (kW)	COP
40	-3.9	56.63	3.04
40	-1.1	57.28	3.36
40	1.7	57.98	3.66
40	4.4	58.64	3.95
40	7.2	59.14	4.22
40	10	59.47	4.51
40	12.8	60.18	4.74
40	15.6	59.95	5.03

3-3-2- Hourly Analysis and PV System

As mentioned before, the ESM receives hourly demand data from urban building modeling. After preprocessing the load curves, some statistical analysis, including maximum demand, average demand (Non-zero values), heating and cooling degree days, and different percentiles will be calculated. Based on these data, the model will select a heat pump capacity among available HPs in the energy library, which matches the building load curve best.

In each time step (1 hour), ESM takes heating and cooling demand (kW) as well as outdoor temperature (°C) and solar irradiation from an input file. INSEL energy systems' library offers a comprehensive list of PV panels and inverters with various specifications and manufacturers, from

which a 300 W panel with 17.24% efficiency and an appropriate inverter were selected. INSEL's available blocks were used to calculate direct and diffused solar radiation on a 31 degrees tilted panels facing south to feed the PV block. a maximum power point tracker was added to ensure the system's optimum output. Finally, DC/AC electricity generation of PV system was used to cover HPs' electricity demand and the excessive portion will be exported to the grid.

3-4-   Hydraulic and Thermal Modeling of the Distribution Network

As mentioned before, it is crucial to study the hydraulic and thermal behavior of the distribution network to understand the effects of the heat losses and pressure drops on the energy
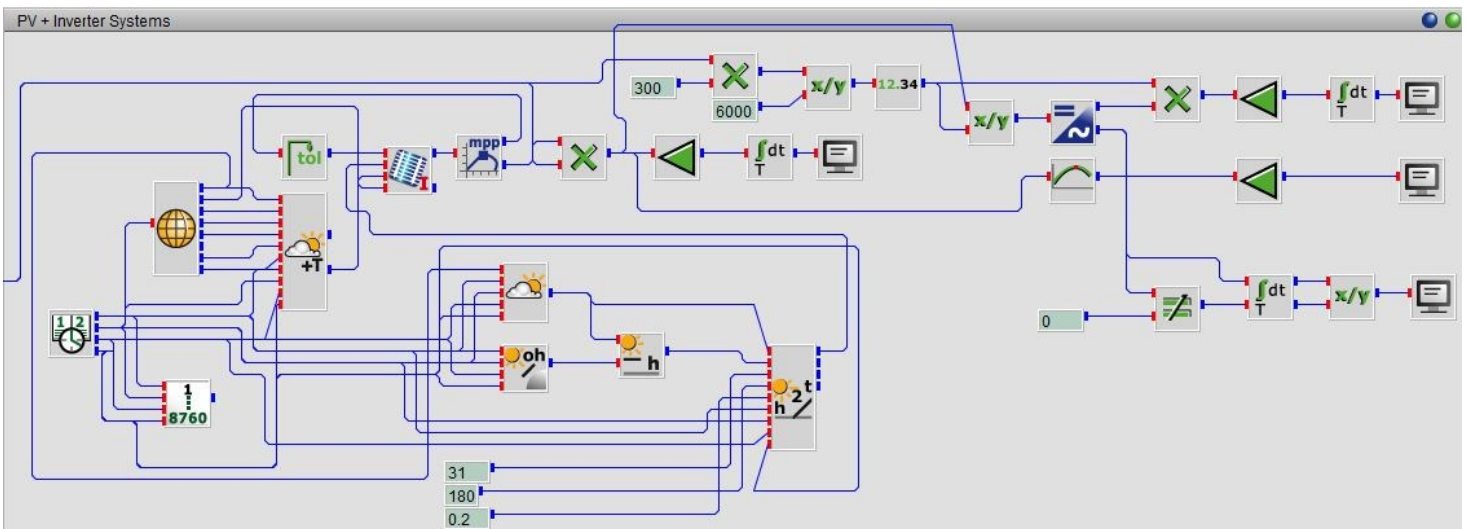
Figure 3-4 A screenshot from PV system modeled in INSEL, including weather block, PV panels. inverter and MPPT.

system. To do so, at first, a distribution network for supply and return pipes was designed. Figure 3-5 shows the configuration of the buildings and the designed network system for heating and cooling, supply, and return lines. A MATLAB code was then developed based on the graph theory to introduce the geometry to the code. Finally, the proper form of the related equation is derived and solved to obtain the network's mass flow rate and temperature levels.
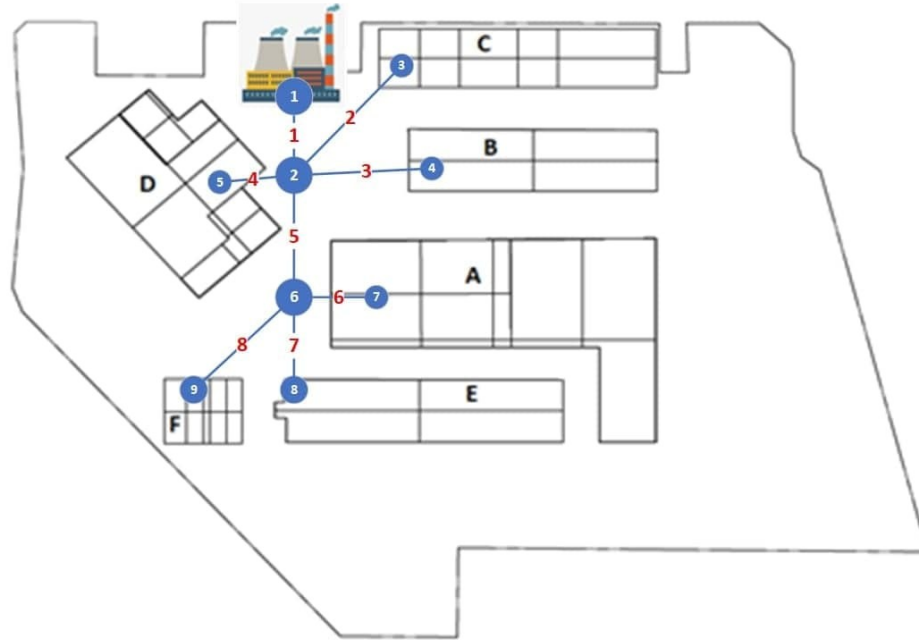
Figure 3-5 Configuration of the buildings in the newly designed geometry and designed supply and return network for heating and cooling.

3-4-1- Network Modeling Using Graph Theory

A graph represents a set of connected objects by nodes and edges. In the context of the district heating network (DHN), edges are interpreted as pipes, and nodes demonstrate the junctions and the consumer stations. To be able to implement the concept of graphs in a mathematical model, an incident matrix A is defined which its elements are 0, +1, and -1. The Incident matrix shows the interconnection of the nodes and the edges. The rows and columns of the incident matrix represent the number of nodes and pipes, respectively. In the incidence matrix, +1 is assigned to the inlet node of a pipe, while -1 is assigned to the outlet node of the pipe. Therefore, 0 is assigned to the nodes that do not have any interaction with a specific pipe (Shakerin 2017). Incident matrix is the mathematical representation of the network's configuration, which can be combined with the conservation equations to calculate the mass flow rates, and temperature distribution in the network (equations 3-3 and 3-4).

3-4-2-Hydraulic Modeling

For a pipe in the network, connecting two junctions, the one-dimensional, steady-state momentum equation was derived as Equation (1) (Shakerin 2017).

$$P_{out} - P_{in} = -\dot{m}\left(\frac{1}{2}f\frac{8L\dot{m}}{D^5\rho^2\pi^2 g} + \frac{8\dot{m}}{D^4\rho^2\pi^2}\sum_k \beta_k\right) + \Delta P_{pump} \tag{3-1}$$

where P_{out} is the outlet pressure, P_{in} is the inlet pressure, g is the acceleration of the gravity, $\dot{m}$ is the mass flow rate in the specified pipe, f is the friction factor, L and D are the length and diameters of the specified pipe, respectively, and β is the total loss coefficient. Also, the associated equation for the calculation of the mass conservation could be derived. Equation (3-2) shows the simplified mass conservation equation (Shakerin 2017).

$$\sum_i \dot{m}_{out} - \sum_i \dot{m}_{in} = 0 \rightarrow \sum_i \dot{m}_i = \dot{m}_{ext} \tag{3-2}$$

where $\dot{m}_{ext}$ is the flow rate leaving each node. In consumer stations, $\dot{m}_{ext}$ is obtained by using the energy demand calculated in the previous sections ($\dot{m}_{ext} = \frac{Demand\ of\ the\ building}{c_p(T_{supply} - T_{return})}$). By employing the incident matrix, the above-mentioned equations will turn into the following forms (Shakerin 2017):

$$A \times \dot{m} = \dot{m}_{ext} \tag{3-3}$$

$$-A^T \times P = -\dot{m} \times C + \Delta P_{pump} \tag{3-4}$$

where C is $\frac{1}{2}f\frac{8L\dot{m}}{D^5\rho^2\pi^2 g} + \frac{8\dot{m}}{D^4\rho^2\pi^2}\sum_k \beta_k$. A MATLAB code was written to solve the above equations using the Newton algorithm to solve the system of non-linear equations.

2.3.3. Thermal Modeling

Once the mass flow rate in each pipe is determined, the mentioned code uses the one-dimensional energy conservation law (Equation (3-5)) to calculate the temperature level in each

node. The energy equation is discretized in time by Euler backward method. An upwind scheme translates the temperatures at the boundary to the node upstream (Shakerin 2017).

$$\frac{(\rho_i c_{p,i} T_i)^t - (\rho_i c_{p,i} T_i)^{t-\Delta t}}{\Delta t} \left(\sum_j \frac{S_j L_j}{2} \right) + \sum_j (\dot{m}_i c_{p,i} T_i)^t = - \sum_j \frac{L_j}{2} \tag{3-5}$$

where c_p is specific heat capacity, S is the area of the pipe, L is the length of the pipe, P is the perimeter of the pipe, and U is the global heat transfer coefficient. In order to calculate the pipe diameters, Equation (3-6) can be used (Shakerin 2017).

$$D = \sqrt{\frac{4\dot{m}}{\rho v \pi}}, \tag{3-6}$$

where v is the design velocity that should not exceed specific limits in order to avoid noise and damaging of pipes. Thus, the design velocity for the water system is considered to be 1.5 m/s for sizing calculations (Shakerin 2017)(The Engineering ToolBox 2017). Once the mass flow rate in each pipe is determined, the pipe sizing can be completed.

3-5-   Economic Assessment

Among various cost estimation methods, levelized cost of energy (LCOE) is a good indicator of the cost-effectiveness of renewable energy systems. The LCOE of both scenarios is calculated to investigate the economic feasibility of central and decentral district heating and cooling systems in the current study. The LCOE is defined as the total lifetime cost of an investment divided by the cumulated generated energy by this investment. An alternative (but mathematically identical) approach is the definition by means of the net present value (NPV). The LCOE is the (average) internal price at which the energy is sold to achieve a zero NPV. The formula to calculate LCOE is shown in Equation (3-7).

$$LCOE = \frac{\sum_{t=1}^{n} \frac{I_t + M_t + F_t}{(1+r)^t}}{\sum_{t=1}^{n} \frac{E_t}{(1+r)^t}}$$ (3-7)

where I_t is investment expenditures in year t, M_t is operations and maintenance costs in year t, F_t is fuel expenditures in year t, E_t is energy generation in year t, r is interest rate, and n is lifetime of the technology.

As mentioned earlier, the location of the current study is in Montreal, Quebec. all the prices, including equipment and labor costs, are obtained from a local company named Marmott Energy, based on their previous large-scale projects. Table 3-3 includes the detailed costs of different items involved in the economic assessments.

Table 3-3 Costs of the items for economic assessment.

	Central Systen	Decentral System
Heat pump cost (CAD/ton)		$675
Drilling and filling of the borehole (CAD/m)		$18
Labor (CAD/ton)		$1470
Distribution network cost (CAD/m) *	$1020	-
Electricity cost (Cents/kWh)		8

* This value shows the cost of digging the trench, purchase, and installation of the pipes in there per each meter of the trench.

3-6- Results and Discussion

3-6-1- Demand Results

For the configuration of the buildings shown in Figure 3-5, the hourly heating demand is calculated. As mentioned above, different factors affect heating and cooling demands, such as building surface area, its application, location, etc.

Figure 3-6 shows the heating and cooling curves of the buildings in the area. Based on this figure, building A has the highest heating and cooling demand which is due to its heated surface area which is the largest of all the buildings.

To better analyze the results, Table 3-4 shows the maximum heating and cooling for each building throughout the year.

Table 3-4 Maximum heating and cooling loads for each building.

Building	A	B	C	D	E	F
Maximum Heating Load (MW)	5.161	0.999	2.331	2.411	0.516	0.785
Maximum Cooling Load (MW)	4.608	0.940	1.902	1.739	0.318	0.619
Tot. Floor Area (m^2)	136,136	31,056	54,693	39,410	11,798	16,908

Figure 3-6 shows that in specific periods (around 3000hr or 6500hr) there is a demand for both heating and cooling. Predefined heating and cooling and transitional seasons method can be implemented to avoid having heating and cooling demand at the same time, since this would not be feasible according to the high thermal inertia of the network. In this method, two specified periods are allocated to cooling and heating separately, and two other periods (one before autumn and one before spring) are defined as transitional seasons, which does not need heating or cooling. In this case, optic-variable walls (OVW) has high solar absorption during Winter and low solar absorption during summer and can be useful to provide thermal comfort during the transitional seasons (Wang, Zhu, and Guo 2019). However, in the current study, two separate distribution networks are considered for heating and cooling so that the heating and cooling thermal demand will be answered without causing problems. These calculated demands are the starting point for network analysis and energy system design. The following section discusses the energy system modeling results.

3-6-2- Energy System Results

ESM was used for each of the six buildings in the district plus the central district heating and cooling scenario. ESM results are summarized in Table 3-5. It is worth mentioning that supply temperatures for both heating and cooling are assumed to be constant, while fluid temperature leaving boreholes are dependent on the outdoor temperature. Moreover, ESM determines the number of HPs in each iteration that covers the maximum demand, and the required number of required HPs is added to the results. Also, HPs are considered to have single-stage compressors and either work with 100 percent capacity or zero. Besides calculating metered parameters like electricity to/from the grid, only HP electricity demand has been considered.

Table 3-5 ESM result summary for 7 cases.

Case \ Output	Building A	Building B	Building C	Building D	Building E	Building F	Central
Heating SCOP	3.29	3.29	3.33	3.30	3.41	3.44	3.27
Cooling SCOP	5.62	5.64	5.63	5.61	5.56	5.66	5.61
Tot. HP Electricity Demand (kWh/yr)	3,564,448	804,703	1,762,696	1,729,678	560,527	819,814	7,890,552
Electricity Exported to grid (kWh/yr)	882,280	400,524	283,253	451,334	533,010	33,232	2,863,273
Electricity from grid (kWh/yr)	2,681,697	558,383	1,349,154	1,316,139	369,986	655,697	5,859,504
Tot. PV generation (kWh/yr)	1,836,502	673,004	724,968	899,873	752,852	205,323	5,092,522
Tot. AC electricity generation (kWh/yr)	1,765,031	646,845	696,795	864,873	723,550	197,348	4,894,320
PV Electricity Direct Use (kWh/yr)	882,751	246,321	413,542	413,539	190,541	164,117	2,031,048
PV Self-Consumption Ratio	0.50	0.38	0.59	0.48	0.26	0.83	0.41
Number of panels	4,347	1,593	1,716	2,130	1,782	486	12,054
Heat Pumps in service (Heating)	30	6	14	15	3	5	71
Heat Pumps in service (Cooling)	20	4	8	8	2	3	42
Heat Pump capacity (ton)	70	70	70	70	70	70	70
Tot. Floor Area (m^2)	136,136	31,056	54,693	39,410	11,798	16,908	290,001
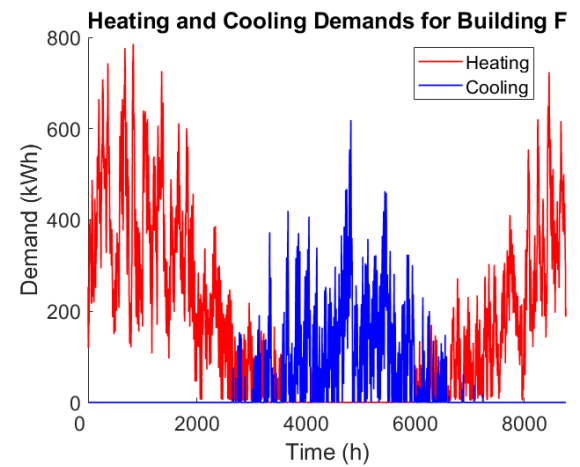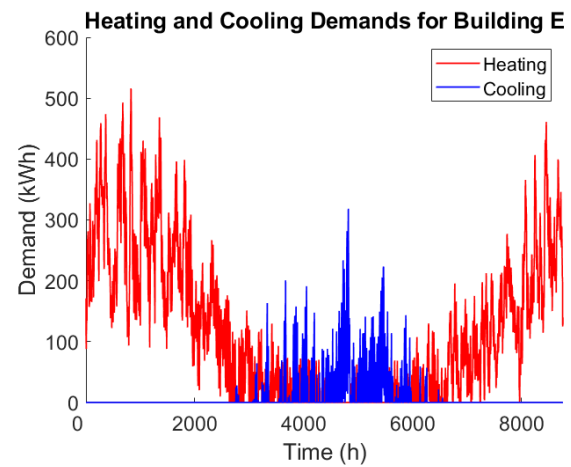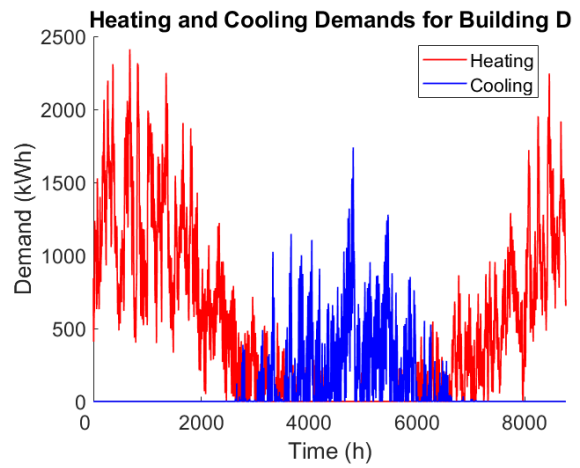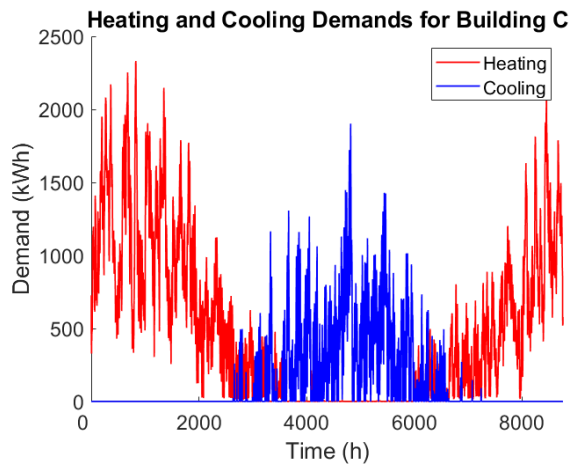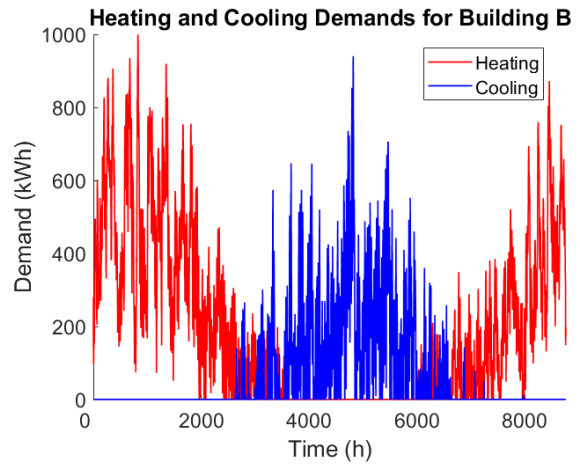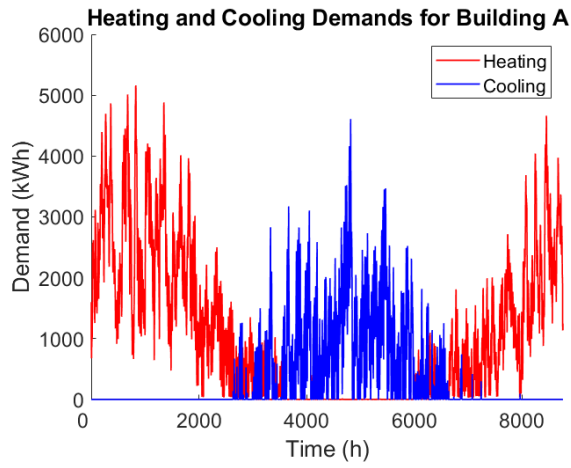
Figure 3-6 Load curves for all buildings.

Since a single COP value cannot reflect the fluctuations of COP during different weather conditions, the Seasonal COP (SCOP) was used to understand HP performance better. SCOP for heating and cooling seasons are defined as follows:

$$SCOP_H = \frac{\sum_{i=1} Q_H}{\sum_{i=1} E_H},$$ (3-8)

$$SCOP_H = \frac{\sum_{i=1} Q_C}{\sum_{i=1} E_C},$$ (3-9)

where Q_H, Q_C are HP heat output (kWh) and and E_H, E_C electricity consumption (kWh) in the heating and cooling cycle.

Since the selected HPs are single staged and the model requires them to cover the maximum demand, almost in all time steps, a surplus of energy will be available. It is clear that sizing the energy system relying on maximum demand results in an over-sized system for most operating hours that will lower the system's total efficiency and lifespan by causing numerous on/off cycles.

Comparing the central scenario with the decentralized system output shows notable differences regarding electricity balance and the number of HPs required. The central scenario's total HP electricity consumption is 17 % lower than that of the decentral systems, while the central scenario has higher electricity export and lower import from the grid with 10 and 18 percent respectively. The central system requires 2 HPs for heating and 3 HPs for cooling less than the decentral scenario because the demand profile of the buildings are not similar, and in the central scenario, the peak demand in one building might be covered by a simultaneous valley in another building's demand. Also, in some hours, especially in peak demand hours, the total amount of surplus energy of 6 buildings in each hour is higher than the capacity of a single 70-ton HP (responsible for the extra number of HPs in the decentralized scenario).

3-6-3- Distribution Network Hydraulic and Thermal Results

In this section, the calculated mass flow rate, heat losses, and the piping system are presented. At first, the mass flow rate for each pipe is determined. Figure 3-7 shows the mass flow rate of the supply line of the heating system in the network.
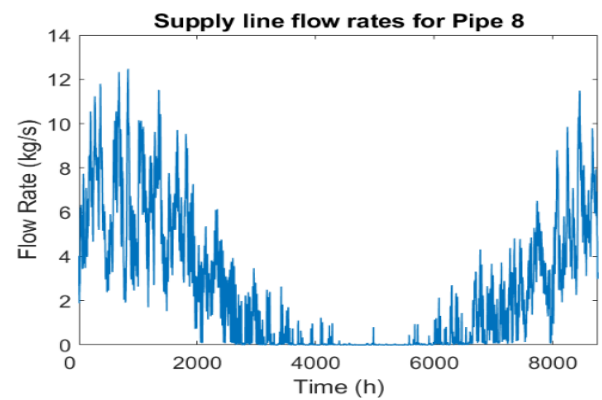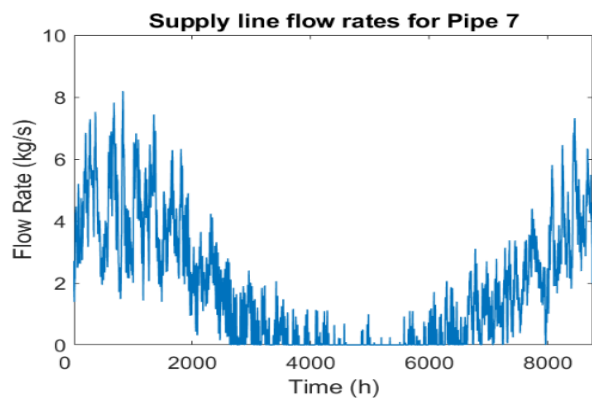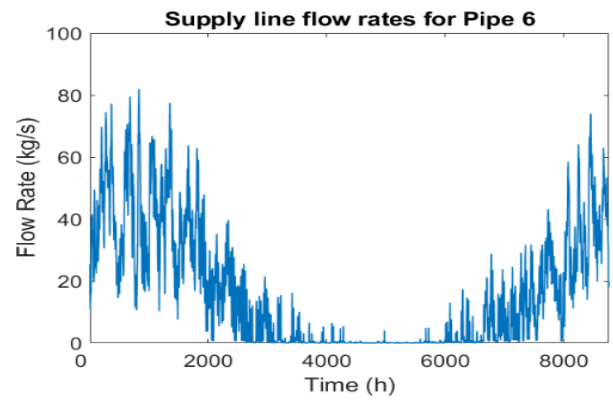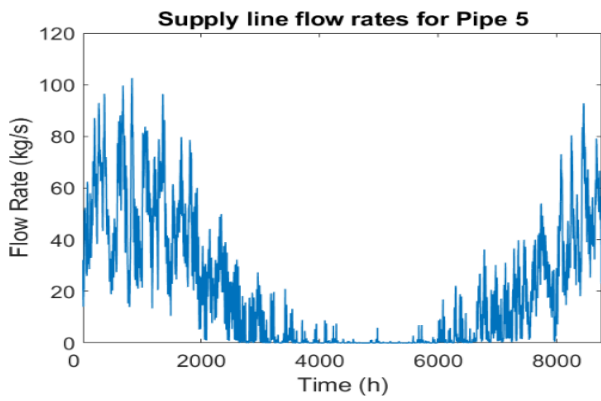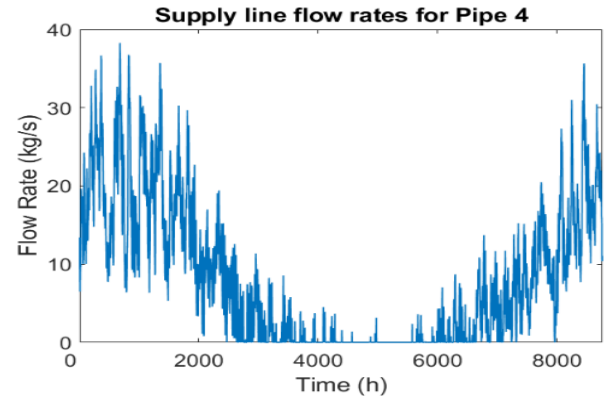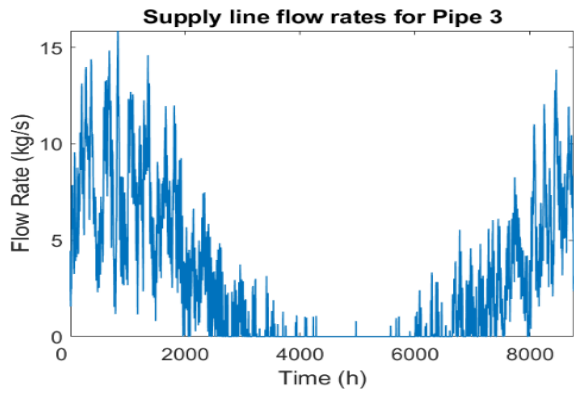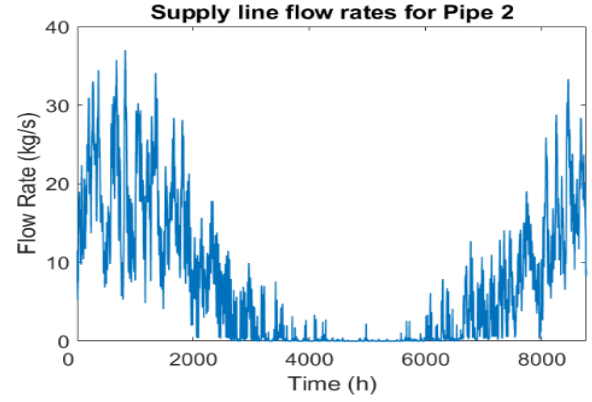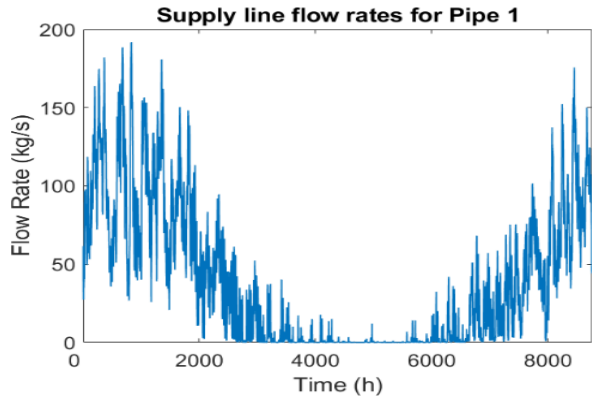
Figure 3-7 Supply line mass flow rates for the heating system in each pipe.

Figure 3-7 shows that the mass flow rates in the main pipes, with pipe 1 and pipe 5 having the highest value. Moreover, the flow rate in pipe 6, which transfers energy from the plant to building A, has a higher value compared to the other pipe, because building A has the highest energy demand in the configuration. This is also true for the cooling system operation. After calculating the mass flow rate in the system, the size of the pipes can be determined. Table 3-6 shows the piping results for the heating and cooling systems. The mentioned results will be used in economic assessment.

Table 3-6 Pipe sizing results.

Cooling		Heating	
Length (m)	Diameter (in)	Length (m)	Diameter (in)
71	16	71	16
53.25	8	53.25	8
71	6	71	6
35.5	8	35.5	8
159.75	12	159.75	12
17.75	12	17.75	12
71	4	71	4
35.5	6	35.5	6

After obtaining the flow rates and sizes of the pipes, it is possible to calculate the temperature levels in the network. This calculation helps to evaluate the heat losses in the grid and, more importantly, to make sure that the demand will be responded to properly by the system. Figure 3-8 shows the temperature variation of the heating system in building A's consumer substation. The temperature setpoint for heating in Montreal is 22 °C, and Figure 3-8 shows that this energy system scenario can respond to the energy demands of this building properly.

The minimum temperature of the supply line for the heating system was 28 °C and the maximum temperature of the supply line for the cooling system was calculated as 19 °C. Thus, the centralized scenario can properly provide energy for consumption. The calculation showed that the heat loss for this configuration of the network is 2.15×10^6 kWh, which is 10.1% of the total demand.
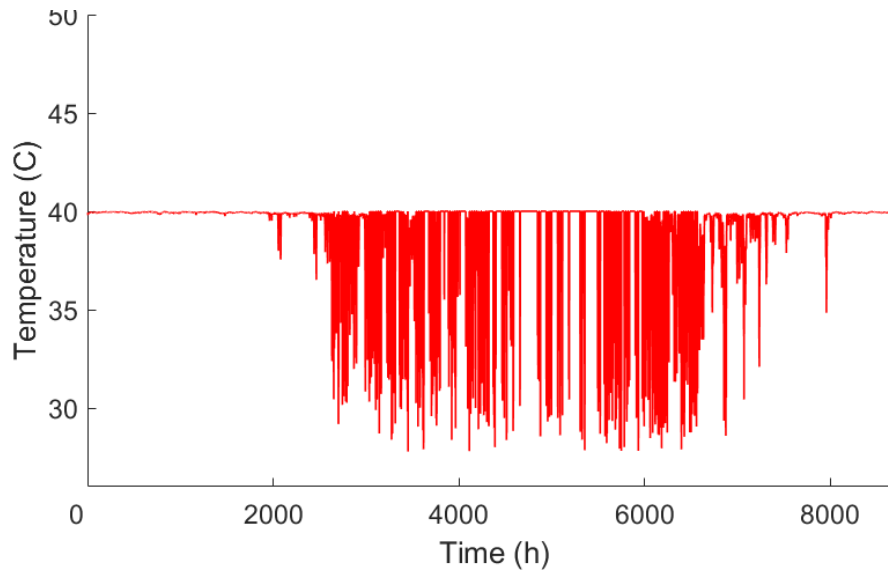
Figure 3-8 Temperature variation of the heating system supply line in building A's consumer substation.

3-6-4- Economic Assessment Results

In this section, the results of the economic assessment are presented. LCOE is used as an indicator for evaluating the economic performance of both scenarios. Table 3-7 shows the results of calculating LCOE for the first scenario where each building has an individual geothermal loop. The electricity cost in the province of Quebec is 8 CAD/kWh. Based on the table's data, the LCOE for all the buildings is less than this value. Therefore, using the geothermal loop for buildings in the Lachine area is cheaper than using direct electrical heating systems commonly used in Montreal.

Table 3-7 Economic assessment of the first scenario (decentralized energy system).

Building Name	A	B	C	D	E	F
Investment Costs						
Heat pump capacity (ton)	30x70	6x70	14x70	15x70	3x70	5x70
Heat pump cost (CAD)	$1,417,500	$283,500	$661,500	$708,750	$141,750	$236,250
Drilling and filling of borehole (CAD)	$1,728,216	$345,643	$806,501	$864,108	$172,822	$288,036
Labour (CAD)	$3,087,000	$617,400	$1,440,600	$1,543,500	$308,700	$514,500
Total Capital Cost (CAD)	$6,232,716	$1,246,543	$2,908,601	$3,116,358	$623,272	$1,038,786
Profit (%)	22.00	22.00	22.00	22.00	22.00	22.00
Total Capital Cost after profit (CAD)	$7,603,914	$1,520,783	$3,548,493	$3,801,957	$760,391	$1,267,319
Annual Capital Cost (CAD/year)	$341,085	$68,217	$159,173	$170,542	$34,108	$56,847

58

Economic Factors						
Project Lifetime	35	35	35	35	35	35
Discount rate (%)	2.75	2.75	2.75	2.75	2.75	2.75
Fuel Costs						
Heat pump Electricity consumption (MWh)	3565	805	1763	1730	561	820
Fuel cost (CAD/year)	$285,200	$64,400	$141,040	$138,400	$44,880	$65,600
Energy Generation						
Yearly Heating Energy Generation (MWh)	8899	1605	4056	4352	997	1385
Yearly Cooling Energy Generation (MWh)	2940	552	1153	863	77	356
LCOE (CAD/kWh)	*$0.053*	*$0.061*	*$0.058*	*$0.059*	*$0.074*	*$0.070*

In Figure 3-9 the left axis and the bars represent LCOE. The right axis and the circles represent building surface area. In addition, the size of circles represents building surface area to show a comparison between them. It is shown in the figure that the bigger the building is, the cheaper the system be-comes. The LCOE for building E, the smallest building, is 0.07 CAD/kWh, while this number for building A, the biggest building in the area, is 0.05 CAD/kWh.
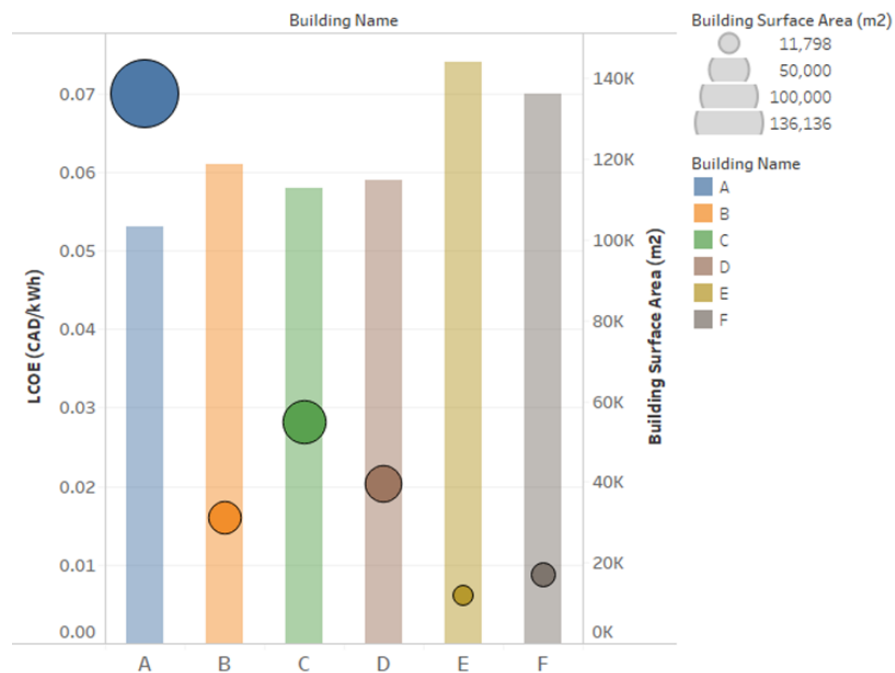
Figure 3-9 Surface area and LCOE for each building.

Table 3-8 shows the results of the economic assessment of the centralized system under two different sets of assumptions. In the first case, the system's detailed costs are equal to the values used for the distributed system. The cost of heat pump, labor, and borehole drilling and filling are the same as the ones used for the decentral system. In the second case, the economies of scale are considered. Hence, either a discount on different items has been received and/or the project is subsidized. The results show that in both cases, the LCOE is lower than the electricity price in Quebec, which proves that using a geothermal district heating and cooling network is cost beneficial when compared to direct electrical heating. Moreover, in both cases the LCOE of the central system is lower than or equal to the LCOE in decentral system. In the unsubsidized system, only for the building A, the LCOE of both central and decentral systems are the same, while for all other buildings LCOE decreased. This reduction in LCOE is more significant in smaller buildings. On the other hand, in subsidized case, the LCOE for all buildings decreased which proves that the heating cost could become even cheaper in case of governmental support.

Table 3-8 Economic assessment of the second scenario (centralized energy system).

	Unsubsidized	Discounts/Subsidized
Investment Costs		
Heat pump capacity (ton)	71x70	71x70
Heat pump cost (CAD)	$3,354,750	$2,180,588
Drilling and filling of borehole (CAD)	$4,090,111	$2,454,067
Labour (CAD)	$7,305,900	$4,383,540
Distribution Network Cost (CAD)	$1,722,589	$1,722,589
Total Capital Cost (CAD)	$16,473,350	$10,740,783
Profit (%)	22.00	22.00
Total Capital Cost including profit margin (CAD)	$20,097,487	$13,103,755
Annual Capital Cost (CAD/year)	$901,502	$587,788
Economic Factors		
Project Lifetime	35	35
Discount rate (%)	2.75	2.75
Fuel Costs		
Heat pump Electricity consumption (MWh)	3565	805
Fuel cost (CAD/year)	$285,200	$64,400
Energy Generation		
Yearly Heating Energy Generation (MWh)	8899	1605
Yearly Cooling Energy Generation (MWh)	2940	552
LCOE (CAD/kWh)	**$0.05**	**$0.04**

3-7- Conclusion

The present paper proposed a new method for district scale automated building energy modeling and energy system simulation. This method was implemented to design an economic and efficient energy system for a Montreal case study district called Dominion Bridge. An automated urban building energy modeling (AUBEM) method was used to calculate the energy demand of the buildings. This method carries out the whole process of 3D building modeling for the energy demand analysis and the entire process of energy system modeling in an automatic manner. Using the energy demand results from the AUBEM, an energy system model for decentral and central reversible heat pumps was prepared in the INSEL 8.2 simulation environment. Moreover, a heating network model was designed and implemented for a centralized heat pump system in MATLAB. This code provides the pipe sizing, mass flow rates, temperature distribution and heat losses in the distribution network. Finally, LCOE was used as an indicator for evaluating the economic performance of both scenarios.

Although the centralized scenario experienced heat losses through the grid, according to ESM results, this scenario required lower electricity consumption and lower numbers of HPs to meet demands. Moreover, the economic assessment results revealed that the LCOE of both scenarios varies from 0.04 to 0.07 CAD/kWh, which is cheaper than the electricity cost in Quebec (0.08 CAD/kWh). The LCOE for the bigger buildings was lower compared to the smaller ones. A comparison between centralized and decentralized scenarios revealed that the centralized system is cost beneficial for all buildings. Also, it was shown that if discounts are received due to the economy of scale, or government subsidize the project, the cost of heating could decrease further. If the central project is subsidized and/or discounts are received on different items, the LCOE decreases to 0.04 CAD/kWh.

The ESM results also showed that system sizing for 100% of hours (8760 in a year) results in an over-sized system for most operating hours. Adding storage, short or long term, and system sizing for lower percentiles of the maximum load (i.e., P=0.98) will have a better outcome. The optimal percentile determination requires detailed investigation on load profiles, peaks and valleys, and the number of hours with consecutive high demand.

Chapter 4: Other Applications and Case Studies

4-1- Introduction

In this chapter rest of the framework's applications are introduced, and different case studies have been presented. In chapters 2 and 3, the framework was put into work on scenarios to compare GSHP and ASHP in centralized and decentral energy systems from energy and economic perspectives. However, since the framework is being developed and improved regularly, other capabilities are added to the framework after preparing two papers provided in previous chapters.

4-2- DHW Generation Using HP

Hot water has always been an essential part of final energy consumption in buildings, and despite the reduction in space heating energy consumption thanks to recent highly efficient façade and construction, the portion of DHW has stayed relatively constant (Pomianowski et al. 2020). Consequently, the DHW share of total energy consumption is rising from 15-25% in older constructions to 40-50% in highly efficient or nearly zero buildings (Erhorn and Erhorn-Kluttig 2014). Hence, the importance of an energy-efficient DHW generation is system is becoming more understandable.

A missing link in providing a complete solution to energy system needs in addition to meeting heating and cooling demands is DHW. As a result, a DHW tank model is added, and a HP system, similar to the heating system, is responsible for meeting DHW demands. Although the HP modeling section is identical to what is presented in the previous chapters for heating demands, the critical factor in DHW is the hot water supply temperature. Previously mentioned that high water temperature (60 °C and over) causes scalding and low temperature (below 35 °C) has a higher chance of Legionella infection (Lee 2018). There are preventing actions such as making regular fluctuations in stored water temperature (raising temperature once or twice every four hours), eliminating storage tank, and implementing point of use heating and regular system cleaning, which are not in the focus of this work.

4-2-1-DHW Demand Profile

Similar to what the integrated UBEM+UESM workflow does, determining the DHW demand profile is the first step. To do so, DHW-Calc (Jordan and Vajen 2017) is used, which is a free statistical tool for generating DHW profiles developed by Kassel University, Germany. The tool can provide a DHW profile in various time steps over an adjustable time frame for a single-family house, multi-family house, or multiple buildings (district) in the Beta version (under development). Four load distribution probabilities are considered, which are the default values based on IEA-Task 26 (Figure 4-1). Time steps, water draw offs (flowrate and duration), simulation time frame, and probabilities are all adjustable, and other features like weekdays/weekends, holidays, and daylight saving are included. The output can be either DHW demand (lit/hr/time step), flowrate and duration of draw off per time step, or daily sum of draw-offs (Jordan and Vajen 2017).
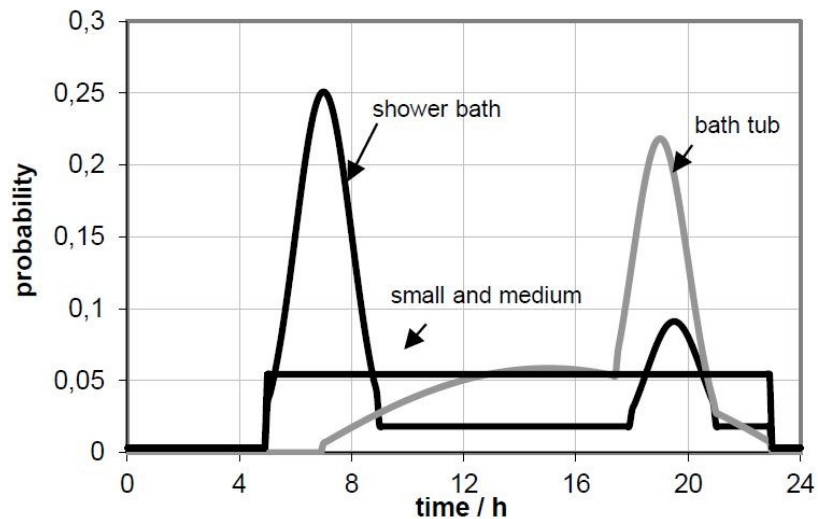
Figure 4-1 Probability distribution load during a day. Category 1 and 2: For small and medium draw-offs Category 3: Bath Category, 4: Shower (Jordan and Vajen 2017).

4-2-2- Hot Water Tank and HP

By having the DHW profile (lit/hr), the required energy to raise the temperature of the fresh makeup city water to generate hot water can easily be calculated using the equation below:

$$Q_{DHW} = \dot{m} \cdot C_p \cdot (T_{supp} - T_{city}) \tag{4-1}$$

where Q_{DHW} is the energy required to generate hot water, $\dot{m}$ is the hot water flow rate, C_p is water heat capacity (4.19 kJ/kg °C) and T_{supp} and T_{city} are hot water supply temperature and fresh make up city water temperature (assumed 10 °C). The HP system's supplied energy in each time step will be calculated using the same equation. Although the HTF in the HP system is usually a mixture of glycol and water, for simplifying the calculations, pure water's heat capacity (4.19 kJ/kg °C) is used. Moreover, the HP system's return line temperature is considered equal to the temperature of the bottom of the stratified tank model.

As mentioned in section 2-6, the framework rounds the number HPs up to the closest integer to ensure that the system meets or exceeds the required energy. Thus, in each time step, there might be excessive generated energy by HPs valued at a percent of the HP capacity. This energy can be either directed to thermal storage or a hot water tank. The latter would be a better choice as it might reduce the number HPs required to provide DHW. That being said, the excessive energy generated by heating HPs, will be subtracted from Q_{DHW} and the rest should be provided by the HPs dedicated to DHW. It is worth mentioning that the same sizing approach for heating HPs is used for the DHW generation system. However, it should be noted that in case of having excessive heat after meeting heating and DHW demands, there should be thermal storage added to store and redirect the energy when needed. Otherwise, the number of HPs should not be rounded up, and an auxiliary electrical heater should provide the extra energy to prevent any unbalancing in the system energy-wise.
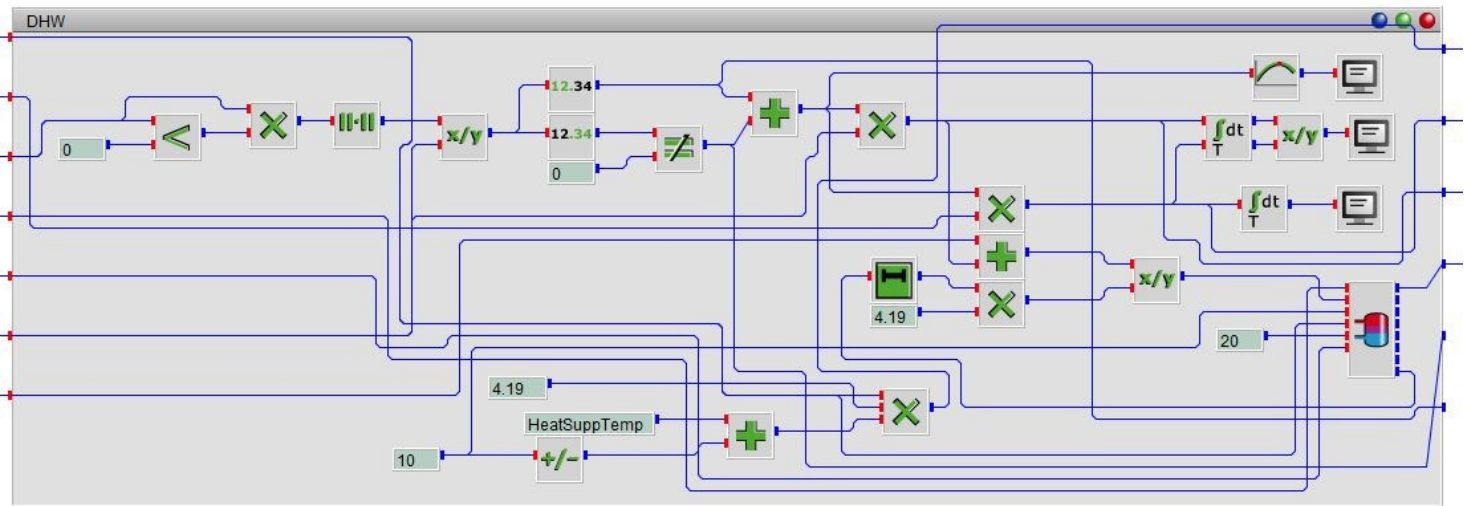
Figure 4-2 A screenshot of DHW generation/ stratified tank system modeled in INSEL.

4-2-3- DHW Case Study

As a case study, the DHW generation model has been added to the framework. In this case study, two scenarios will be studied to compare generating DHW with HP only or with a combination of HP and an auxiliary electrical heater. The studied building is a residential, low-rise three-story building located in Lachine-Est, Montreal. The general specification of the building as well as occupancy and DHW demand density values used in calculations are summarized in Table 4-1. Occupant density and DHW demand values are extracted from literature (The Engineering ToolBox 2017; Engineering ToolBox 2003), and the values are in the standard range.

DHW demand profile is determined using the DHW-Calc tool regarding the assumptions summarized in Table 4-1. As a result, the DHW system should provide DHW to 80 people (20 households) with an average daily hot water consumption of 120 liters/day. DHW daily average demand profile is shown in Figure 4-3. Heating and cooling demands are also determined using the UBEM used in previous chapters.

Table 4-1 The case study building specification and general assumptions used in the calculation.

Number of stories	3
Total floor area (m^2)	2161
Total Roof area (m^2)	667 (23x29)
Occupant density (m^2/person)	27
DHW demand (liter/day/person)	120

The HP system is designed to provide heating and cooling supply temperature of 40°C and 11°C, respectively, which are approved temperatures complying with low-temperature heating and high-temperature cooling concepts. Regarding low-temperature heating, the literature is provided in previous chapters. For high-temperature cooling, it is shown in many studies that a supply temperature of up to 18 °C can provide thermal comfort while can reduce cooling energy consumption by 6-41% depending on the location and control strategies (Saber, Tham, and

Leibundgut 2016). Also, for DHW temperature, 40 °C is set for domestic use in either scenario and in case HP is not sufficient for meeting the setpoint, an auxiliary electrical heater (point of use) will raise the DHW temperature.
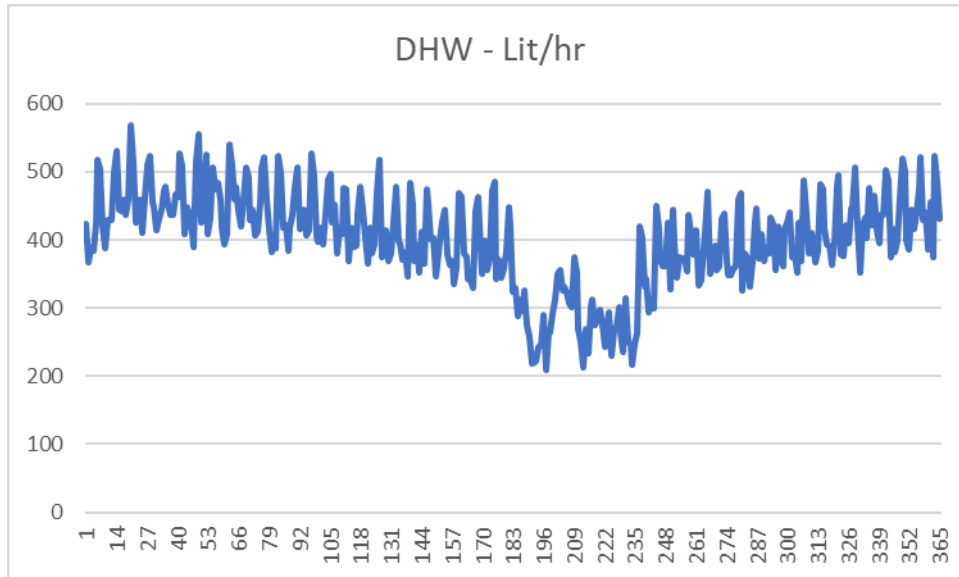
Figure 4-3 DHW daily average demand profile for 20 households.

In the first scenario, after sizing the heating and cooling HP system (with rounded up number), the extra available heat will be directed to the DHW tank in each time step. If the energy is sufficient to provide 40 °C hot water, the HP system will be bypassed until the next time step. Otherwise, the DHW HP sizing system will turn on HPs dedicated to DHW to cover the demand. On the other hand, in the second scenario, if the heating system's excessive energy is not sufficient and DHW dedicated HPs are required, the system will round down the number of HPs and provide extra energy via an auxiliary electrical heater. Based on the calculations, for 20 households with typical DHW usage such as shower/ bathtub, toilet, laundry, dishwasher, and the kitchen sink, considering storage factor and demand factors of 1 and 0.3 respectively, a 1.5 m^3 storage tank is needed. To check schematic system formation/ overview, please refer to Figure 1-2. Moreover, for the heating system, 30 ton (105 kW) ASHP and for DHW generation, 12 ton (42 kW) ASHP are used in both scenarios.

The results for both scenarios are summarized in Table 4-2. In both scenarios, the setpoint constraints must be met, but adding an auxiliary electrical heater will add flexibility to the system due to its low inertia and working range, i.e., providing heat as much as needed and at the time it is needed. Moreover, when the system is sized for the highest demand (which may occur only 1-4 % a year), reducing the number of HPs will not affect the thermal comfort, and in a worst-case scenario, the auxiliary electrical heater will save the system purpose of either heating or generating DHW.

$$Seasonal\ Performance\ factor = \frac{\sum Demand}{\sum Energy\ Consumed\ for\ Meating\ Demand}, \qquad (4\text{-}1)$$

Table 4-2 Result of DHW generation scenarios using HP with and without auxiliary electrical heater.

	HP + Electric heater	HP Only
Total Excessive Energy (kWh)	0	139,704
DHW HP Seasonal COP	3.22	3.55
HP Electicity Consumption (kWh/yr) (DHW)	68,558	128,113
Aux. Electric. Heater Consumption (kWh/yr)	94,116	0
Number of Heat Pumps (DHW)	3	4
Seasonal Performance Factor	2.45	2.67

Since a stratified DHW tank model is used, monitoring the supply (top) and return (bottom) temperatures will indicate the system's performance. By referring to Figure 4-4, as anticipated, the HP-only system works smoothly, and the system can keep the hot water at the set point almost at all times during the highest demand times (January and February). It can be seen that this service is coming at the cost of having an extra HP and consuming more electricity compared to the combination of HP and electrical heater. Also, it is worth mentioning that in HP+ electric heater scenario, the system reduces the HP counts by one number to prevent energy unbalancing. As a result, the supply and return temperature of DHW fluctuates in a more extensive range, and the

electric heater will work similarly to the point of use systems to instantly increase the hot water temperature. However, these fluctuations and lower return temperature have impacted the system
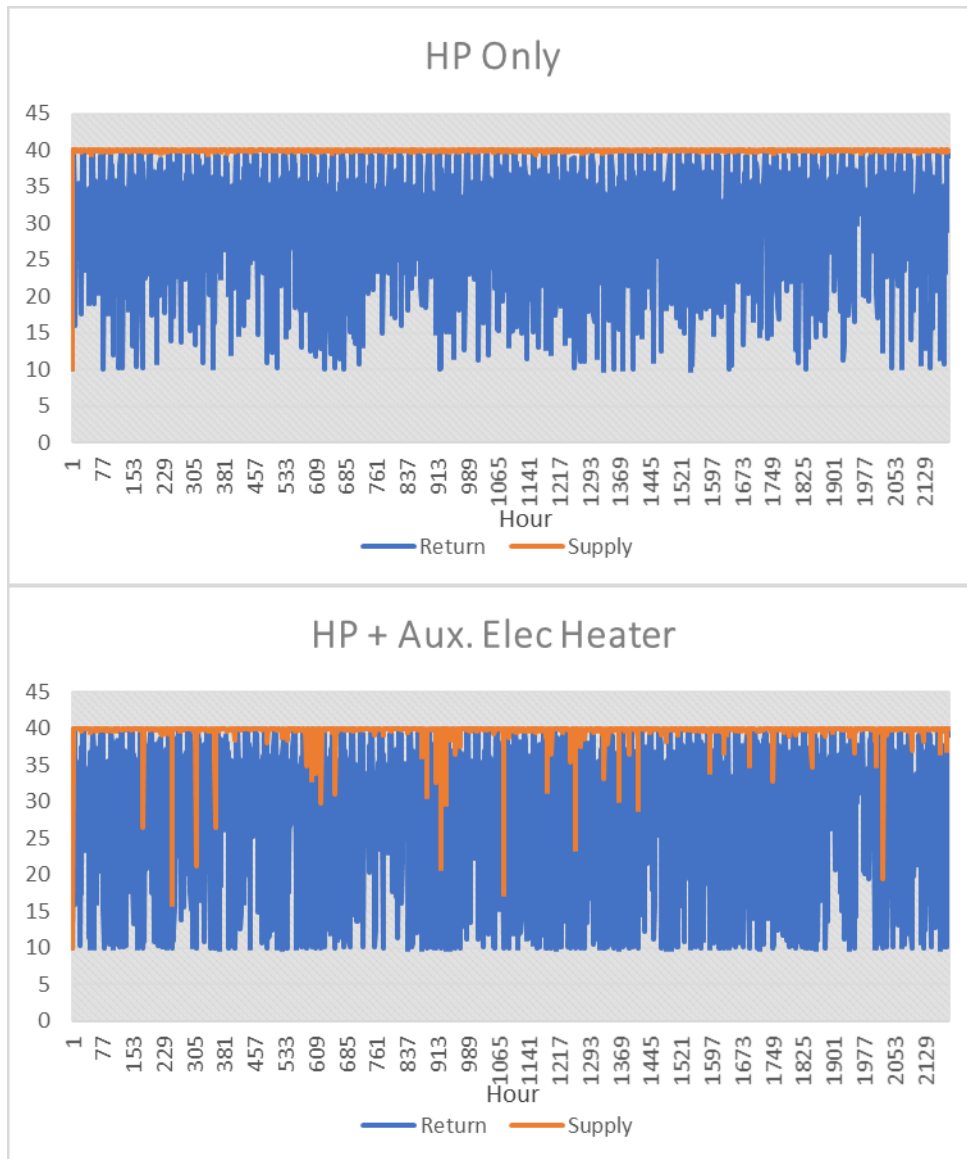
Figure 4-4 Three months overview of the Supply and return temperature of DHW tank in both scenarios.

COP.

4-3- Optimizing Model Parameters Using Python

The model prepared in INSEL's graphical user interface can be coupled with Python to conduct various justifications using INSEL's text input files. By defining and associating global constants to parameters wish to optimize or change, these parameters can be treated as optimization

parameters, and various actions from making changes manually to using evolutionary algorithms like Genetic Algorithm (GA) can be taken.

4-3-1-Optimization Case Study- PV Slope

Finding the optimum PV inclination can significantly affect the system's output from economic, efficiency, and occupant comfort level aspects (In standalone cases). Although there are estimated values and rules of thumb for PV slope values based on the location's latitude, these values may differ from the optimum angle. Thus, an optimization using models with a high temporal resolution is recommended. Moreover, the INSEL library gives the chance to use available equipment in the market, including PV panels and inverters.

The procedure starts with assembling a PV system model including PV, MPPT, and inverter accompanied by a sizing algorithm (both topics are addressed in section 2-3-3-HP System) in INSEL graphical interface, and selecting PV slope as the parameter and the total yearly power generation as the objective function. Then with using PyCharm (an integrated development environment for Python), DEAP library (which includes templates for optimization, including GA), and defining GA parameters, the model is ready. In each time step, a set of values (population) will be generated and used as an input for the PV system's inclination. The INSEL model will then run and write the yearly power generated (system output) in a text file that will be used as parents to generate the population in each time step. This goes on until a criterion is met (e.g., number of iterations). The inclination degree associate with the highest yearly power generation is the optimum value.

For the case study, the building investigated in the previous section (4-2-3-DHW Case Study) will be discussed. Similarly, the building's specifications are summarized in Table 4-1. In the calculations, 65% of the roof area will be assigned for PV panels, and shadowing effects from other buildings and surroundings are neglected. The PV panel is assumed to be similar to what was used in the previous chapter, and its specifications are summarized in Table 2-2. However, the slope (inclination angle) is not fixed and will be optimized to generate the highest possible PV power. The parameters and assumptions used in GA and the PV model are shown in Table 4-3.

Table 4-3 Parameters used in GA optimizer.

Generation (Num)	Population (Num)	Crossed Individual Prob.	Individual Mutation Prob.	Low Boundary (Angle)	High Boundary (Angle)
30	30	0.9	0.3	0	90

The PyCharm returns 31 degrees as the optimum angle with 83'650 and 80'431 total PV generation and total AC electricity generated in a year, respectively (kWh/yr). Furthermore, the INSEL output file contains the model's output for each slope shown in Table 4-4.

Table 4-4 INSEL output for each PV slope.

Slope (degree)	AC Electricity Generation (kWh/yr)	Inverter Efficiency (%)	Total PV Generation (kWh/yr)
0	70802	91.50	73809
10	75641	92.41	78750
25	71808	93.14	74694
28	80336	93.26	83549
29	80386	93.22	83601
30	80405	93.21	83623
31	80431	93.18	83650
32	80424	93.12	83644
33	75905	93.00	78960
34	75859	92.98	78914
35	75801	92.94	78855
40	70652	92.92	73486
60	40737	91.14	42407
80	9706	90.54	10233
86	error	error	3125
90	error	error	error

By reviewing the literature, different optimum angles are mentioned like 30, 34, 35,37 while the INSEL model calculates inverter efficiency in each time step and returns 31 degrees as the angle with the highest yearly AC power generation.

4-4- Sensitivity Analysis Using Python

Sensitivity analysis is a crucial part of analyzing, designing, or planning a new or existing system. It shows the most effective parameters in the system's efficiency and output and reveals the system's vulnerability to small and significant changes in that parameter. Knowing the components of the system and the interaction between each part of it is required for performing sensitivity analysis which can make it difficult in some cases, especially in complex systems. A complete model that captures the effects and interaction of the system's components is of high value due to maximizing possible time saving and minimizing errors.

According to previous sections and chapters, modeling an HP behavior can be a tricky task, let alone having a system with many more complex systems interacting with each other. Also, it is a known fact that one of the essential parameters in heating systems analysis is heating supply temperature as it affects energy and exergy efficiencies. Besides, HP performance is highly susceptible to the heating supply temperature, so that a higher set point is putting the system under pressure, and as a result, the system's COP will drop. Throughout this thesis, the heating supply temperature is selected concerning low-temperature heating (40 °C), while the conventional heating systems are set on temperatures around 80 °C or higher.

4-4-1- Sensitivity Analysis Case Study

For the case study, the same building used in previous sections of chapter 4 is used. Since standard heat pumps usually are working at temperatures lower than 60 °C, it is worth comparing a system's performance with heating supply temperatures from 30 °C (floor heating) to 55 °C and check how the system's COP is affected. The same formerly prepared model for optimization is investigated. However, instead of using GA to generate input values, predefined values for the heating supply temperature, starting from 30 °C up to 55 °C with an increment of 5 degrees, will be used.

Figure 4-5 depicts the system behavior in different supply temperatures. It can be seen that providing higher temperatures puts HPs under pressure. Consequently, the system's efficiency drops and increases electricity consumption, which, other than imposing a higher economic burden on the user, contrasts with zero-carbon design concepts. Furthermore, by comparing electricity consumption values, the minimum, maximum and average increase in consumption for 5 degrees

higher supply temperature are 4%, 20%, and 13%, respectively. The same trend in the opposite direction is evident for COP values, where the COP values diminish with the average rate of 11% for every 5 degrees increase in heating setpoint.
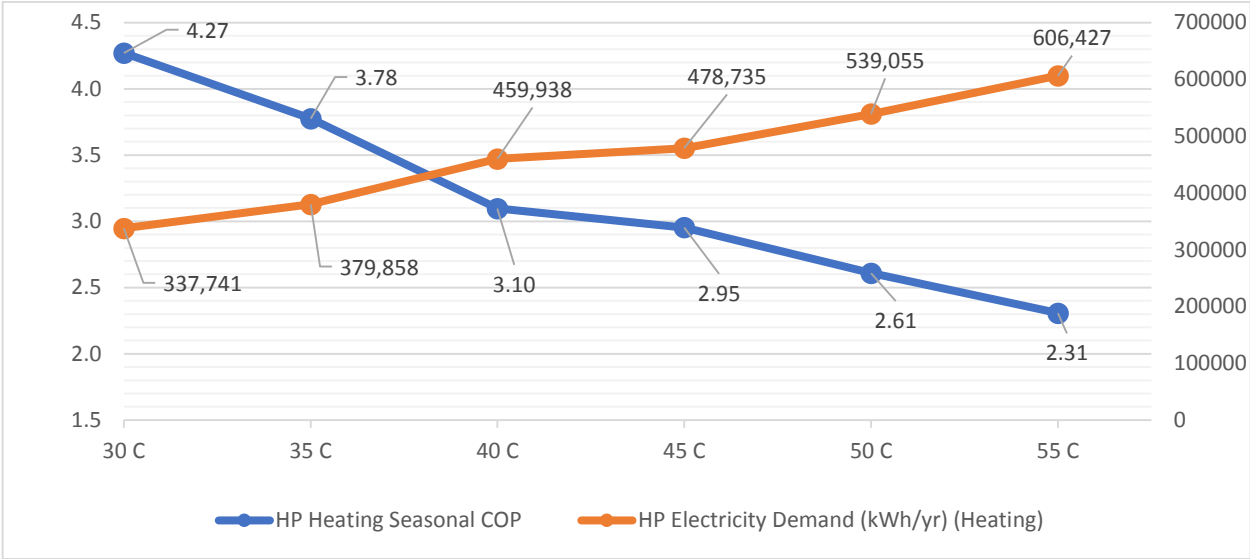
Figure 4-5 HP heating system results in different heating supply temperatures.

Chapter 5: Summary, Conclusion, and Future Works

5-1- Summary

This research's main focus was to provide an automated framework for energy system design in an urban context to cover the gap in the literature regarding available urban energy simulation modeling (UESM). That being said, an open-source physical model was introduced, using INSEL 8.2 and Python with detailed modeled components, featuring adjustable temporal scale and the flexibility of integrating system simulations with building energy modeling tools (UBEM), adding and adjusting components, and undertaking analyses such as optimization or sensitivity analysis.

The proposed energy system model provides a complete solution for sizing HP systems for covering heating, cooling, and hot water demands in addition to modeling and sizing a PV system integrated with MPPT and inverter. Also, to enable the analysis of flexibility and demand-side management strategies such as peak shaving and load shifting, simplified battery and thermal storage models are included in the system model. Moreover, this study's HP system modeling approach enables the framework to calculate the HP system's efficiency (COP) with hourly resolution compared to monthly or yearly averaged COP as common parameters in the literature.

The framework has been put into practice in three major case studies in chapters 2 to 4. In the first case study (chapter 2), a new urban geometry within a zoning process in Lachine-Est, Montreal, is analyzed. In addition to comparing ASHP and GSHP systems, the district's status regarding the energy positivity definition is analysed. Although numerous parameters influence the energy analysis of a system and case studies' results should not be overgeneralized to other contexts, it has been shown that the power supply of a district by local PV as the only renewable source does not meet the needs. It should be noticed that in this case study, only heating and cooling demands were considered, yet the limited PV power that can be installed on the roof areas was insufficient to cover this demand.

In chapter 3, the framework was used to compare centralized heating and cooling scenario and decentralized systems economically. Also, a low-temperature heating concept was analyzed, and the centralized network temperature was investigated to ensure the system can meet the demands. The energy system modeling revealed that the centralized scenario requires fewer HPs and,

consequently, consumes 17% less electricity than the decentralized scenario. Furthermore, the economic assessment showed that the levelized cost of energy of the ground source heat pump system decreases when the building's floor area (energy consumption) increases and the centralized system has a LCOE of 0.04-0.05 CAD/kWh. Also, it was mentioned that energy system sizing based on the peak demand would result in oversizing, which adds burden to cost and system's efficiency. Other peak demand percentiles (e.g., 0.98) were suggested.

Finally, in chapter 4, a building was used in three case studies of DHW generation with HP and hot water tank, optimizing PV slope and carrying out a sensitivity analysis of the HP system's COP regarding changes in heating supply temperature. First, it was shown that although the HP system can provide DHW with small temperature fluctuations, the combination of HP and auxiliary electrical heater could meet the demand while using fewer HPs and consuming less energy, besides increasing the system's flexibility due to the electric heater's low inertia. In the next section, optimization was performed using Python and DEAP library to determine the PV system's optimum slope in Montreal. The slope of 31 degrees was shown to be the slope with which the system can generate the highest AC electricity after taking the inverter's efficiency into account. Lastly, the HP heating system was studied to address the impact of changing heating supply temperature on the system's COP. The analysis revealed that the HP's electricity consumption increases at the rate of 13%, and the COP decreases by 11% by changing heating supply temperature by 5 degrees.

5-2- Conclusion

The extensive literature review showed the lack of transparency and flexibility of available UESMs, which prevents these tools from being used in designing and planning in the energy sector as they should. UESMs are potent tools contributing to analyzing existing and future strategies and policies for reaching carbon neutrality by 2050. By introducing a flexible framework that integrates both demand calculation and energy system modeling parts, a foundation is provided for other researchers to add, justify or extend the model to fit their field best.

The energy system model is a complete solution for sizing PV and HP systems to cover heating, cooling, and DHW demands. Moreover, having a detailed model has made it possible to study the model in different conditions and scenarios. Also, integrating the energy model to Python

and its powerful libraries, has made sensitivity analysis and parameter optimization much more straightforward, even in complex models like the one introduced.

5-3-   Future Works

The current workflow has many advantages, which were addressed in previous chapters. However, some improvement points should not go unnoticed for future works, which can be divided into two sections related to energy system modeling and result post-processing.

- In the energy system modeling section of the framework, PV and HP are the only energy systems included in the design, whereas many other energy systems should be added later.
- HPs are considered single-stage machines, which is not an unrealistic assumption; however, considering inverter HPs can cover more market shares.
- PV system does not take shadowing effects from other buildings and surroundings into account, which might change the system's output drastically if considered.
- Battery and thermal storage models are simplified, and the current model can not capture storage systems' actual performance.
- Results either in INSEL or Python are generally available in text files, and for visualisation of results other tools should be used.

References

Abergel, Thibaut. 2020. "Heat Pumps – Analysis - IEA." *Tracking Report*. https://www.iea.org/reports/heat-pumps.

Aditya, G. Riyan, Olga Mikhaylova, Guillermo A. Narsilio, and Ian W. Johnston. 2020. "Comparative Costs of Ground Source Heat Pump Systems against Other Forms of Heating and Cooling for Different Climatic Conditions." *Sustainable Energy Technologies and Assessments* 42 (December): 100824. https://doi.org/10.1016/j.seta.2020.100824.

Aguilar, F., D. Crespí-Llorens, and P. V. Quiles. 2019. "Techno-Economic Analysis of an Air Conditioning Heat Pump Powered by Photovoltaic Panels and the Grid." *Solar Energy* 180 (March): 169–79. https://doi.org/10.1016/j.solener.2019.01.005.

Ancrossed D Signelković, Aleksandar S., Igor Mujan, and Stojanka Dakić. 2016. "Experimental Validation of a EnergyPlus Model: Application of a Multi-Storey Naturally Ventilated Double Skin Façade." *Energy and Buildings* 118 (April): 27–36. https://doi.org/10.1016/j.enbuild.2016.02.045.

Arpagaus, Cordin, Frédéric Bless, Michael Uhlmann, Jürg Schiffmann, and Stefan S. Bertsch. 2018. "High Temperature Heat Pumps: Market Overview, State of the Art, Research Status, Refrigerants, and Application Potentials." *Energy*. Elsevier Ltd. https://doi.org/10.1016/j.energy.2018.03.166.

Asaee, S. Rasoul, V. Ismet Ugursal, and Ian Beausoleil-Morrison. 2017. "Techno-Economic Feasibility Evaluation of Air to Water Heat Pump Retrofit in the Canadian Housing Stock." *Applied Thermal Engineering* 111 (January): 936–49. https://doi.org/10.1016/j.applthermaleng.2016.09.117.

Bach, Bjarne, Jesper Werling, Torben Ommen, Marie Münster, Juan M. Morales, and Brian Elmegaard. 2016. "Integration of Large-Scale Heat Pumps in the District Heating Systems of Greater Copenhagen." *Energy* 107 (July): 321–34. https://doi.org/10.1016/j.energy.2016.04.029.

Bloess, Andreas, Wolf Peter Schill, and Alexander Zerrahn. 2018. "Power-to-Heat for Renewable

Energy Integration: A Review of Technologies, Modeling Approaches, and Flexibility Potentials." *Applied Energy*. Elsevier Ltd. https://doi.org/10.1016/j.apenergy.2017.12.073.

Brand, Marek, and Svend Svendsen. 2013. "Renewable-Based Low-Temperature District Heating for Existing Buildings in Various Stages of Refurbishment." *Energy* 62: 311–19. https://doi.org/10.1016/j.energy.2013.09.027.

Brange, Lisa, Jessica Englund, and Patrick Lauenburg. 2016. "Prosumers in District Heating Networks - A Swedish Case Study." *Applied Energy* 164 (February): 492–500. https://doi.org/10.1016/j.apenergy.2015.12.020.

Brockway, Anna M., and Pierre Delforge. 2018. "Emissions Reduction Potential from Electric Heat Pumps in California Homes." *Electricity Journal* 31 (9): 44–53. https://doi.org/10.1016/j.tej.2018.10.012.

C40. 2019. "C40 Cities Annual Report," 1–31. https://c40-production-images.s3.amazonaws.com/other_uploads/images/2574_C40_2019_Annual_Report.original.pdf?1587634742%0Awww.c40.org.

Cajot, S., M. Peter, J. M. Bahu, F. Guignet, A. Koch, and F. Maréchal. 2017. "Obstacles in Energy Planning at the Urban Scale." *Sustainable Cities and Society* 30 (April): 223–36. https://doi.org/10.1016/j.scs.2017.02.003.

Calikus, Ece, Sławomir Nowaczyk, Anita Sant'Anna, Henrik Gadd, and Sven Werner. 2019. "A Data-Driven Approach for Discovering Heat Load Patterns in District Heating." *Applied Energy* 252 (October): 113409. https://doi.org/10.1016/j.apenergy.2019.113409.

Chowdhury, Ashfaque Ahmed, M. G. Rasul, and M. M.K. Khan. 2016. "Parametric Analysis of Thermal Comfort and Energy Efficiency in Building in Subtropical Climate." In *Thermofluid Modeling for Energy Efficiency Applications*, 149–68. https://doi.org/10.1016/B978-0-12-802397-6.00007-5.

Collins, Seán, John Paul Deane, Kris Poncelet, Evangelos Panos, Robert C. Pietzcker, Erik Delarue, and Brian Pádraig Ó Gallachóir. 2017. "Integrating Short Term Variations of the Power System into Integrated Energy System Models: A Methodological Review." *Renewable and Sustainable Energy Reviews*. Elsevier Ltd.

https://doi.org/10.1016/j.rser.2017.03.090.

Çomakli, Kemal, Bedri Yüksel, and Ömer Çomakli. 2004. "Evaluation of Energy and Exergy Losses in District Heating Network." *Applied Thermal Engineering* 24 (7): 1009–17. https://doi.org/10.1016/j.applthermaleng.2003.11.014.

Commission, European, European Commission, Clean Planet, and Arias Ca. 2018. "The Commission Calls for a Climate Neutral Europe by 2050 *." https://ec.europa.eu/commission/presscorner/detail/en/IP_18_6543.

Connolly, D., H. Lund, B. V. Mathiesen, and M. Leahy. 2010. "A Review of Computer Tools for Analysing the Integration of Renewable Energy into Various Energy Systems." *Applied Energy*. Elsevier Ltd. https://doi.org/10.1016/j.apenergy.2009.09.026.

Crawley, Drury, Shanti Pless, and Paul Torcellini. 2009. "Getting to Net Zero." *ASHRAE Journal* 51 (9): 18–25. https://doi.org/10.1002/9781119347101.ch18.

Dalla Rosa, A., and J. E. Christensen. 2011. "Low-Energy District Heating in Energy-Efficient Building Areas." *Energy* 36 (12): 6890–99. https://doi.org/10.1016/j.energy.2011.10.001.

DOE. 2020. "Commercial Prototype Building Models | Building Energy Codes Program." *U.S. Department of Energy*. https://www.energycodes.gov/development/commercial/prototype_models.

Dominković, D. F., I. Bačeković, B. Ćosić, G. Krajačić, T. Pukšec, N. Duić, and N. Markovska. 2016. "Zero Carbon Energy System of South East Europe in 2050." *Applied Energy* 184: 1517–28. https://doi.org/10.1016/j.apenergy.2016.03.046.

Dotzauer, Erik. 2002. "Simple Model for Prediction of Loads in District - Heating Systems." *Applied Energy* 73 (3–4): 277–84. https://doi.org/10.1016/S0306-2619(02)00078-8.

Eicker, Ursula, Jürgen Schumacher, Marcus Brennenstuhl, and Verena Weiler. 2020. "SWC 2019 Renewable Energy Supply Concepts for next Generation Cities Using the Integrated Urban Modeling Platform INSEL 4D." In *Proceedings of the ISES Solar World Congress 2019 and IEA SHC International Conference on Solar Heating and Cooling for Buildings and Industry 2019*, 2479–87. https://doi.org/10.18086/swc.2019.51.02.

Eicker, Ursula, Verena Weiler, Jürgen Schumacher, and Reiner Braun. 2020. "On the Design of an Urban Data and Modeling Platform and Its Application to Urban District Analyses." *Energy and Buildings* 217 (June). https://doi.org/10.1016/j.enbuild.2020.109954.

"Energy Technology Perspectives 2017 Catalysing Energy Technology Transformations INTERNATIONAL ENERGY AGENCY." 2017. www.iea.org/t&c/.

Engineering ToolBox. 2003. "Hot Water Consumption per Occupant." 2003. https://www.engineeringtoolbox.com/hot-water-consumption-person-d_91.html.

Erhorn, H., and Heike Erhorn-Kluttig. 2014. "Selected Examples of Nearly Zero- Energy Buildings." *Detailed Report. Report for the Concerted Action on Energy Performance of Buildings, Www. Epbd-ca. Eu*, no. September: 74. http://www.rehva.eu/fileadmin/news/CT5_Report_Selected_examples_of_NZEBs-final.pdf.

European Commission. 2020. "State of the Union: Commission Raises Climate Ambition." 2020. https://ec.europa.eu/commission/presscorner/detail/en/IP_20_1599.

Ferrando, Martina, and Francesco Causone. 2020. "An Overview Of Urban Building Energy Modelling (UBEM) Tools." *Proceedings of Building Simulation 2019: 16th Conference of IBPSA* 16: 3452–59. https://doi.org/10.26868/25222708.2019.210632.

Fonseca, Jimeno A., Thuy An Nguyen, Arno Schlueter, and Francois Marechal. 2016. "City Energy Analyst (CEA): Integrated Framework for Analysis and Optimization of Building Energy Systems in Neighborhoods and City Districts." *Energy and Buildings* 113: 202–26. https://doi.org/10.1016/j.enbuild.2015.11.055.

Gaur, Ankita Singh, Desta Z Fitiwi, and John Curtis. 2021. "Heat Pumps and Our Low-Carbon Future: A Comprehensive Review." *Energy Research and Social Science* 71. https://doi.org/10.1016/j.erss.2020.101764.

Government of Canada. 2020. "CER − Canada's Energy Future 2020." 2020.

Green, Amy. 2018. "Why a Feasibility Study Is Your First Step Towards a Successful Building Project." New York.

Gröger, Gerhard, Thomas H Kolbe, Angela Czerwinski, and Claus Nagel. 2008. "OpenGIS City

Geography Markup Language (CityGML) Encoding Standard." *Open Geospatial Consortium August 2008*, no. 08-007r1: 234. http://www.opengis.net/spec/citygml/2.0.

Gröger, Gerhard, Thomas Kolbe, Claus Nagel, and Karl-Heinz Häfele. 2012. "OGC City Geography Markup Language (CityGML) En-Coding Standard." *Ogc*, 1–344.

Guelpa, Elisa, Ludovica Marincioni, and Vittorio Verda. 2019. "Towards 4th Generation District Heating: Prediction of Building Thermal Load for Optimal Management." *Energy* 171 (March): 510–22. https://doi.org/10.1016/j.energy.2019.01.056.

Halil, Faridah Muhamad, Nasyairi Mat Nasir, Ahmad Azlee Hassan, and Ani Saifuza Shukur. 2016. "Feasibility Study and Economic Assessment in Green Building Projects." *Procedia - Social and Behavioral Sciences* 222 (June): 56–64. https://doi.org/10.1016/j.sbspro.2016.05.176.

Hall, Lisa M.H., and Alastair R. Buckley. 2016. "A Review of Energy Systems Models in the UK: Prevalent Usage and Categorisation." *Applied Energy* 169 (May): 607–28. https://doi.org/10.1016/j.apenergy.2016.02.044.

Hansen, Kenneth. 2019. "Decision-Making Based on Energy Costs: Comparing Levelized Cost of Energy and Energy System Costs." *Energy Strategy Reviews* 24 (April): 68–82. https://doi.org/10.1016/j.esr.2019.02.003.

Happle, Gabriel, Jimeno A. Fonseca, and Arno Schlueter. 2018. "A Review on Occupant Behavior in Urban Building Energy Models." *Energy and Buildings*. https://doi.org/10.1016/j.enbuild.2018.06.030.

Hassine, Ilyes Ben, and Ursula Eicker. 2013. "Impact of Load Structure Variation and Solar Thermal Energy Integration on an Existing District Heating Network." In *Applied Thermal Engineering*, 50:1437–46. Pergamon. https://doi.org/10.1016/j.applthermaleng.2011.12.037.

Heat Pump & Thermal Storage Technology Center of Japan. 2010. "Survey of Availability of Heat Pumps in the Food and Beverage Sector." http://www.hptcj.or.jp/e/publication/tabid/360/Default.aspx.

Hennessy, Jay, Hailong Li, Fredrik Wallin, and Eva Thorin. 2018. "Towards Smart Thermal Grids:

Techno-Economic Feasibility of Commercial Heat-to-Power Technologies for District Heating." *Applied Energy* 228 (October): 766–76. https://doi.org/10.1016/j.apenergy.2018.06.105.

Hesaraki, Arefeh, Adnan Ploskic, and Sture Holmberg. 2015. "Integrating Low-Temperature Heating Systems into Energy Efficient Buildings." In *Energy Procedia*, 78:3043–48. Elsevier Ltd. https://doi.org/10.1016/j.egypro.2015.11.720.

Hong, Tianzhen, Jared Langevin, and Kaiyu Sun. 2018. "Building Simulation: Ten Challenges." *Building Simulation*. https://doi.org/10.1007/s12273-018-0444-x.

Hsieh, Shanshan, Akomeno Omu, and Kristina Orehounig. 2017. "Comparison of Solar Thermal Systems with Storage: From Building to Neighbourhood Scale." *Energy and Buildings* 152: 359–72. https://doi.org/10.1016/j.enbuild.2017.07.036.

Hu, Bin, R. Z. Wang, Biao Xiao, Lin He, Wei Zhang, and Shihang Zhang. 2019. "Performance Evaluation of Different Heating Terminals Used in Air Source Heat Pump System." *International Journal of Refrigeration* 98 (February): 274–82. https://doi.org/10.1016/j.ijrefrig.2018.10.014.

Huang, Shifang, Wangda Zuo, Huixia Lu, Caihua Liang, and Xiaosong Zhang. 2019. "Performance Comparison of a Heating Tower Heat Pump and an Air-Source Heat Pump: A Comprehensive Modeling and Simulation Study." *Energy Conversion and Management* 180: 1039–54. https://doi.org/10.1016/j.enconman.2018.11.050.

Intergovernmental Panel on Climate Change. 2014. *Climate Change 2014 Mitigation of Climate Change. Climate Change 2014 Mitigation of Climate Change*. Cambridge University Press. https://doi.org/10.1017/cbo9781107415416.

Jarre, M., M. Noussan, and M. Simonetti. 2018. "Primary Energy Consumption of Heat Pumps in High Renewable Share Electricity Mixes." *Energy Conversion and Management* 171 (September): 1339–51. https://doi.org/10.1016/j.enconman.2018.06.067.

Jesper, Mateo, Florian Schlosser, Felix Pag, Timothy Gordon Walmsley, Bastian Schmitt, and Klaus Vajen. 2021. "Large-Scale Heat Pumps: Uptake and Performance Modelling of Market-Available Devices." *Renewable and Sustainable Energy Reviews*.

https://doi.org/10.1016/j.rser.2020.110646.

Johari, F., G. Peronato, P. Sadeghian, X. Zhao, and J. Widén. 2020. "Urban Building Energy Modeling: State of the Art and Future Prospects." *Renewable and Sustainable Energy Reviews* 128 (September 2019). https://doi.org/10.1016/j.rser.2020.109902.

Jordan, Ulrike, and Klaus Vajen. 2017. "Tool for the Generation of Domestic Hot Water (DHW) Profiles on a Statistical Basis Version 2.02b."

Keirstead, James, Mark Jennings, and Aruna Sivakumar. 2012. "A Review of Urban Energy System Models: Approaches, Challenges and Opportunities." *Renewable and Sustainable Energy Reviews*. Pergamon. https://doi.org/10.1016/j.rser.2012.02.047.

Kim, Young Jin, Seong Hwan Yoon, and Cheol Soo Park. 2013. "Stochastic Comparison between Simplified Energy Calculation and Dynamic Simulation." *Energy and Buildings* 64 (September): 332–42. https://doi.org/10.1016/j.enbuild.2013.05.026.

Kontu, Kaisa. 2014. "District Heating and Cooling as Part of Smart Energy Systems." https://danskfjernvarme.dk/sitetools/english/climate-policy.

Lake, Andrew, Behanz Rezaie, and Steven Beyerlein. 2017. "Review of District Heating and Cooling Systems for a Sustainable Future." *Renewable and Sustainable Energy Reviews*. Elsevier Ltd. https://doi.org/10.1016/j.rser.2016.09.061.

Larsen, Helge V., Halldór Pálsson, Benny Bøhm, and Hans F. Ravn. 2002. "Aggregated Dynamic Simulation Model of District Heating Networks." *Energy Conversion and Management* 43 (8): 995–1019. https://doi.org/10.1016/S0196-8904(01)00093-0.

Lee, Susanne. 2018. "An Overview of the European Technical Guidelines for the Prevention, Control and Investigation of Infections Caused by Legionella Species." *Perspectives in Public Health*. Vol. 138. Stockholm. https://doi.org/10.1177/1757913918790922.

Li, Peifeng, Natasa Nord, Ivar Ståle Ertesvåg, Zhihua Ge, Zhiping Yang, and Yongping Yang. 2015. "Integrated Multiscale Simulation of Combined Heat and Power Based District Heating System." *Energy Conversion and Management* 106: 337–54. https://doi.org/10.1016/j.enconman.2015.08.077.

Lindholm, Oscar, Hassam Ur Rehman, and Francesco Reda. 2021. "Positioning Positive Energy Districts in European Cities." *Buildings* 11 (1): 1–31. https://doi.org/10.3390/buildings11010019.

Lizana, Jesús, Ricardo Chacartegui, Angela Barrios-Padura, and José Manuel Valverde. 2017. "Advances in Thermal Energy Storage Materials and Their Applications towards Zero Energy Buildings: A Critical Review." *Applied Energy*. https://doi.org/10.1016/j.apenergy.2017.06.008.

Lund, H., B. Möller, B. V. Mathiesen, and A. Dyrelund. 2010. "The Role of District Heating in Future Renewable Energy Systems." *Energy* 35 (3): 1381–90. https://doi.org/10.1016/j.energy.2009.11.023.

Lund, Henrik, Sven Werner, Robin Wiltshire, Svend Svendsen, Jan Eric Thorsen, Frede Hvelplund, and Brian Vad Mathiesen. 2014. "4th Generation District Heating (4GDH). Integrating Smart Thermal Grids into Future Sustainable Energy Systems." *Energy* 68: 1–11. https://doi.org/10.1016/j.energy.2014.02.089.

Lund, Rasmus, Danica Djuric Ilic, and Louise Trygg. 2016. "Socioeconomic Potential for Introducing Large-Scale Heat Pumps in District Heating in Denmark." *Journal of Cleaner Production* 139: 219–29. https://doi.org/10.1016/j.jclepro.2016.07.135.

Lund, Rasmus, Dorte Skaarup Østergaard, Xiaochen Yang, and Brian Vad Mathiesen. 2017. "Comparison of Low-Temperature District Heating Concepts in a Long-Term Energy System Perspective." *International Journal of Sustainable Energy Planning and Management* 12 (March): 5–18. https://doi.org/10.5278/ijsepm.2017.12.2.

Mai, Trieu, Jeffrey Logan, Nate Blair, Patrick Sullivan, and Morgan Bazilian. 2013. "RE-ASSUME: A Decision Maker's Guide to Evaluating Energy Scenarios, Modeling, and Assumptions Implementing Body: National Renewable Energy Laboratory." *National Renewable Energy Laboratory, Golden CO, USA*, no. January 2015: 1–73.

Maritime Geothermal. 2018. "Commercial W-Series & WH-Series Water to Water Heat Pumps - Installation and Service Manual."

Mohajeri, Nahid, Dan Assouline, Berenice Guiboud, Andreas Bill, Agust Gudmundsson, and Jean

Louis Scartezzini. 2018. "A City-Scale Roof Shape Classification Using Machine Learning for Solar Energy Applications." *Renewable Energy* 121: 81–93. https://doi.org/10.1016/j.renene.2017.12.096.

Monsalvete, Pilar, Darren Robinson, and Ursula Eicker. 2015. "Dynamic Simulation Methodologies for Urban Energy Demand." In *Energy Procedia*, 78:3360–65. Elsevier Ltd. https://doi.org/10.1016/j.egypro.2015.11.751.

Montr, Sustainable. 2020. "Sustainable Montréal 2016-2020."

Mustafa Omer, Abdeen. 2008. "Ground-Source Heat Pumps Systems and Applications." *Renewable and Sustainable Energy Reviews*. Pergamon. https://doi.org/10.1016/j.rser.2006.10.003.

Nordman, R, O Kleefkens, P Riviere, T Nowak, A Zottl, C Arzano-Daurelle, A Lehmann, et al. 2009. "Seasonal Performance Factor and Monitoring for Heat Pump Systems in the Building Sector SEPEMO-Final Report."

NREL. 2018. "Building Component Library." National Renewable Energy Laboratory. 2018. https://bcl.nrel.gov/.

Østergaard, Dorte Skaarup, and Svend Svendsen. 2016. "Theoretical Overview of Heating Power and Necessary Heating Supply Temperatures in Typical Danish Single-Family Houses from the 1900s." *Energy and Buildings* 126: 375–83. https://doi.org/10.1016/j.enbuild.2016.05.034.

Østergaard, Poul Alberg, and Henrik Lund. 2011. "A Renewable Energy System in Frederikshavn Using Low-Temperature Geothermal Energy for District Heating." *Applied Energy* 88 (2): 479–87. https://doi.org/10.1016/j.apenergy.2010.03.018.

Petkov, Ivalin, and Paolo Gabrielli. 2020. "Power-to-Hydrogen as Seasonal Energy Storage: An Uncertainty Analysis for Optimal Design of Low-Carbon Multi-Energy Systems." *Applied Energy* 274. https://doi.org/10.1016/j.apenergy.2020.115197.

Pfenninger, Stefan. 2017. "Dealing with Multiple Decades of Hourly Wind and PV Time Series in Energy Models: A Comparison of Methods to Reduce Time Resolution and the Planning

Implications of Inter-Annual Variability." *Applied Energy* 197 (July): 1–13. https://doi.org/10.1016/j.apenergy.2017.03.051.

Pfenninger, Stefan, Adam Hawkes, and James Keirstead. 2014. "Energy Systems Modeling for Twenty-First Century Energy Challenges." *Renewable and Sustainable Energy Reviews*. Elsevier Ltd. https://doi.org/10.1016/j.rser.2014.02.003.

Pietra, B. Di, F. Zanghirella, and G. Puglisi. 2015. "An Evaluation of Distributed Solar Thermal 'Net Metering' in Small-Scale District Heating Systems." In *Energy Procedia*, 78:1859–64. Elsevier Ltd. https://doi.org/10.1016/j.egypro.2015.11.335.

Pilpola, Sannamari, Vahid Arabzadeh, Jani Mikkola, and Peter D. Lund. 2019. "Analyzing National and Local Pathways to Carbon-Neutrality from Technology, Emissions, and Resilience Perspectives—Case of Finland." *Energies* 12 (5). https://doi.org/10.3390/en12050949.

Pless, Shanti, and Ben Polly. 2018. "Communities of the Future : Accelerating Zero Energy District Master Planning Preprint," no. September.

Pomianowski, M Z, H Johra, A Marszal-Pomianowska, and C Zhang. 2020. "Sustainable and Energy-Efficient Domestic Hot Water Systems: A Review." *Renewable and Sustainable Energy Reviews* 128: 109900. https://doi.org/10.1016/j.rser.2020.109900.

Rao, Sagar, David Conant-Gilles, Yiyuan Jia, and Brittany Carl. 2018. "Rapid Modeling of Large and Complex High Performance Buildings Using Energyplus." In *SimBuild 2018*, 9–16.

Reinhart, Christoph F., and Carlos Cerezo Davila. 2016. "Urban Building Energy Modeling - A Review of a Nascent Field." *Building and Environment*. https://doi.org/10.1016/j.buildenv.2015.12.001.

Remmen, Peter, Moritz Lauster, Michael Mans, Marcus Fuchs, Tanja Osterhage, and Dirk Müller. 2018. "TEASER: An Open Tool for Urban Energy Modelling of Building Stocks." *Journal of Building Performance Simulation* 11 (1): 84–98. https://doi.org/10.1080/19401493.2017.1283539.

Renaldi, R., A. Kiprakis, and D. Friedrich. 2017. "An Optimisation Framework for Thermal

Energy Storage Integration in a Residential Heat Pump Heating System." *Applied Energy* 186 (January): 520–29. https://doi.org/10.1016/j.apenergy.2016.02.067.

Ringkjøb, Hans Kristian, Peter M. Haugan, and Ida Marie Solbrekke. 2018. "A Review of Modelling Tools for Energy and Electricity Systems with Large Shares of Variable Renewables." *Renewable and Sustainable Energy Reviews*. Elsevier Ltd. https://doi.org/10.1016/j.rser.2018.08.002.

Rinne, S, and S Syri. 2013. "Heat Pumps versus Combined Heat and Power Production as CO2 Reduction Measures in Finland." *Energy* 57: 308–18. https://doi.org/10.1016/j.energy.2013.05.033.

Saber, Esmail M., Kwok Wai Tham, and Hansjürg Leibundgut. 2016. "A Review of High Temperature Cooling Systems in Tropical Buildings." *Building and Environment*. Elsevier Ltd. https://doi.org/10.1016/j.buildenv.2015.11.029.

Safa, Amir A., Alan S. Fung, and Rakesh Kumar. 2015. "Comparative Thermal Performances of a Ground Source Heat Pump and a Variable Capacity Air Source Heat Pump Systems for Sustainable Houses." *Applied Thermal Engineering* 81 (April): 279–87. https://doi.org/10.1016/j.applthermaleng.2015.02.039.

Sarbu, Ioan, and Calin Sebarchievici. 2014. "General Review of Ground-Source Heat Pump Systems for Heating and Cooling of Buildings." *Energy and Buildings*. Elsevier Ltd. https://doi.org/10.1016/j.enbuild.2013.11.068.

Sarfraz, Omer, Christian K. Bach, and Christopher K. Wilkins. 2018. "Plug Load Design Factors." *ASHRAE Journal* 60 (1): 14–19.

Shakerin, Mohammad. 2017. "Analysis of District Heating Systems Integrating Distributed Sources Mohammad Shakerin," no. May. https://ntnuopen.ntnu.no/ntnu-xmlui/handle/11250/2454936.

Sinha, Sunanda, and S. S. Chandel. 2014. "Review of Software Tools for Hybrid Renewable Energy Systems." *Renewable and Sustainable Energy Reviews*. Pergamon. https://doi.org/10.1016/j.rser.2014.01.035.

Soutullo, S, L. A. Bujedo, J Samaniego, D. Borge, J. A. Ferrer, R. Carazo, and M. R. Heras. 2016. "Energy Performance Assessment of a Polygeneration Plant in Different Weather Conditions through Simulation Tools." *Energy and Buildings* 124: 7–18. https://doi.org/10.1016/j.enbuild.2016.04.031.

Spreiregen, Paul D, and De Paz Beatriz. 2007. *Pre-Design*. Chicago, IL : Kaplan AEC Education,.

Strzalka, Aneta, Jürgen Bogdahn, Volker Coors, and Ursula Eicker. 2011. "3D City Modeling for Urban Scale Heating Energy Demand Forecasting." *HVAC and R Research* 17 (4): 526–39. https://doi.org/10.1080/10789669.2011.582920.

Tabar, Vahid Sohrabi, Mehrdad Tarafdar Hagh, and Mehdi Ahmadi Jirdehi. 2021. "Achieving a Nearly Zero Energy Structure by a Novel Framework Including Energy Recovery and Conversion, Carbon Capture and Demand Response." *Energy and Buildings* 230. https://doi.org/10.1016/j.enbuild.2020.110563.

Talebi, Behrang, Parham A. Mirzaei, Arash Bastani, and Fariborz Haghighat. 2016. "A Review of District Heating Systems: Modeling and Optimization." *Frontiers in Built Environment* 2 (October): 22. https://doi.org/10.3389/fbuil.2016.00022.

Tanguay, Denis. 2016. "Fundamental Economic Analysis of Ground Source Heat Pump Markets in North America." *12th IEA Heat Pump Conference (2017)*, 1–11.

The Engineering ToolBox. 2017. "Maximum Flow Velocities in Water Systems." The Engineering Toolbox. 2017. https://www.engineeringtoolbox.com/flow-velocity-water-pipes-d_385.html.

Thomaßen, Georg, Konstantinos Kavvadias, and Juan Pablo Jiménez Navarro. 2021. "The Decarbonisation of the EU Heating Sector through Electrification: A Parametric Analysis." *Energy Policy* 148. https://doi.org/10.1016/j.enpol.2020.111929.

Trane. 2015. "Multi-Pipe Units with Scroll Compressors, Model CMAA 012 to 140."

U.S. Department of Energy. 2020. "EnergyPlus | EnergyPlus." U.S. Department of Energy's. 2020. https://energyplus.net/.

US DOE. 2013. "Commercial Prototype Building Models | Building Energy Codes Program." U.S.

Department of Energy. 2013.

Vesaoja, Eero, Heikki Nikula, Seppo Sierla, Tommi Karhela, Paul G. Flikkema, and Chen Wei Yang. 2014. "Hybrid Modeling and Co-Simulation of District Heating Systems with Distributed Energy Resources." In *2014 Workshop on Modeling and Simulation of Cyber-Physical Energy Systems, MSCPES 2014 - Held as Part of CPS Week, Proceedings*. IEEE Computer Society. https://doi.org/10.1109/MSCPES.2014.6842395.

Wang, Cheng, Ye Zhu, and Xiaofeng Guo. 2019. "Thermally Responsive Coating on Building Heating and Cooling Energy Efficiency and Indoor Comfort Improvement." *Applied Energy* 253 (November): 113506. https://doi.org/10.1016/j.apenergy.2019.113506.

Weiler, Verena, Jonas Stave, and Ursula Eicker. 2019. "Renewable Energy Generation Scenarios Using 3D Urban Modeling Tools—Methodology for Heat Pump and Co-Generation Systems with Case Study Application." *Energies* 12 (3). https://doi.org/10.3390/en12030403.

Welsch, Manuel, Paul Deane, Mark Howells, Brian O Gallachóir, Fionn Rogan, Morgan Bazilian, and Hans Holger Rogner. 2014. "Incorporating Flexibility Requirements into Long-Term Energy System Models - A Case Study on High Levels of Renewable Electricity Penetration in Ireland." *Applied Energy* 135 (December): 600–615. https://doi.org/10.1016/j.apenergy.2014.08.072.

Wilkins, C.; Hosni, M. 2011. "Plug Load Design Factors." *ASHRAE Journal*, no. 53: 30–34.

Wiseman, John. 2018. "The Great Energy Transition of the 21st Century: The 2050 Zero-Carbon World Oration." *Energy Research and Social Science* 35 (October): 227–32. https://doi.org/10.1016/j.erss.2017.10.011.

Xu, Wei, Changping Liu, Angui Li, Ji Li, and Biao Qiao. 2020. "Feasibility and Performance Study on Hybrid Air Source Heat Pump System for Ultra-Low Energy Building in Severe Cold Region of China." *Renewable Energy* 146: 2124–33. https://doi.org/10.1016/j.renene.2019.08.079.

Yang, Xiaochen, and Svend Svendsen. 2018. "Ultra-Low Temperature District Heating System with Central Heat Pump and Local Boosters for Low-Heat-Density Area: Analyses on a Real Case in Denmark." *Energy* 159: 243–51. https://doi.org/10.1016/j.energy.2018.06.068.

Yazdanie, M., and K. Orehounig. 2021. "Advancing Urban Energy System Planning and Modeling Approaches: Gaps and Solutions in Perspective." *Renewable and Sustainable Energy Reviews*. Elsevier Ltd. https://doi.org/10.1016/j.rser.2020.110607.

Yuan, Jiaqi, Chengliao Cui, Ziwei Xiao, Chong Zhang, and Wenjie Gang. 2020. "Performance Analysis of Thermal Energy Storage in Distributed Energy System under Different Load Profiles." *Energy Conversion and Management* 208. https://doi.org/10.1016/j.enconman.2020.112596.

Yunna, Wu, and Xu Ruhang. 2013. "Green Building Development in China-Based on Heat Pump Demonstration Projects." *Renewable Energy*. Pergamon. https://doi.org/10.1016/j.renene.2012.11.021.

Zoellner, Jan, Petra Schweizer-Ries, and Christin Wemheuer. 2008. "Public Acceptance of Renewable Energies: Results from Case Studies in Germany." *Energy Policy* 36 (11): 4136–41. https://doi.org/10.1016/j.enpol.2008.06.026.

Appendix

In this section an example from one of the used models are shown which is the output of INSEL's text output. INSEL automatically translate the connections and parameters in the graphical user interface to text files which can be the linkage between INSEL and other software like Python.

The following screenshot and INSEL text file are for the case study-3, explained in chapter 4. The model includes 70 ton heat pumps for heating and cooling and 6 ton heat pumps for domestic hot water production. An auxiliary electrical heater is used when the heat pumps' out put is not sufficient to cover demands. Rest of the model is similar to what was discussed in previous chapters including PV system, Heat pump system, and DHW generation. Battery and thermal storages are available in the model, however, their capacities are considered zero as they are used in the case study.

As discussed in the previous chapters, the model can either round up the number HPs for heating to have excessive heat, or round it down and the heat deficit to be covered by auxiliary electrical heater. In case of having excessive energy, after meeting the demands, the extra energy can either get directed to DHW tank, or stored in the thermal storage to justify the next time-step's energy production, or use at a later desired situation (e.g., accumulate energy until the storage capacity reaches an specific value).
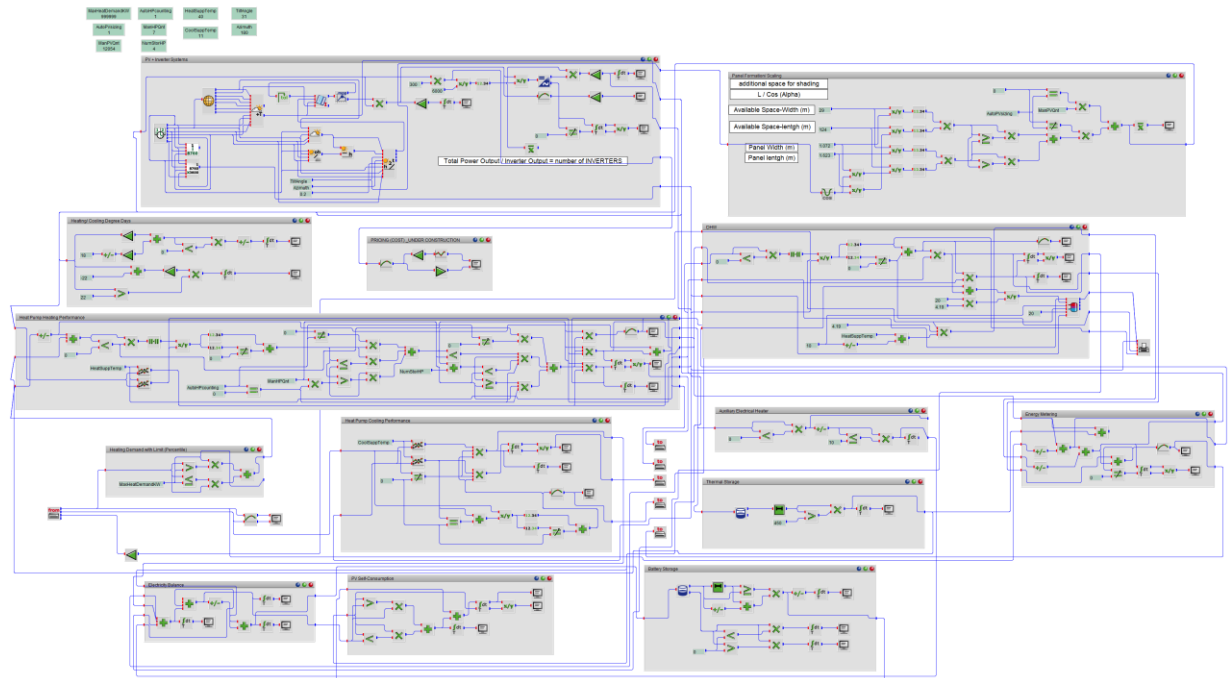
Figure 1 Screenshot from INSEL graphical user interface of the used model

B 15 PLOT

  308.1

  302.1

P 15

  'insel.gnu'   % Gnuplot file name

B 16 MUL

  302.8

  77.1

B 17 MUL

  170.2

  147.1

B 18 MUL

  211.1

  199.1

B 19 MUL

  21.1

  177.1

B 20 MUL

  207.1

  148.1

B 21 MUL

  252.1

  257.1

B 22 MUL   % Number of Inverters

  258.1

  309.1

B 23 MUL   % HP Electricity Demand (kW) (Cooling)

262.1

217.1

205.1

B 24 MUL

  266.1

  65.1

B 25 MUL

  170.2

  176.1

B 26 MUL

  200.1

  216.1

B 27 MUL

  313.1

304.1

B 28 MUL   % HPs Heat Output HEATING(kW)

188.1

261.1

B 29 MUL   % HEAT PUMP OUTPUT (DHW) (kW)

201.1

260.1

B 30 MUL

197.1

149.1

B 31 MUL

227.1

172.1

B 32 MUL

306.1

196.1

B 33 MUL

45.1

173.1

B 34 MUL

179.1

304.1

B 35 MUL   % To electric heater

77.1

223.1

195.1

B 36 MUL   % Number of Panels (Scaling)

315.2

183.1

B 37 MUL   % HP Cooling Output (kW)

263.1

217.1

205.1

B 38 MUL

187.1

144.1

B 39 MUL

253.1

256.1

B 40 MUL

64.1

171.1

B 41 MUL

183.1

93.1

B 42 MUL

218.1

204.1

B 43 MUL

305.1

74.1

268.1

B 44 MUL   % HPs Electricity Demand (Heating-kW)

188.1

264.1

B 45 MUL

74.1

268.1

B 46 MUL   % DHW Energy Demand (10Cto 40C) (kW)

223.1

77.1

198.1

B 47 MUL

175.1

193.1

B 48 MUL

190.1

174.1

B 49 MUL

182.1

145.1

B 50 MUL

220.1

142.1

B 51 MUL

39.1

307.1

B 52 MUL   % HP Electricity Demand (DHW) (kW)

201.1

265.1

B 53 MUL

199.1

314.1

B 54 MUL

143.1

184.1

146.1

268.1

B 55 MUL

178.1

206.1

B 56 CONST   % Heating Supply Temperature (C)

P 56

HeatSuppTemp   % Constant value

B 57 CONST

P 57

0   % Constant value

B 58 CONST   % Panel Width (m)

P 58

1.072   % Constant value

B 59 CONST

P 59

0   % Constant value

B 60 CONST

P 60

0   % Constant value

B 61 CONST

P 61

0   % Constant value

B 62 CONST   % base temperature (C)

P 62

22   % Constant value

B 63 CONST

P 63

0   % Constant value

B 64 CONST

P 64

MaxHeatDemandKW   % Constant value

B 65 CONST

P 65

ManPVQnt   % Constant value

B 66 CONST   % base temperature (C)

P 66

-22   % Constant value

B 67 CONST   % HP Supply Temperature (C) (Cooling)

P 67

CoolSuppTemp   % Constant value

B 68 CONST   % Azimuth Degree

P 68

Azimuth   % Constant value

B 69 CONST   % Tilt angle

P 69

TiltAngle   % Constant value

B 70 CONST   % Available Space-Width (m)

P 70

29   % Constant value

B 71 CONST

P 71

AutoHPcounting   % Constant value

B 72 CONST

P 72

0   % Constant value

B 73 CONST   % Inverter Nominal Capacity (W)

P 73

6000   % Constant value

B 74 CONST

P 74

ManHPQnt   % Constant value

B 75 CONST   % base temperature (C)

P 75

18   % Constant value

B 76 CONST

P 76

0   % Constant value

B 77 CONST   % Cp water (kJ/kgC)

P 77

4.19   % Constant value

B 78 CONST

P 78

```
        0          % Constant value

B 79 CONST

P 79

        0          % Constant value


B 80 CONST

P 80

        0          % Constant value


B 81 CONST

P 81

        0          % Constant value


B 82 CONST

P 82

        0          % Constant value


B 83 CONST

P 83

        AutoPVsizing      % Constant
value


B 84 CONST

P 84

        100        % Constant value


B 85 CONST

P 85

        0          % Constant value


B 86 CONST

P 86

        0          % Constant value


B 87 CONST        % HP Supply
Temperature (C) (Heating)

        P 87
```

```
        HeatSuppTemp      % Constant
value


        B 88 CONST        % Panel lentgh
(m)

P 88

        1.623        % Constant value


B 89 CONST

P 89

        NumStorHP         % Constant
value


        B 90 CONST        % Available
Space-lentgh (m)

        P 90

        124        % Constant value


        B 91 CONST        % HP Supply
Temperature (C) (Heating)

        P 91

        HeatSuppTemp      % Constant
value


        B 92 CONST        % City Cold
water Temperature (C)

        P 92

        10         % Constant value


        B 93 CONST        % PV Panel
Nominal Power (W)

        P 93

        300        % Constant value


B 94 CONST

P 94

        0.2        % Constant value


B 95 CONST

P 95

        0          % Constant value
```

```
        B 96 CONST        % Environment
Temp (C)

P 96

        20         % Constant value


        B 97 SCREEN       % Total AC
Electricity Generation (kWh/yr)

        244.1

P 97

        '*'        % Format

        'Total AC Electricity Generation
(kWh/yr)' % Headline


        B 98 SCREEN       % HP DHW
Seasonal COP

        165.1

P 98

        '*'        % Format

        'HP DHW Seasonal COP' %
Headline


        B 99 SCREEN       % Total HP
Electricity Demand (kWh/yr)

        245.1

P 99

        '*'        % Format

        'Total HP Electricity Demand
(kWh/yr)' % Headline


        B 100 SCREEN          % HP
Heating Seasonal COP

        151.1

P 100

        '*'        % Format

        'HP Heating Seasonal COP' %
Headline


        B 101 SCREEN          % Total
Battery Discharge (kWh/yr)

        249.1

P 101
```

'*'   % Format

'Total   Battery   Discharge
(kWh/yr)' % Headline

B 102 SCREEN   % Total
DHW Demand (kWh/yr)

233.1

P 102

'*'   % Format

'Total DHW Demand (kWh/yr)'
% Headline

B 103 SCREEN   % Total Self-
Consumption- INC. Battery(kWh/yr)

240.1

P 103

'*'   % Format

'Total Self-Consumption- INC.
Battery(kWh/yr)' % Headline

B 104 SCREEN   % MAX
EXCESSIVE ENERGY(kWh)

284.1

P 104

'*'   % Format

'MAX   EXCESSIVE
ENERGY(kWh)' % Headline

B 105 SCREEN   % Cooling
Degree Days

251.1

P 105

'*'   % Format

'Cooling   Degree   Days'   %
Headline

B 106 SCREEN   % PV Self-
Consumption-INC.Battery (%)

160.1

P 106

'*'   % Format

'PV   Self-Consumption-
INC.Battery (%)' % Headline

B 107 SCREEN   % Number
of Heat Pumps (Cooling)

288.1

P 107

'*'   % Format

'Number of   Heat   Pumps
(Cooling)' % Headline

B 108 SCREEN   % Electricity
Balance (kWh/yr)

250.1

P 108

'*'   % Format

'Electricity   Balance   (kWh/yr)'
% Headline

B 109 SCREEN   % HP
Electricity Demand (kWh/yr) (DHW)

243.1

P 109

'*'   % Format

'HP   Electricity   Demand
(kWh/yr) (DHW)' % Headline

B 110 SCREEN   % Total Th-
Storage Discharge (kWh/yr)

248.1

P 110

'*'   % Format

'Total   Th-Storage   Discharge
(kWh/yr)' % Headline

B 111 SCREEN   % PV cost
(Interpolation)/ Fixed Estimated cost (2.7
$/W)

312.1

292.1

P 111

'*'   % Format

'PV cost (Interpolation)/ Fixed
Estimated cost (2.7 $/W)' % Headline

B 112 SCREEN   %
AVERAGE   EXCESSIVE   ENERGY
(kWh)

167.1

P 112

'*'   % Format

'AVERAGE   EXCESSIVE
ENERGY (kWh)' % Headline

B 113 SCREEN   % Total
EXCESSIVE ENERGY (KWH/YR)

247.1

P 113

'*'   % Format

'Total EXCESSIVE ENERGY
(KWH/YR)' % Headline

B 114 SCREEN   % HP
Cooling Seasonal COP

162.1

P 114

'*'   % Format

'HP Cooling Seasonal COP' %
Headline

B 115 SCREEN   % Maximum
PV Generation (kWh)

221.1

P 115

'*'   % Format

'Maximum   PV   Generation
(kWh)' % Headline

B 116 SCREEN   % Heating
Degree Days

237.1

P 116

'*'   % Format

'Heating   Degree   Days'   %
Headline

B 117 SCREEN   % Aux. Electric. Heater Demand (kWh/yr)

229.1

P 117

'*'   % Format

'Aux. Electric. Heater Demand (kWh/yr)' % Headline

B 118 SCREEN   % Inverter Average Efficiency

152.1

P 118

'*'   % Format

'Inverter Average Efficiency' % Headline

B 119 SCREEN   % Total PV Direct Use (kWh/yr)

236.1

P 119

'*'   % Format

'Total PV Direct Use (kWh/yr)' % Headline

B 120 SCREEN   % Maximum Heating/ Cooling Demand (kW)

285.1

285.2

P 120

'*'   % Format

'Maximum Heating/ Cooling Demand (kW)' % Headline

B 121 SCREEN   % Number of Panels

270.1

P 121

'*'   % Format

'Number of Panels' % Headline

B 122 SCREEN   % Total Electricity Demand (kWh/yr)

234.1

P 122

'*'   % Format

'Total Electricity Demand (kWh/yr)' % Headline

B 123 SCREEN   % Electricity Exported to Grid (kWh/yr)

238.1

P 123

'*'   % Format

'Electricity Exported to Grid (kWh/yr)' % Headline

B 124 SCREEN   % SEASONAL PERFORMANCE FACTOR

168.1

P 124

'*'   % Format

'SEASONAL PERFORMANCE FACTOR' % Headline

B 125 SCREEN   % Electricity from Grid (kWh/yr)

230.1

P 125

'*'   % Format

'Electricity from Grid (kWh/yr)' % Headline

B 126 SCREEN   % Number of Heat Pumps (DHW)

283.1

P 126

'*'   % Format

'Number of Heat Pumps (DHW)' % Headline

B 127 SCREEN   % HP Electricity Demand (kWh/yr) (Cooling)

235.1

P 127

'*'   % Format

'HP Electricity Demand (kWh/yr) (Cooling)' % Headline

B 128 SCREEN   % HP Electricity Consumption (kWh/yr) (Heating)

241.1

P 128

'*'   % Format

'HP Electricity Consumption (kWh/yr) (Heating)' % Headline

B 129 SCREEN   % Number of Heat Pumps (Heating)

286.1

P 129

'*'   % Format

'Number of Heat Pumps (Heating)' % Headline

B 130 SCREEN   % Total PV Generation (kWh/yr)

228.1

P 130

'*'   % Format

'Total PV Generation (kWh/yr)' % Headline

B 131 CHS

38.1

B 132 CHS   % (-)Total Electricity Demand (kW)

193.1

B 133 CHS

32.1

96

B 134 CHS
170.1

B 135 CHS
92.1

B 136 CHS   % (-) heating demand
185.1

B 137 CHS
185.1

B 138 CHS
169.1

B 139 CHS
302.1

B 140 CHS   % (-) DHW demand
46.1

B 141 CHS
75.1

B 142 LT
220.1
193.1

B 143 LT
200.1
74.1

B 144 LT
187.1
72.1

B 145 LT
182.1
79.1

B 146 LT
184.1
74.1

B 147 LT
170.2
63.1

B 148 LT
207.1
86.1

B 149 LT
197.1
61.1

B 150 DIV
295.1
260.1

B 151 DIV   % HP Heating Seasonal COP
239.1
239.2

B 152 DIV
232.1
232.2

B 153 DIV
90.1
157.1

B 154 DIV

36.1
258.1

B 155 DIV
70.1
88.1

B 156 DIV
304.2
186.1

B 157 DIV
88.1
291.1

B 158 DIV
90.1
161.1

B 159 DIV
294.1
261.1

B 160 DIV   % PV Self-Consumption-INC.Battery (%)
240.1
240.2

B 161 DIV
58.1
291.1

B 162 DIV
246.1
246.2

B 163 DIV
48.1

16.1

B 164 DIV

41.1

73.1

B 165 DIV   % HP DHW Seasonal COP

231.1

231.2

B 166 DIV

70.1

58.1

B 167 DIV   % AVERAGE EXCESSIVE ENERGY (kWh)

247.1

247.2

B 168 DIV

242.1

242.2

B 169 BUCKET   % Thermal Storage

189.1

P 169

0   % Minimum contents

0   % Maximum contents

0   % Initial contents

B 170 BUCKET   % Battery Storage

192.1

P 170

0   % Minimum contents

0   % Maximum contents

0   % Initial contents

B 171 GT

304.1

64.1

B 172 GT

310.2

62.1

B 173 GT

199.1

45.1

B 174 GT

190.1

82.1

B 175 GT

220.1

193.1

B 176 GT

170.2

63.1

B 177 GT

21.1

39.1

B 178 GT

208.1

169.1

B 179 GT

304.1

84.1

B 180 SUM   % Total PV Direct Use (kWh/yr)

47.1

50.1

B 181 SUM   % Total HP Electricity Demand(HEAT/COOL/DHW) (kW)

44.1

23.1

52.1

B 182 SUM   % Storage Dis + (-) Heating Demand

137.1

209.1

B 183 SUM

24.1

42.1

B 184 SUM

200.1

89.1

B 185 SUM   % Heating Demand (kW)

34.1

B 186 SUM

263.1

267.1

B 187 SUM

224.1

225.1

B 188 SUM   % Total Number of Heat Pumps (Heating)

26.1

54.1

43.1

B 189 SUM

30.1

29.1

B 190 SUM   % Heating HP output + DHW HP output (-) Heating demand

28.1

136.1

29.1

B 191 SUM   % Battery Discharged Amount (kW)

32.1

180.1

B 192 SUM   % Electricity Generation - Electricity Demand (kW)

132.1

220.1

B 193 SUM   % Total Electricity Demand (kW)

293.1

181.1

B 194 SUM   % Heating HP + DHW HP + Aux. elec. heater Electricity Consumption

52.1

44.1

293.1

B 195 SUM

139.1

56.1

B 196 SUM

210.1

134.1

B 197 SUM

28.1

136.1

140.1

B 198 SUM

56.1

135.1

B 199 SUM   % First Stage-Number of Heat Pumps (Heating)

255.1

B 200 SUM   % Number of Heat Pumps (Heating)

18.1

53.1

33.1

B 201 SUM   % Number of Heat Pumps (DHW)

254.1

B 202 SUM

310.2

66.1

B 203 SUM   % HEATING + DHW DEMAND (kW)

185.1

46.1

B 204 SUM

51.1

19.1

B 205 SUM   % Number of Heat Pumps (Cooling)

259.1

213.1

B 206 SUM

208.1

138.1

B 207 SUM

29.1

30.1

B 208 DELAY

169.1

P 208

0   % Initial value

B 209 DELAY

55.1

P 209

0   % Initial value

B 210 DELAY

170.1

P 210

0   % Initial value

B 211 NE

57.1

71.1

P 211

0   % Error tolerance

B 212 NE

189.1

76.1

P 212

    0   % Error tolerance

B 213 NE

    299.1

    95.1

P 213

    0   % Error tolerance

B 214 NE

    297.1

    80.1

P 214

    0   % Error tolerance

B 215 NE

    309.2

    81.1

P 215

    0   % Error tolerance

B 216 NE

    71.1

    59.1

P 216

    0   % Error tolerance

B 217 NE

    304.2

    95.1

P 217

    0   % Error tolerance

B 218 NE

    60.1

    83.1

P 218

    0   % Error tolerance

B 219 NE

    298.1

    85.1

P 219

    0   % Error tolerance

B 220 ATT   % W to kW

    22.1

P 220

    1000   % Attenuation factor
a

B 221 ATT   % W to kW

    287.1

P 221

    1000   % Attenuation factor
a

B 222 ATT   % W to kW

    289.1

P 222

    1000   % Attenuation factor
a

B 223 ATT   % DHW lit/hr to lit/s

    304.3

P 223

    3600   % Attenuation factor
a

B 224 ATT   % 1 hour of a day (1/24)

    310.2

P 224

    24   % Attenuation factor
a

B 225 ATT   % 1 hour of a day (1/24)

    141.1

P 225

    24   % Attenuation factor
a

B 226 ATT   % W to kW

    36.1

P 226

    1000   % Attenuation factor
a

B 227 ATT   % 1 hour of a day (1/24)

    202.1

P 227

    24   % Attenuation factor
a

B 228 CUM   % Total PV Generation (kWh/yr)

    226.1

B 229 CUM   % Total Auxiliary Heater Required Output (kWh/yr)

    293.1

B 230 CUM   % Electricity from Grid (kW)

    17.1

B 231 CUM   % HP DHW Seasonal COP

    29.1

    52.1

B 232 CUM

    309.2

    215.1

B 233 CUM

46.1

B 234 CUM   % Total
Electricity Demand (kWh/yr)

193.1

B 235 CUM   % HP
Electricity Demand (kW) (Cooling)

23.1

B 236 CUM   % Total PV
Direct Use (kWh/yr)

180.1

B 237 CUM

131.1

B 238 CUM   % Electricity
Exported to Grid (kWh/yr)

25.1

B 239 CUM   % HP Heating
Seasonal COP

28.1

44.1

B 240 CUM

191.1

220.1

B 241 CUM   % HP
Electricity Demand (kWh/yr) (Heating)

44.1

B 242 CUM

203.1

194.1

B 243 CUM   % HP
Electricity Demand (kWh/yr) (DHW)

52.1

B 244 CUM   % Total AC
Electricity Generation (kWh/yr)

220.1

B 245 CUM   % Total HP
Electricity Demand (kWh/yr)

181.1

B 246 CUM

37.1

23.1

B 247 CUM

189.1

212.1

B 248 CUM

55.1

B 249 CUM   % Total Battery
Discharge (kWh/yr)

133.1

B 250 CUM   % Electricity
Balance (kWh/yr)

192.1

B 251 CUM

31.1

B 252 INT

155.1

B 253 INT

166.1

B 254 INT

150.1

B 255 INT

159.1

B 256 INT

153.1

B 257 INT

158.1

B 258 INT

164.1

B 259 INT

156.1

B 260 POLYG2   % Tsupply
Tsource Heat_Output (Heating)

87.1

310.2

P 260

    0   % Mode

    8   % Number of nodes

    40 -30 15

40 -25 17

40 -5 19.5

40 0 22.25

40 7 26.55

40 10 28.65

40 15 32.45

40 25 33.5 % p x y coordinates

B 261 POLYG2   % Tsupply
Tsource Heat_Output (Heating)

91.1

310.2

P 261

  0   % Mode

  8   % Number of nodes

  40 -30 80

40 -25 83

40 -5 89.9

40 0 102.2

40 7 121.6

40 10 131.1

40 15 148.4

40 25 156 % p x y coordinates

    B 262 POLYG2   % Tsupply Tsource Pelec (Cooling)(kW)

  67.1

  310.2

P 262

  0   % Mode

  8   % Number of nodes

  11 15 49

11 20 50

11 25 51.5

11 30 57.1

11 32 59.6

11 35 63.5

11 40 70.8

11 45 78.8 % p x y coordinates

    B 263 POLYG2   % Tsupply Tsource Heat_Output (Cooling)

  67.1

  310.2

P 263

  0   % Mode

  8   % Number of nodes

  11 15 260

11 20 255

11 25 252.7

11 30 238.6

11 32 232.8

11 35 223.6

11 40 208.2

11 45 191.6 % p x y coordinates

    B 264 POLYG2   % Tsupply Tsource Pelec (Heating)(kW)

  91.1

  310.2

P 264

  0   % Mode

  8   % Number of nodes

  40 -30 40

40 -25 45

40 -5 31.5

40 0 31.6

40 7 31.8

40 10 31.8

40 15 31.9

40 25 32.5 % p x y coordinates

    B 265 POLYG2   % Tsupply Tsource Pelec (Heating)(kW)

  87.1

  310.2

P 265

  0   % Mode

  8   % Number of nodes

  40 -30 9

40 -25 7.5

40 -5 6.6

40 0 6.65

40 7 6.75

40 10 6.8

40 15 6.85

40 25 7 % p x y coordinates

B 266 EQ

  60.1

  83.1

P 266

  0   % Error tolerance

B 267 EQ

  263.1

  95.1

P 267

  0   % Error tolerance

B 268 EQ

  71.1

  78.1

P 268

  0   % Error tolerance

B 269 GENG

  272.1

  301.1

  301.2

  301.3

  301.4

P 269

  45.50   % Latitude

  73.62   % Longitude

  5   % Time zone

  1   % Gordon Reddy variance factor

  0   % Year-to-year variability

  0.3   % Autocorrelation coefficient lag one

  0.171   % Autocorrelation coefficient lag two

  4712   % Initialisation of random number generator

    B 270 AVE

183.1

B 271 AVE   % Number of Inverters

258.1

B 272 MTM

301.2

P 272

'Montreal'   % Location

C TiltAngle

31   % Tilt Angle (Degree)

C NumStorHP

4   % Number of Heat Pumps Charging Storage Tank

C CoolSuppTemp

11   % Cooling Supply Temperature (C)

C HeatSuppTemp

40   % Heating Supply Temperature (C)

C MaxHeatDemandKW

999999   % Define global constant: 277

C ManPVQnt

12054   % Manual Number of PV panels

C AutoPVsizing

1   % Automatic PV sizing = 1/ Otherwise =0

C AutoHPcounting

1   % Automatic HP Counting = 1 / Otherwise = 0

C Azimuth

180   % Azimuth (180=south)

C ManHPQnt

1   % Manual Maximum Heat Pump Quantity

B 283 MAXX   % Number of HPs in Service (DHW)

201.1

B 284 MAXX

189.1

B 285 MAXX   % Maximum Heating/ Cooling Demand (kW)

304.1

304.2

B 286 MAXX   % Number of Heat Pumps in Service (Heating)

188.1

B 287 MAXX

36.1

B 288 MAXX

205.1

B 289 MAXX

41.1

B 290 TOL

315.1

B 291 COS

69.1

P 291

0   % Unit of angle

B 292 GAIN   % Fixed Estimated cost (2.7 $/W)

289.1

P 292

2.7   % Gain factor g

B 293 ABS

20.1

B 294 ABS

49.1

B 295 ABS

30.1

B 296 GH2GT

269.1

311.1

69.1

68.1

94.1

301.1

301.2

301.3

301.4

P 296

8   % Model

45.50   % Latitude

73.62   % Longitude

5   % Time zone

B 297 FRAC

159.1

B 298 FRAC

150.1

B 299 FRAC

156.1

B 300 HOY

301.1

301.2

301.3

301.4

B 301 CLOCK

P 301

2019	% Start year
1	% Start month
1	% Start day
0	% Start hour
0	% Start minute
0	% Start second
2020	% End year
1	% End month
1	% End day
0	% End hour
0	% End minute
0	% End second
1	% Increment
'h'	% Unit

B 302 TANKST

56.1

163.1

92.1

223.1

96.1

308.1

P 302

1.5	% Tank volume
8	% Number of temperature nodes
3	% Tank diameter
4190	% Specfic heat of fluid
1000	% Fluid density
0.5	% Overall heat-loss coefficient
0.025	% Effective heat conductivity
10	% Initial tank temperature

B 303 PVI

290.1

296.1

310.2

272.2

P 303

0	% Temperature mode
96	% Number of cells in series per module
1	% Number of cells in parallel per module
1	% Number of modules in series
1	% Number of modules in parallel
0.0181	% Single cell area
1.740	% Single module area
1.12	% Band gap
0.2285	% Coefficient of short-circuit current density
0.326E-03	% Temperature coefficient of short-circuit current
0.334236E-04	% Coefficient of saturation current density (Shockley diode)
0	% Coefficient of saturation current density (Recombination diode)
0.00017223	% Series resistance
0.05295855	% Parallel resistance
0.6126541	% Diode ideality factor alpha
2	% Diode ideality factor beta
0	% Bishop parameter a
0	% Bishop parameter M
0	% Bishop parameter Vbr
2.0	% Module tolerance plus
-2.0	% Module tolerance minus

1.623	% Characteristic module length
20.000	% Module weight
0.70	% Absorption coefficient
0.85	% Emission factor
900.0	% Specific heat of a module
47.7	% Nominal operating cell temperature
25	% Initial cell temperature
1E-5	% Single cell voltage error tolerance
100	% Maximum number of iterations
'002368'	% Product ID

B 304 READ

P 304

3	% Number of values to be read per record
0	% Number of records to be skipped on the first call

'C:\Users\Bahador\Desktop\THESIS\INSEL MODEL\DHW_CASE STUDY_INSEL INPUT FILE.txt' % File name

'*'	% Fortran format

B 305 GE

184.1

74.1

P 305

0	% Error tolerance

B 306 GE

210.1

170.1

P 306

0	% Error tolerance

B 307 GE

39.1

21.1

P 307

0   % Error tolerance

B 308 SOY

301.1

301.2

301.3

301.4

301.5

301.6

B 309 IVP

154.1

P 309

6300.00   % Nominal DC power

0.00951   % Normalized self consumption

-0.00956   % Normalized voltage losses

0.04304   % Normalized ohmic losses

'0817'   % Inverter ID

B 310 GENGT

272.1

272.3

272.4

272.5

272.7

272.8

301.1

301.2

301.3

301.4

P 310

45.50   % Latitude

73.62   % Longitude

5   % Time zone

1   % Variance factor of the Gordon Reddy correlation

0   % Year-to-year variability

0.3   % Autocorrelation coefficient lag one

0.171   % Autocorrelation coefficient lag two

4711   % Initialisation of random number generator

2   % Maximum allowed mean temperature deviation

100   % Maximum number of iterations

B 311 G2GDH

269.1

316.1

P 311

0   % Model

B 312 POLYG   % PV price related to PV max power

222.1

P 312

15   % Number of nodes

2.5   10000

5   15000

10   28666.25

15   35369.8125

20   42034

24   47337

70   106510.25

100.5   143907.2531

200 255721

300 352386

500 498466

800 800000

1000 1000000

2000 2000000

3000 3000 % x y coordinates

B 313 LE

304.1

64.1

P 313

0   % Error tolerance

B 314 LE

199.1

45.1

P 314

0   % Error tolerance

B 315 MPP

303.1

P 315

10   % Lower limit

700   % Upper limit

0.01   % Error tolerance

B 316 GOH

301.1

301.2

301.3

301.4

P 316

45.50   % Latitude

73.62   % Longitude

5   % Time zone